# DEVELOPMENT OF A QUASI-2DH MODEL FOR NUMERICAL MODELING OF SHORELINE CHANGES

A THESIS SUBMITTED TO
THE GRADUATE SCHOOL OF NATURAL AND APPLIED SCIENCES
OF
MIDDLE EAST TECHNICAL UNIVERSITY

BY

CAN ÖZSOY

IN PARTIAL FULFILLMENT OF THE REQUIREMENTS
FOR
THE DEGREE OF MASTER OF SCIENCE
IN
CIVIL ENGINEERING

FEBRUARY 2021

Approval of the thesis:

**DEVELOPMENT OF A QUASI-2DH MODEL FOR NUMERICAL MODELING OF SHORELINE CHANGES**

submitted by **CAN ÖZSOY** in partial fulfillment of the requirements for the degree of **Master of Science** i**n Civil Engineering, Middle East Technical University** by,

Prof. Dr. Halil Kalıpçılar
Dean, Graduate School of **Natural and Applied Sciences** _____

Prof. Dr. Ahmet Türer
Head of the Department, **Civil Engineering** _____

Assist. Prof. Dr. Cüneyt Baykal
Supervisor, **Civil Engineering, METU** _____

**Examining Committee Members:**

Prof. Dr. Ahmet Cevdet Yalçıner
Civil Engineering, METU _____

Assist. Prof. Dr. Cüneyt Baykal
Civil Engineering, METU _____

Assoc. Prof. Dr. Havva Anıl Güner
Civil Engineering, Yıldız Teknik Üniversitesi _____

Assoc. Prof. Dr. Mustafa Tuğrul Yılmaz
Civil Engineering, METU _____

Assist. Prof. Dr. Gülizar Özyurt Tarakcıoğlu
Civil Engineering, METU _____

Date: 15.02.2021

**I hereby declare that all information in this document has been obtained and presented in accordance with academic rules and ethical conduct. I also declare that, as required by these rules and conduct, I have fully cited and referenced all material and results that are not original to this work.**

Name, Last name : Can Özsoy

Signature :

# ABSTRACT

## DEVELOPMENT OF A QUASI-2DH MODEL FOR NUMERICAL MODELING OF SHORELINE CHANGES

Özsoy, Can
Master of Science, Civil Engineering
Supervisor: Assist. Prof. Dr. Cüneyt Baykal

February 2021, 105 pages

The scope of this thesis is to develop a quasi-2-dimensional numerical model to numerically modeling shoreline response under wave action in the vicinity of various coastal defense implementation. The developed quasi-2-dimensional model is applicable in both the medium and the long term. The model is utilizing a spectral wave model, which solves the energy balance equation. Longshore sediment transport is solved through the bulk sediment transport formula, and it is distributed over the surf-zone. The aim is to develop an accurate sediment transport model combining a spectral wave model with directly computed sediment transport expressions without prolonging computation time. The model consists of cross-shore and swash zone sand transport for maintaining an equilibrium profile. The developed quasi-2-dimensional numerical model is compared with theoretical cases and validated through Gravens and Wang's (2007) laboratory experiments. For theoretical cases, beach cusps, model's scope of cross-shore sediment transport, and a single groin case investigated. Moreover, series of experimental results in an offshore breakwater's vicinity are compared with the model results for laboratory experiments. In initial cases of laboratory experiments, the model successfully represents both the shoreline and the areal changes. As the shoreline advances

through the offshore breakwater and tombolo starts to form, incoming wave and local orientation angles start to increase; the model results deviate from laboratory measurements.

Keywords: Sediment Transport, Shoreline Change Model, Quasi-2DH

# ÖZ

## KIYI ÇİZGİSİ DEĞİŞİMLERİNİN SAYISAL MODELLENMESİ İÇİN YARI IKI BOYUTLU MODEL GELİŞTİRİLMESİ

Özsoy, Can
Yüksek Lisans, İnşaat Mühendisliği
Tez Yöneticisi: Dr. Öğr. Üyesi Cüneyt Baykal

Şubat 2021, 105 sayfa

Bu tezin kapsamında kıyı çizgisi değişimlerinin dalga etkisi altında ve çeşitli kıyı yapısı alternatifleri varlığında sayısal olarak modellenmesi için yarı iki boyutlu bir sayısal model geliştirilmiştir. Geliştirilen yarı iki boyulu model orta ve uzun dönem kıyı çizgisi değişimleri için uygulanabilir bir modeldir. Geliştirilen model, dalga taşınımı için, enerji denge denklemini çözen spektral dalga modeli içermektedir. Kıyı boyu kum taşınımı toplu kum taşınımı denklemleriyle hesaplanıp, sörf bölgesine dağıtılmıştır. Böylece, spektral dalga modeli ile toplu kum taşınımı denklemleri birlikte çalışarak hızlı hesaplama yapan ama doğruluğu yüksek bir model geliştirilmesi amaçlanmıştır. Modelde kıyıya dik taşınım ve plajın çalkantı bölgesinde kum taşınımı denge kıyı profilini koruma amacıyla tanımlanmıştır. Geliştirilen yarı iki boyutlu model teorik sonuçlarla karşılaştırılmış ve Gravens ve Wang (2007) laboratuvar sonuçlarıyla doğrulanmıştır. Teorik sonuçlarda, sahil çıkıntıları çevresindeki taşınımlar, kıyıya dik kum taşınımı etkisi altında kıyı profili değişimi ve kıyıya dik tek mahmuz çevresindeki birikme ve oyulma durumları incelenmiştir. Ek olarak, laboratuvar sonuçlarında bir açıkdeniz dalgakıran çevresinde oluşan kum taşınımları karşılaştırılmıştır. Laboratuvar sonuçlarıyla yapılan karşılaştırmalara göre; model kum taşınımının ve kıyı çizgisinin ilerlemeye

başladığı ilk fazlarda kıyı çizgisi ve alansal sonuçlar incelendiğinde başarılı olduğu gözlenmiştir. Kıyı çizgisi açıkdeniz dalgakıranına doğru ilerlemeye başladığı ve tombolo oluştuğu durumlarda ise model sonuçlarının laboratuvar sonuçlarından uzaklaşmaya başladığı gözlemlenmiştir.

Anahtar Kelimeler: Kum Taşınımı, Kıyı Çizgisi Değişimi Sayısal Modeli, Yarı İki Boyutlu Model

To my family & my beloved ones…

## ACKNOWLEDGMENTS

I would like to express my uttermost gratitude to my supervisor Dr. Cüneyt Baykal who encouraged and guided me through completing this thesis with his enlightening guidance. His expertise in the field of coastal engineering is impressive. I am grateful to learn from him.

I would like to thank Dr. Ayşen Ergin, who shows the coastal engineering family's path to me. Being one of her students is honorable for me. If I didn't meet her, I would never be a part of the coastal engineering family. With her encouraging, cheerful and enlightening perspective, she is a mentor for all coastal engineers.

I would like to express my thanks to Dr. Işıkhan Güler, Dr. Hasan Gökhan Güler, Dr. Ahmet Cevdet Yalçıner, and Dr. Gülizar Özyurt Tarakcıoğlu for their continuous support, sharing their knowledge and experience throughout graduate studies.

I would like to thank eleven fifty group, Ghazal Khodkar Kadir Karakaş, Cem Bingöl, Sedat Gözlet, Koray Göral, for their support in all aspects of life. We shared plenty of joyful moments with them.

I would like to extend my thanks to coastal engineer family, Arda Çiçek, Barış Ufuk Şentürk, Berkay Akyol, Emre Yıldırım, Gözde Güney Doğan, İlker Çoban, Mert Yaman, Utku Uzun for their presence and all the things we shared.

I want to thank my dearest friends, Hazal Çağlan, Mertcan Gültekin, Ulaş Canberk Ayan, İsmail Ortakcı, Erkin Cem Göze and Umut Kağan "George" Yıldırım for their valuable friendship and support throughout my life.

Finally, I would like to express my heartfelt gratitude to my mother Banu Göle, my father İhsan Özsoy, and Özlem Özsoy for their support and everything they have done for me. They always inspired me to be a better person.

## TABLE OF CONTENTS

## LIST OF TABLES

TABLES

## LIST OF FIGURES

FIGURES

## LIST OF ABBREVIATIONS

| | |
|---|---|
| 1-D | 1 Dimensional |
| 2-D | 2 Dimensional |
| 2-DH | 2 Dimensional Horizontal |
| 2-DV | 2 Dimensional Vertical |
| Q-2D | Quasi 2 Dimensional |
| Q-2DH | Quasi 2 Dimensional Horizontal |
| Q-2DV | Quasi 2 Dimensional Vertical |
| 3-D | 3 Dimensional |
| Q-3D | Quasi 3 Dimensional |
| BSS | Brier Skill Score |
| CEM | Coastal Engineering Manual |
| CERC | Coastal Engineering Research Center |
| MAPE | Mean Absolute Percent Error |
| MEV | Morphology Evolution |
| NSW | Nearshore Spectral Wave Model |
| SPM | Shore Protection Manual |
| STD | Sediment Transport Distributions |
| T1C1 | Test 1 Case 1 |
| T1C2 | Test 1 Case 2 |
| T1C3 | Test 1 Case 3 |

| | |
|---|---|
| T1C4 | Test 1 Case 4 |
| T1C5 | Test 1 Case 5 |
| T1C6 | Test 1 Case 6 |
| T1C7 | Test 1 Case 7 |
| T1C8 | Test 1 Case 8 |

## LIST OF SYMBOLS

SYMBOLS

| | |
|---|---|
| $\alpha$ | Local Orientation |
| $\alpha_b$ | Breaking Wave Angle |
| $\alpha_e$ | Effective Breaking Angle |
| $\alpha_s$ | Orientation at The Shoreline |
| $\beta$ | Angle Between Local Wave Angle and Bottom Orientation |
| $\beta_b$ | Angle Between Breaking Wave Angle and The Coastline |
| $b$ | Constant Controls Residual Value Beyond Closure Depth |
| $c$ | Calibration Constant |
| $C_1$ | Depth Distribution for Longshore Sediment Transport |
| $C_2$ | Wave Height Distribution for Longshore Sediment Transport |
| $C_3$ | Total Distribution for Longshore Sediment Transport |
| $\overline{C_3}$ | Normalized Total Distribution |
| $C_{gb}$ | Wave Group Celerity |
| $d$ | Bottom Depth |
| $d^a$ | Recomputed Water Depth After Avalanching |
| $d_c$ | Closure Depth |
| $d_e$ | Assumed Equilibrium Profile |
| $d_p$ | Profile Depth |
| $d^{stg}$ | Depth of The Staggered Bathymetry System |

| | |
|---|---|
| $D_{50}$ | Median Grain Size |
| $D_b$ | Dissipation Rate Due to Random Wave Breaking |
| $D_d$ | Diffraction Term |
| $\Delta d_a$ | Depth Change in Avalanching |
| $E_b$ | Breaking Wave Energy |
| $\varepsilon_x$ | Constant for Cross-Shore Sediment Transport |
| $\varepsilon_y$ | Constant for Alongshore Diffusivity Transport |
| $f(x)$ | Density Function |
| $\varphi(x)$ | Shape Function |
| $g$ | Gravitational Acceleration |
| $\gamma_b$ | Breaking Index |
| $\gamma_x$ | Cross-Shore Diffusivity Constant |
| $\gamma_y$ | Alongshore Diffusivity Constant |
| $\gamma_s$ | Shore Relaxation Coefficient |
| $H_s$ | Significant Wave Height |
| $H_{s,0}$ | Deep Water Significant Wave Height |
| $H_{s,12}$ | Significant Wave Height Which Exceeded 12 Hours Per Year |
| $H_{sb}$ | Breaking Wave Height |
| $H_{rms,b}$ | Root Mean Square Breaking Wave Height |
| $H_{rms,0}$ | Deep Water Root-Mean-Square Wave Height |
| $K$ | Empirical Coefficient |
| $K_b$ | Dimensionless Constant |

| | |
|---|---|
| $\zeta$ | Wave Set-Up for Oblique Incident Wave |
| $\zeta_{\theta_0=0}$ | Wave Set-Up for Perpendicular Incident Waves |
| $L$ | Surf-Zone Width Parameter |
| $L_0$ | Deep Water Wave Length |
| $L_d$ | Length Scale Decay Control Parameter |
| $L_p$ | Peak Wave Length |
| $m$ | Average Bottom Slope of The Surf-Zone |
| $m_b$ | Beach Slope Near Breaking |
| $m_{cr}$ | Critical Slope |
| $m_f$ | Morphological Acceleration Factor |
| $m_s$ | Local Slope at The Shoreline |
| $\mu$ | Empirical Constant |
| $p$ | Porosity Index |
| $q_{crs}$ | Cross-Shore Sediment Transport |
| $q_{lst}$ | Longshore Sediment Flux |
| $q_{lst,x}$ | Longshore Sediment Flux In X |
| $q_{lst,y}$ | Longshore Sediment Flux In Y |
| $q_x$ | Total Sediment Transport in X Direction |
| $q_y$ | Total Sediment Transport in Y Direction |
| $q_Y$ | Representation of Sand Sources / Sinks Along the Shoreline |
| $Q$ | Bulk Sediment Transport |

| | |
|---|---|
| $r$ | Empirical Constant |
| $\rho$ | Density of Water |
| $\rho_s$ | Density of Sand |
| $S$ | Directional Wave Spectral Density |
| $t$ | Time |
| $T_p$ | Peak Wave Period |
| $T_r$ | Relaxation Time |
| $T_s$ | Significant Wave Period |
| $\theta_0$ | Offshore Incoming Wave Angle |
| $\theta_b$ | Wave Angle at Breaking |
| $u_0$ | Maximum Horizontal Bottom Orbital Velocity |
| $v_1$ | Vector One for Orientation |
| $v_2$ | Vector Two for Orientation |
| $v_{ref}$ | Free Surface Normal Vector |
| $v_{proj}$ | Projected Surface Vector |
| $V_l$ | Longshore Current Velocity |
| $\vartheta_\theta$ | Propagation Velocity in Directional Space |
| $\vartheta_x$ | Propagation Velocity In X |
| $\vartheta_y$ | Propagation Velocity In Y |
| $x$ | Longshore Position/Cross-Shore Position |
| $x_i$ | True Value for MAPE |
| $X_b$ | Surf-Zone Width |

| | |
|---|---|
| $X_l$ | Decay Distance |
| $X^{stg}$ | X Coordinate of The Staggered Bathymetry System |
| $y$ | Longshore Position/Cross-Shore Position |
| $y_i$ | Prediction Value for MAPE |
| $Y^{stg}$ | Y Coordinate of The Staggered Bathymetry System |

# CHAPTER 1

# INTRODUCTION

## 1.1 Motivation and Problem Definition

In coastal engineering, the phenomenon of shoreline change is an important issue due to its wide impact on the coastal field; it affects both the magnitude and directions of waves, currents, sediment transport rates, and even biological activities. Ever-increasingly development in the coastal areas and human interventions cause changes in the shorelines. Hence, determining the change of shoreline in a condition/state is a must to thoroughly understand the process during this condition and counteract against it. Some measures prevent these changes or minimize their effects and maybe restore the coastline's natural state; soft and hard measures. Soft measures include; nourishments, sand traps, etc., and hard measures include; placing a shore protection structure in the nearshore area. Whether soft measures or hard measures, minimizing measures' effects on the coast and maximizing counter-action against previous conditions should restore natural processes in the coast and conserve the restored natural state. It is crucial to understand these measures and their effects on the shoreline to design a shore-protection structure effectively.

Engineers and scientists have been trying to estimate coastline changes in various external forces such as sea level change, presence of a coastal structure, presence of a river mouth, etc. Coastal areas are under the effect of many complex natural phenomena. When any measures or interventions are implemented in the nearshore, these natural phenomena change to adapt to the new environment. Thus, estimation of changes of coastlines is a difficult task.

The construction of coastal structures affects the coastline; different coastal structures affect the shoreline separately. Groins cause sand accumulation on the windward side, while erosion on the leeward side. Offshore breakwaters cause accumulation and erosion on the leeward side of the breakwater. General behavior may follow the same pattern, yet changes in wave height, wave period, wave direction, and structure dimensions result in different behavior. There are analytical, empirical, and numerical solutions to estimate shoreline changes around coastal structures.

With the advancements in computer technology, numerical models are becoming more convenient than before. Implementing and executing numerical models are much faster and easier than before. Various numerical models are implemented on the problem of shoreline change. These numerical models vary from simple one-dimensional (1-D) models for shorelines or cross-shore profiles and three dimensional (3-D) models for near-shores. 3-D models are sophisticated and complex models. As the model gets complicated and sophisticated, computation times accumulate. This results in high computation, calibration, and verification times. Therefore, these complicated 3-D models fail to represent the long-term changes (more than 5-10 years) in the shorelines. On the other hand, 1-D models are idealizing coastal profiles and near-shore processes; thus, it lowers computation, calibration, and verification times. This reduced computation times allow the modeler to model longer durations since computation times do not limit the modeler. While it reduces computation times, an idealized shoreline only gives a solution under idealized conditions; thus, results do not fully represent the real case; it only gives an "idealized" result for the modeler.

In one-line models, wave transformations and computations are done mostly parametrically or geometrically. Thus, in situations where different types of coastal measures are in the nearshore area, afore mentioned wave computations and transformations become too complex to accurately solved by one-line models. On the other hand, 2 and 3-dimensional numerical models solve an immense number of equations, cause to increase in the "Big O". In studies where quick solutions/interim

results are required, such as coast restoration projects, these models fail to give a quick solution to designing and investigating hard coastal measures' effectiveness. Hence, one-line models are preferred in such fields of applications. One-line models are insufficient to model tombolo formation, estimate accretion and erosion around complex coastal structures (Y-head, T-head groin, multiple structures), the effect of topographical conditions (bars, throughs), and sediment transport in curved shorelines. Although, sediment transport in curved shorelines is partially modeled by Larson et al. (2006). Developed quasi-two-dimensional-horizontal (Q-2DH) model within the scope of this thesis combines the quick one-line methodology of sediment transport with a 2-DH spectral wave transformation model to combine the accuracy with computation speed.

## 1.2 Proposed Model

In this study, a quasi-two-dimensional horizontal model is implemented to estimate medium-to-long-term shoreline changes in coastal structures' vicinity. Without the need to idealize the near-shore field and processes, this model computes wave field using wave module and sediment transport rates computed as a one-dimensional model and distributed over the surf zone, making transport field two-dimensional horizontal. In the proposed model, it consists of 3 basic steps. The first step is the wave model (Nearshore Spectral Wave Model (NSW); Baykal, 2012); it solves the energy balance equation to compute the wave field in the near-shore area. In the second step, as in 1-D models, bulk sediment transport is computed with the extended version of the CERC formula (Komar, 1998), and using the wave field information in the nearshore area, bulk sediment transport is distributed over the surf zone from shoreline to the closure depth. Computation of sediment transport with one dimensional approach and distributing it over the surf zone makes the model a quasi-two-dimensional-horizontal model. In the computation of the sediment transport rates, previous work of van den Berg et al. (2011) is implemented to the

model. In the final step, morphology is updated according to sediment transport rates, and the process is repeated until the last time step.

## 1.3 Objectives

This thesis focuses on quasi two dimensional-horizontal numerical modeling of both medium and long-term shoreline changes in the vicinity of coastal structures. Objectives are listed as follows:

- Computation of wave field in the vicinity of structures with the use of a spectral wave model, rather than geometric/parametric computations as in one-line models
- Direct computation of distributed alongshore sediment transport rates based on nearshore wave characteristics
- Computation of cross-shore and swash zone sediment transport mechanisms
- Investigation of computed sediment field with theoretical cases
- To validate the model results with laboratory measurements

## 1.4 Outline of the Thesis

In this chapter, general information about the shoreline change, shoreline dynamics, and importance of shoreline change estimations are briefly discussed. Motivation and problem definition are presented considering the importance of shoreline change models. Shoreline change models are briefly discussed, previously done studies on hybrid modeling, proposed methods, and models are mentioned. Contributions and outline of this thesis are given.

In the second chapter, the time history of this thesis' prior studies and their evolution in the past and conditions made available this thesis are discussed. The detailed information in the literature on sediment transport models, evolution of these transport models in time, detailed information about one-line modeling, and its

difference between other modeling methods, and detailed information on Q-2DH modeling concepts are discussed. Also, beach morphology models, which is applicable for shoreline modeling, are discussed in this chapter.

In the third chapter, a detailed explanation of the developed Q-2DH model, the model's structure, its operating, and its flowchart are given. Briefly, its wave module is explained, sediment transport field and its computations, distributions, morphology module is also explained in this chapter. Assumptions and limitations of the model, governing equations, numerical schemes are presented in this chapter.

In the fourth chapter, the Q-2DH model is benchmarked. It is compared with theoretical cases and laboratory cases. For theoretical cases, sediment transport directions are compared with beach cusps. Accepted cross-shore transport for Q-2DH model and its evolution under solely cross-shore transport is studied. A single groin case is studied to observe the model's behavior in the vicinity of a groin. Gravens and Wang's (2007) laboratory experiments for investigating headland structures are studied, and the model is validated through several laboratory cases.

In the fifth chapter, a summary of the work done in this thesis, the model's results, and further recommendations on the Q-2DH model are presented. The model's importance and contributions are discussed, and the conclusion is given in the fifth chapter.

# CHAPTER 2

# LITERATURE REVIEW

Sediment transport has always been an important issue for human beings. Development in coastal areas increased the importance of the sediment transport mechanism. Without understanding this process, any interaction in the coastal areas may cause fatal consequences for natural habitats in the region, or it may cause loss of sand or even the entire beach.

Sediment transport models are studied for a long time. Whether these models are examined through analytical, empirical, physical or numerical, many scientist and engineer has dealt with this problem. In this chapter, background information about sediment transport models is going to be presented. Moreover, shoreline change models, beach profile change models, 3-D models are discussed and presented.

## 2.1 Overview of Sediment Transport Models

Models are basically categorized as 4; analytical, physical, empirical, and numerical models. Different problems may require different solutions; therefore usage of afore mentioned four methods depends on the problem. Empirical models are derived from field or laboratory observations and measurements. Analytical models are physical expressions derived as a mathematical expression for the problem. Physical models are models that physically imitate the problem that the same conditions are satisfied within a laboratory or in the field. Numerical models are a combination of large mathematical expressions solved within multiple time steps. Analytical and empirical results give quick and accurate results for the problem. Physical models are carried out to understand complex phenomena occurred in coastal processes.

However, physical models are expensive, and it has scaling effects. Therefore, it may distort the desired outcomes. Due to these reasons, numerical models are ever-increasingly used in the modeling of coastal processes.

Numerical models can be applied to problems that last several minutes to decades. These models can be applied to situations with dimensions of several kilometers or can be applied to few centimeters. Coastal planners are interested in temporal scales of years to decades, spatial scales of 10 to 100 kilometers alongshore, 1 to 10 kilometers cross-shore. In coastal zone management, the use of numerical models for estimation of future shoreline, processes involved in this phenomena, and selection of appropriate design conditions are powerful tools. Numerical models give a basis for arranging and examining data and assessing possible future shoreline evolution situations. In conditions where design practices are included, numerical models develop an understanding and evaluation of selected design (Hanson et al. 2003).

While modeling shoreline change, different methodologies conclude differently. Prediction of the shoreline can be simplified by isolating processes individually. Since long-term changes in the shoreline occur due to the alongshore sediment transport process, cross-shore sediment transport mainly affects the change on shorter time scales. Cross-shore transport mechanism can be omitted in the long-term computations. An eminent special case to this speculation is the shoreline change identified with long-term sea variability, which causes to beach profile to re-adapt to the new water level (Miller & Dean, 2004). Morphological models vary from simple 1-D to complex 3-D models, depending on the coastal process and the study, which can be used to predict the study's solution. The availability of numerical models categorized for their spatial and temporal extends are schematized in Figure 2.1.

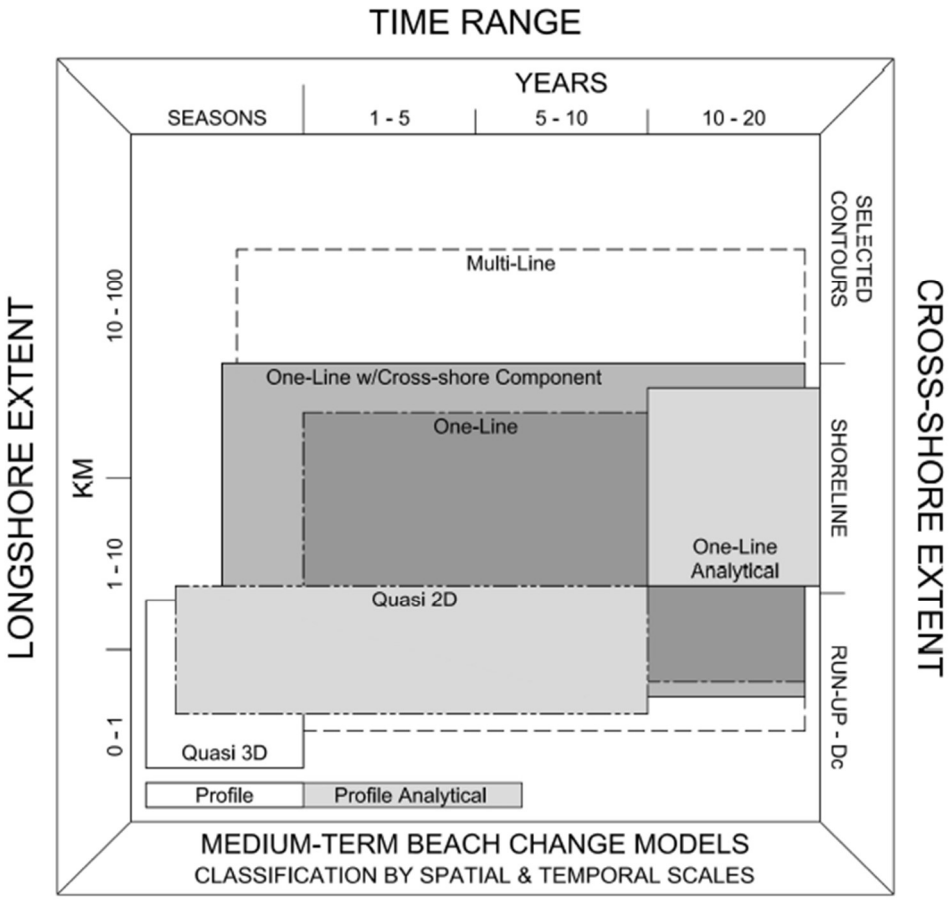


Figure 2.1 Classification of beach change models by spatial & temporal scales (adopted from Hanson et al., 2003)

Figure 2.1 explains the spatial and temporal scales of some medium-term beach change models. Firstly, Profile change models can predict seasons in temporal scales and are very limited in both longshore and cross-shore extent. Analytical profile change models are similar to Profile change models, yet they have more capability to predict long-term changes. Quasi 3-D models can also predict seasonal changes; they have more longshore and cross-shore extent than profile models. Quasi 2-D models are similar to Quasi 3-D models, yet they can represent longer durations than Quasi 3-D models. One-Line, One-Line with a cross-shore component, multi-line models are available, and they are similar to each other considering their applicability. They can predict changes from seasons to decades, they can be used to

predict tens of kilometers in alongshore direction and they can be used to predict all three components (selected contours, shoreline and run-up & closure depth) of cross-shore bathymetry changes. Its wide applicability makes these models preferable when morphology modules are required.

### 2.1.1 Sediment Transport in the Surf Zone

Sediment transport in the surf zone occurs in two ways; longshore sediment transport and cross-shore sediment transport. Longshore sediment transport occurs within the surf zone as a result of the advection of alongshore current. This current is generated by the differences in the wave radiation stress in the breaking zone (Fredsoe & Deigaard, 1992). Alongshore current magnitude depends on wave height, angle of wave incidence, sediment characteristics, and bed shear stress. Longshore sediment transport is a fairly well-known phenomenon. Many formulas have been developed to estimate the quantity of the longshore sediment transport. Inman and Bagnold (1963), CERC formula (SPM, 1984), and Kamphuis (1991) formulas are the most common formulas for longshore sediment transport.

Another phenomenon for the sediment transport in the surf zone is cross-shore sediment transport. This type of process is the conclusion of many sophisticated processes. In this type of sediment transport, each wave moves the sediment back and forth. This transport's long-term behavior can be predicted by computing the net flux over one wave period (Fredsoe & Deigaard, 1992). This type of transport occurs both in the surf zone and outside the surf zone. Cross-shore sediment transport inside the surf zone is generally dominated by a vertically segregated return flow, this causes sediment to move offshore (Kristensen, 2012). Cross-shore sediment transport outside the surf zone is because sediment moves through the onshore direction. This type of transport is mainly occurring due to wave asymmetry from non-linear waves, boundary layer streaming caused by a systematic build-up of boundary layer thickness, and wave drift due to oscillatory particle trajectory (Fredsoe & Deigaard, 1992).

### 2.1.2 Beach Evolution Modeling

Beach evolution modeling's spatial scales can vary from centimeters to kilometers; temporal scales can vary from hours to months. Depending on the research question and the coast's situation, one of these scales can be chosen. For different problems, there exist several solutions; the fastest way to predict long term changes in the shoreline can be done with one-line models. Dune erosion, bar formation, seasonal changes in the shoreline and swash zone dynamics can be predicted with medium to short term beach evolution models (Baykal, 2012).

Numerical modeling of beach evolution firstly started to predict shoreline change and it is studied by Pelnard-Considere in 1956. Pelnard-Considere developed a mathematical model to observe and predict the situation around a groin using the one-line model. A one-line model accepts that seasonal changes in the nearshore region, such as bar formation, storm-induced accretion, and erosion, are canceled during the process. Moreover, it is accepted that a single equilibrium beach profile is representing the whole shoreline. Accepting the cancelation of short-term changes in the nearshore region and accepting an equilibrium beach profile to represent the shoreline, longshore sediment transport becomes the coastal problem's governing process. After these fundamentals of the one-line model, Bakker (1968) included onshore and offshore processes to understand the profile changes within the one-line model and obtained a two-line model, LeMéhauté and Soldate (1978) added wave diffraction and refraction further to extend the capability of this type of model. Fleming and Hunt (1976) included grid points to allow further bathymetry changes over the area (Capobianca et al., 2002).

The general approach for the shoreline models is dividing the shoreline into computational cells or grids. Using desired bulk sediment transport formula, in computational cells computation of the sediment influxes and outfluxes are desired. The movement of sand can be computed with these influxes and outfluxes.

The one-Line theory was first numerically implemented by Price et al. (1973), and followed and developed by many others. Throughout the years, computer technology advancement and lesser computational heaviness allow engineers to use these one-line models for preliminary design and research. Examples of some models are given as follows; GENESIS (Hanson & Kraus, 1989), ONELINE (Dabees & Kamphuis, 1998), and CSIM (Şafak, 2006; Artagan, 2006; Baykal, 2006; Esen, 2007).

Assuming cancelation of short-term changes and accepting an equilibrium shoreline for the entire beach is a major drawback for the one-line models. These assumptions led to long-term shore evolution deviations. To overcome these problems, the addition of some governing processes to solve medium-term and short-term events, the addition of cross-shore modules to one-line models (Hanson et al., 1997; Hanson & Larson, 1998), beach profile models works simultaneously with one-line models (Larson et al., 1990), multiple-line models (Hanson & Larson, 2000; Dabees & Kamphius, 2000) or one-line models linked to two-dimensional depth-averaged (2-DH) models (Shimizu et al., 1996; DHI, 2001; van den Berg et al., 2011; Kristensen et al., 2013) are developed.

One of the major drawbacks of the one-line models is also they are not easily applicable to irregular or curved shorelines. They are aimed to smooth out the shoreline. Curved shorelines are becoming straight, and the shoreline's irregularities tend to smoothed out by the one-line model. This drawback is surpassed by Hanson et al. (2001) by defining fixed representative shoreline, Larson et al. (2002), and Larson et al. (2006) introduced regional shoreline alignments, thus allowing local shoreline advance or retreat aligning regional shoreline. Their study also introduced a wave transformation mechanism that transforms the waves to a representative contour. Hence, without the interruption in alongshore sediment transport of a structure, the shoreline preserves its natural condition. However, the smoothing process of curved shorelines continues to occur in the vicinity of a structure as well. Around these structures, wave transformation, wave refraction, and wave diffraction computations are done geometrically; hence it causes wave height variations and causes this problem to happen as well. An energy balance equation-based wave

transformations module can be added to the sediment transport model to compute wave heights around structures to solve this drawback. Van to Dang (2006)'s N-Line Model can solve both short-term 2-D profile changes and long-term 3-D beach changes. For the wave transformation module Van to Dang incorporates RCPWAVE to solve wave field in the nearshore. RCPWAVE (Ebersole et al., 1986) is one of the simplified linear wave models to solve wave field in a large domain; also it solves Dally's (1985) empirical energy balance equation in the surf zone. Van to Dang's N-Line solves shallow water equation for alongshore and cross-shore current computations. The model uses Bailard's (1981) energetics approach utilized for sediment transport computations. Van to Dang's model is a versatile tool to model nearshore sedimentation. Although Van to Dang's RCPWAVE is based on linear wave theory, it does not accurately compute wave fields around complex structures. Also, it solves shallow water equations for the current field, which causes an increase in computation time. Hoan (2010) utilized the EBED wave model (Mase, 2001) based on the energy balance equation to compute wave transformation in the nearshore. To compute bottom morphology, Hoan used a one-line model with the computed wave field from EBED wave model. Hoan's model is a fast model to simulate shoreline changes. Hoan's sediment approach follows a one-line methodology solely. van den Berg et al. (2011) used the energy balance equation to compute the wave field. To evaluate sediment transport, extended CERC formula with the second term (Komar, 1998; Ozasa & Brampton, 1980) is applied. van den Berg studied shoreline changes in a nourished beach. Smith (2012) modeled the effects of bedforms and sediment grain size on wave energy dissipation and used wave energy dissipations to model the shoreline change with N-Line Model. Model is incorporated into the SWAN wave model (Booij et al., 1999). Similarly, Kristensen et al. (2013) computes the sediment transport field with MIKE21 (DHI, 2005) and integrates those sediment fluxes over the surf zone to continue to compute the sediment transport one-line model.

The aforementioned models are mainly for predicting the changes of shoreline from medium to long temporal scale. There are also numerical models for predicting beach

profile change models. These models are generally used for short to medium-term temporal scales for cross-shore movement of sand. There are also long-term models available for predicting the changes due to sea-level rise. Beach profile models are used to predict the changes that occurred during cross-shore sediment transport such as storm induced beach erosion and the accretion and readjustment of the beach after a beach nourishment application. These models are mainly used in shorter temporal scales since they mainly deal with cross-shore movements and do not consider longshore processes (Dabees, 2000). Beach profile models calculate sediment transport flux in a grid point over an area or profile, a continuity equation that may be implemented implicitly or explicitly is solved over this area or profile. In these computational grids, differences between sediment influxes and outfluxes lead to the calculation of accretions and erosions in the profile for the given wave condition (Baykal, 2006). Various models have been created dependent on breaking waves as the reason for changes in beach profile. (Dally & Dean, 1984; Kriebel & Dean, 1984; Larson & Kraus, 1989). There are some deterministic approaches to cross-shore models; these models compute wave transformation and time-averaged velocities over the profile. The cross-shore sediment transport is calculated as a function of horizontal velocities and local bottom conditions using Bailard's (1981) energetics approach. Examples of these models are; UNIBEST-TC (Stive & Battjes, 1984; Roelvink et al., 1995) and LITCROSS (Brøker-Hedegaard et al., 1991) (Dabees, 2000).

The aforementioned models are effectively used to model sudden response to storm conditions and assess beach nourishment's initial response. These models cannot effectively evaluate the recovery phase successive to storms. Zheng and Dean (1997) have published an inter-comparison of four 'erosion models' based on large scale wave experiments. According to this study, available tools for sediment transport models are successfully handling the erosional conditions; on the other hand, they cannot successfully handle accretional conditions. This is an issue while assessing a single storm or storm season's reaction to assessing long-term development (Capobianco et al., 2002).

This sort of model has been fruitful in predicting short-term events. Nevertheless, using these models under the temporal scales of medium to long term is ineffective due to complications in formulating this process to represent reliable and correct profile development (Hanson et al., 2003). In contrast, these models are successful tools when modeling extensive profile evolution (e.g., profile evolution due to sea-level rise, barrier island formation, and development) (Cowell et al., 1994). Extensive profile evolution models depend on formulas that become in an equilibrium state in this time scale. Hence, when formulating long-term and medium-term profile development, help of this equilibrium state can be satisfied to achieve beach profile development for these scales (Hanson et al., 2003).

Due to the fact, the nearshore process is highly complex and modeling this highly complex process is a difficult task, a different number of approaches have occurred. Roelvink and Broker (1993) and van Rijn et al. (2003) provide us with extensive evaluation and inter-comparison of many state-of-art European cross-shore models. Roelvink and Broker differed cross-shore modeling techniques into 4; descriptive models (e. g., Wright and Short, 1984), equilibrium profile evolution models (e. g., Larson and Kraus, 1989), and process-based (e. g. Dally and Dean, 1984). Davies et al. (2002) divided process-based models into two categories; research models that include extensive descriptions and formulations of the governing process and practical models that simplify the process, hence making them empirical in nature (Miller & Dean, 2004). Advancement in computer technology causes the development and use of physics-based 2-D and 3-D models coupled hydrodynamics, waves, sediment transport, and morphology models in beach profile prediction. Delft3D (Roelvink & van Banning, 1995), XBeach (Roelvink et al., 2010), MIKE21 (DHI, 2005), and ROMS (Warner et al., 2010) solve conservation of mass, the momentum of fluid and sediment to solve nearly all important aspects of coastal morphology evolution. These models are capable of solving the short-term evolution of coastal evolution. However, these models are computationally expensive for predicting long-term and large-scale coastal models (Vitousek et al., 2017).

Advancement in computer technology and numerical modeling techniques are led to more complex and sophisticated models. 2-D and 3-D models are consequences of this development. These models are for predicting morphological change in the nearshore region for short to medium temporal scale. These models are available to overcome the problems aforementioned about one-line models. 2-D and 3-D models are composed couples of wave transformation, nearshore current calculation, sediment transport module and bottom evolution. Quasi-3-D (Q-3D) and 3-D models are commonly used for short-term events. In these models, vertical distribution of current velocities and sediment concentrations are a major issue for precise modeling. Q-3D models are similar to 2-DH models; there is a one-dimensional vertical profile model (1-DV) to include the effects of return flows in the cross-shore process (Briand & Kamphuis, 1993). 3-D models solve hydrodynamic equations in three dimensions (Warner et al., 2008). The grid system of 3-D models is presented in Figure 2.2.

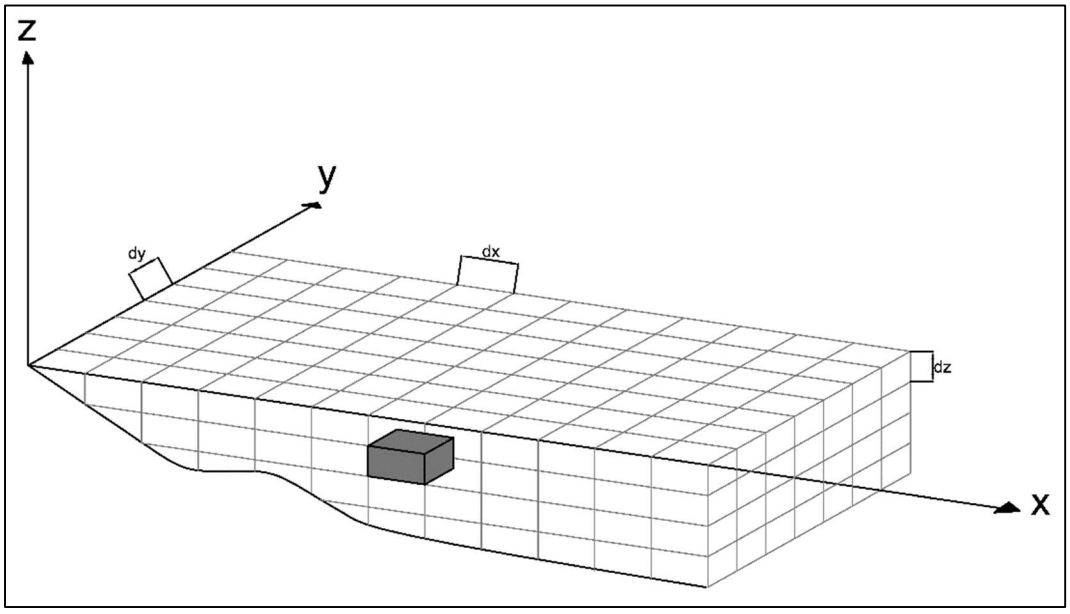


Figure 2.2 3-D modeling

3-D models can be simplified via integrating over the horizontal or vertical plane. Vertically integrated models result in only a computational domain in the horizontal plane (2-DH), whereas horizontally integrated models result in a computational

domain in the vertical plane (2-DV). 2-DH and 2-DV models are less computationally intensive compared to 3-D models. Therefore, they are more capable of long-term modeling (Shimizu et al., 1996). The grid system of 2-DH and 2-DV models can be found in Figure 2.3 and Figure 2.4.

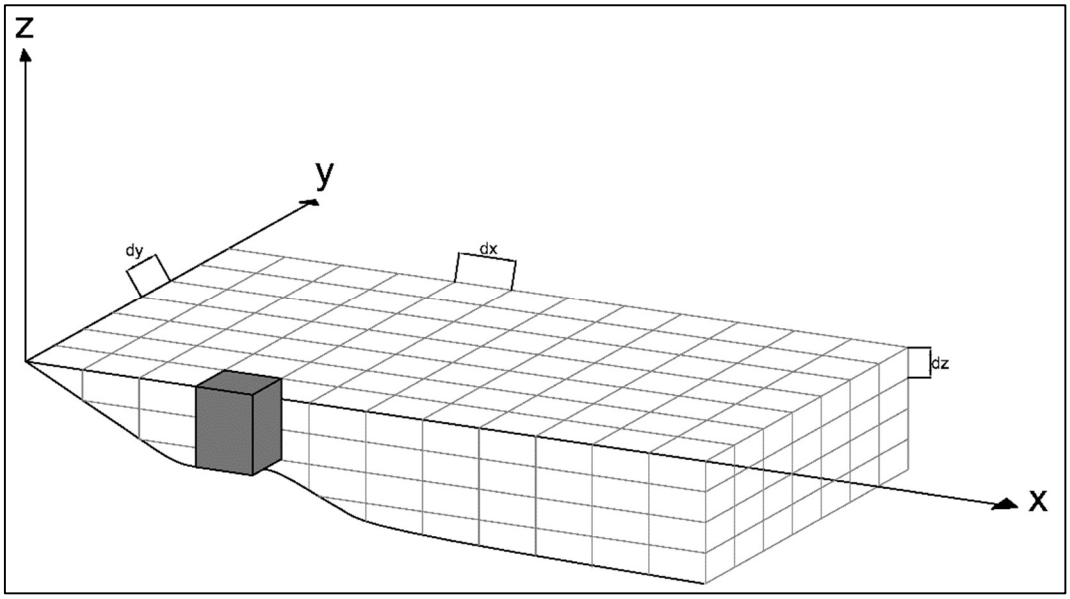


Figure 2.3 2-DH modeling

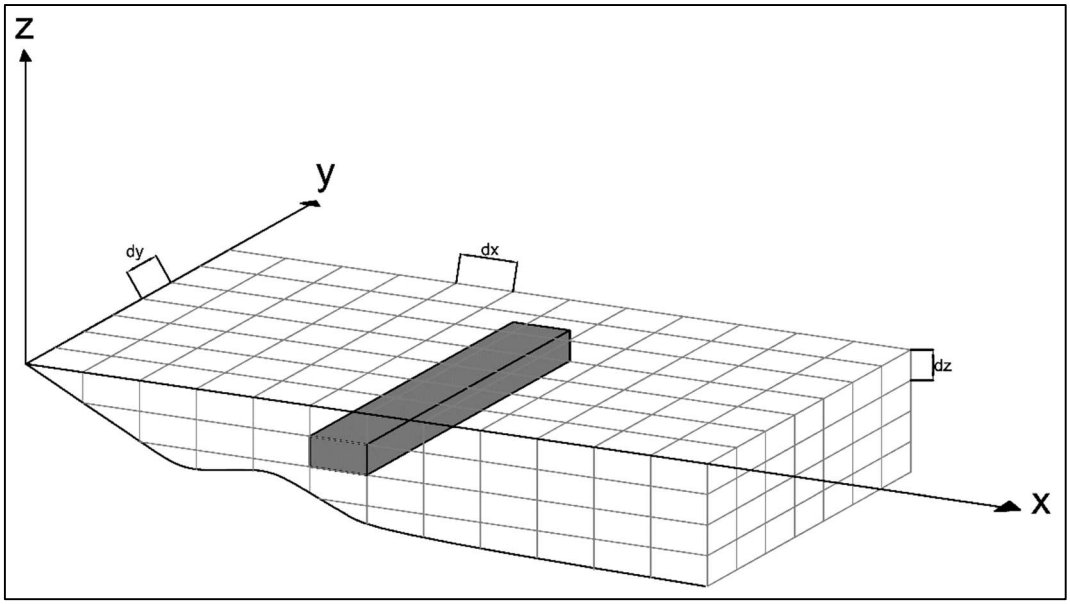


Figure 2.4 2-DV modeling

Example of 2-DH models are as follows; Militello et al. (2004) and Buttolph et al. (2006) developed M2D model (later called as CMS-M2D) which is a 2-DH model solves nearshore currents including sediment transport rates, and it has hard-bottom and avalanching modules. The model can be coupled with STWAVE or WABED for wave forcing. Bruneau et al. (2007) developed a 2-DH model coupled with SWAN with model MARS (Perenne, 2005) and a sediment transport model based on MORPHODYN (Saint-Cast, 2002). Roelvink et al. (2010) developed a 2-DH model called XBEACH to simulate morphological changes in the surf and swash zone during storms and hurricanes (Baykal, 2012).

### 2.1.3 One-Line Theory of Shoreline Change

The fundamental presumption of the one-line theory of shoreline change is that the beach profile moves parallel to a limiting depth of closure where no major sand moves beyond this point. Assumption of beach profile movement parallel to itself, shoreline change becomes related with changes and imbalances in the longshore sediment transport. Cross-shore sediment transport is assumed to cancel itself in the long-term. With this presumption, it is possible to mathematically model long-term shoreline changes using conservation of mass and a sediment transport formula (Dabees, 2000). The illustration of conservation of mass over the shoreline is schematized in Figure 2.5.

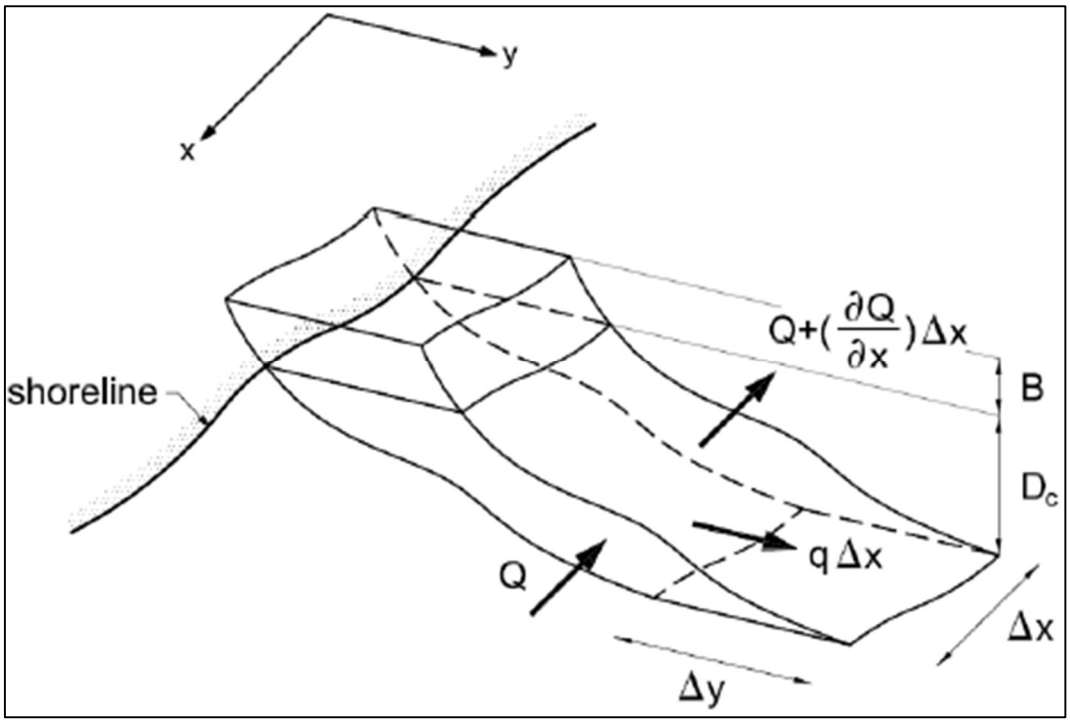


Figure 2.5 Schematization of conservation of mass for a beach system (adopted from Baykal, 2006)

Conservation of sand mass on an infinitesimal element (Δx) on the shoreline system can be expressed in Equation 2.1,

$$\frac{\partial y}{\partial t} = -\frac{1}{d_p}\left(\frac{\partial Q}{\partial x} \pm q_Y\right) \tag{2.1}$$

where $y$ is the location of the shoreline position, $t$ is time, $d_p$ is the profile depth which is equivalent to the summation of closure depth and berm height, $Q$ is the bulk sediment transport, $x$ is the longshore position and $q_Y$ represents sand sources or sinks along the shoreline (e. g. river discharges, beach nourishment, net cross-shore sediment transport). Representation of sediment transport can be done mathematically. There are some common bulk sediment transport formulas that represent the movement of sand caused by incident waves. Inman and Bagnold (1963), CERC (SPM, 1984) and Kamphuis (1993) formulas are the most commonly used formulas for longshore sediment transport; formulas are given in Equation 2.2, Equation 2.3, and Equation 2.4, respectively.

$$Q = \frac{K_b}{(\rho_s - \rho)g(1-p)} C_{gb} E_b cos\theta_b \left(\frac{V_l}{u_0}\right) \quad (2.2)$$

In Equation 2.2, $Q$ is bulk longshore sediment transport rate in volume per unit time, $K_b$ is a dimensionless constant which is given as 0.25 based on field data collected at different beach locations in the United States and Japan (Komar, 1998), $\rho_s$ is the density of sand, $\rho$ is the density of water, $g$ is gravitational acceleration, $p$ is the porosity index, $C_{gb}$ is the wave group velocity at breaking, $E_b$ is the breaking wave energy, $\theta_b$ is the wave angle at breaking, $V_l$ is the longshore current velocity (in practice measured at the middle of surf zone location) and $u_0$ is the maximum horizontal bottom orbital velocity.

$$Q = \frac{\rho K \sqrt{g/\gamma_b}}{16(\rho_s - \rho)(1-p)} H_{sb}^{2.5} sin(2\theta_b) \quad (2.3)$$

In Equation 2.3, $K$ is an empirical coefficient, SPM recommends a value of 0.39. Schoonees and Theron (1993, 1996) recommends a value of 0.20. $\gamma_b$ is the breaker index and $H_{sb}$ is the breaking wave height of significant waves.

$$Q_{im} = 2.27 H_{sb}^2 T_p^{1.5} m_b^{0.75} D_{50}^{-0.25} sin^{0.6}(2\theta_b) \quad (2.4)$$

In Equation 2.4, $Q_{im}$ is bulk longshore sediment transport rate in volume per unit time of immersed mass, $T_p$ is the peak wave period, $m_b$ is the beach slope near the breaking, $D_{50}$ is the median grain size. The immersed weight is related to the volumetric rate as in Equation 2.5.

$$Q_{im} = (\rho_s - \rho)(1-p)Q \quad (2.5)$$

Over time, shoreline conditions change. Therefore, sediment transport conditions change as well. Angle term in Equations 2.2, 2.3 and 2.4, should adapt to changed shoreline. Hence, the use of an effective breaking angle instead of a breaking angle is introduced. Figure 2.6 shows effective breaking angle, and Equation 2.6 gives effective breaking angle formula.

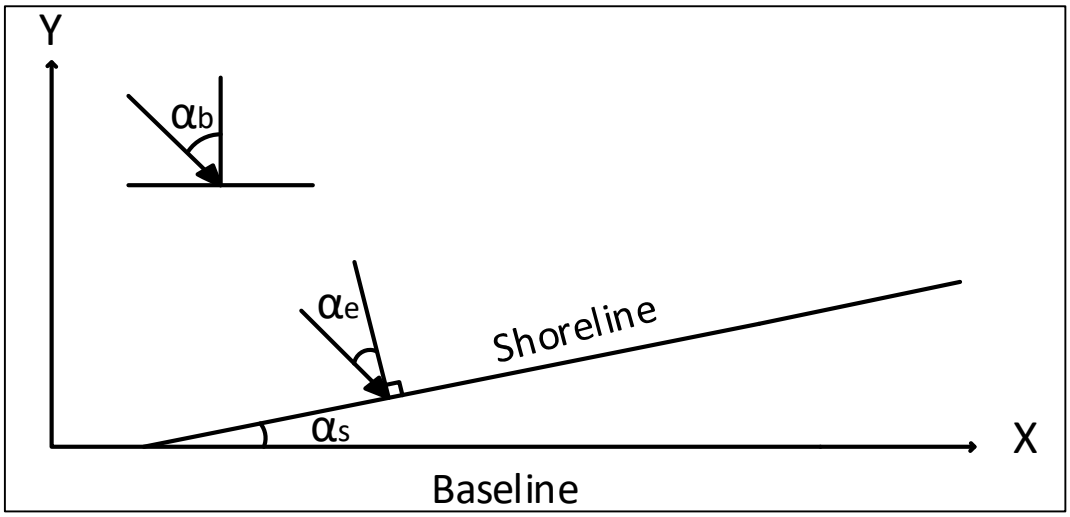


Figure 2.6 Illustration of effective breaking angle

$$\alpha_e = \alpha_b - \alpha_s \tag{2.6}$$

In Equation 2.6, $\alpha_e$ is the effective breaking angle, $\alpha_b$ is the breaking wave angle with respect to Y axis and $\alpha_s$ is the orientation of the shoreline and represented as $\tan^{-1}(\partial y/\partial x)$. However, after the assumption that $\alpha_s$ is very small such that it becomes $\alpha_s = (\partial y/\partial x)$. Equation 2.6 can be written as Equation 2.7;

$$\alpha_e = \alpha_b - \frac{\partial y}{\partial x} \tag{2.7}$$

# CHAPTER 3

# MODEL DEVELOPMENT

In this chapter, the theoretical and numerical structure of the quasi 2-dimensional horizontal model will be explained and presented in detail.

## 3.1 Model Structure

The model consists of three modules. These are listed as follows;

- Nearshore Spectral Wave Model (NSW; Baykal, 2012)
- Sediment Transport Distributions (STD)
- Morphology Evolution (MEV)

MATLAB environment is the platform that is used during the development of the Q-2DH Model. It is a 2-DH model to evaluate shoreline change under constant wave forcing in the vicinity of coastal defense structures. It works on a rectangular grid. Finite difference schematization is followed in solving the governing equations. The Q-2DH model takes bottom topography, structural information, rectangular computational cell intervals (dx, dy), average bottom slope in the surf zone, wave parameters (significant wave height, significant wave period, mean approach angle, etc.), hydrodynamic (updating the wave field) and morphodynamic (updating the sea bed elevations) time steps, material properties (median particle size, the density of material and water, etc.), sediment transport and morphology options. The model's structure is illustrated in Figure 3.1.

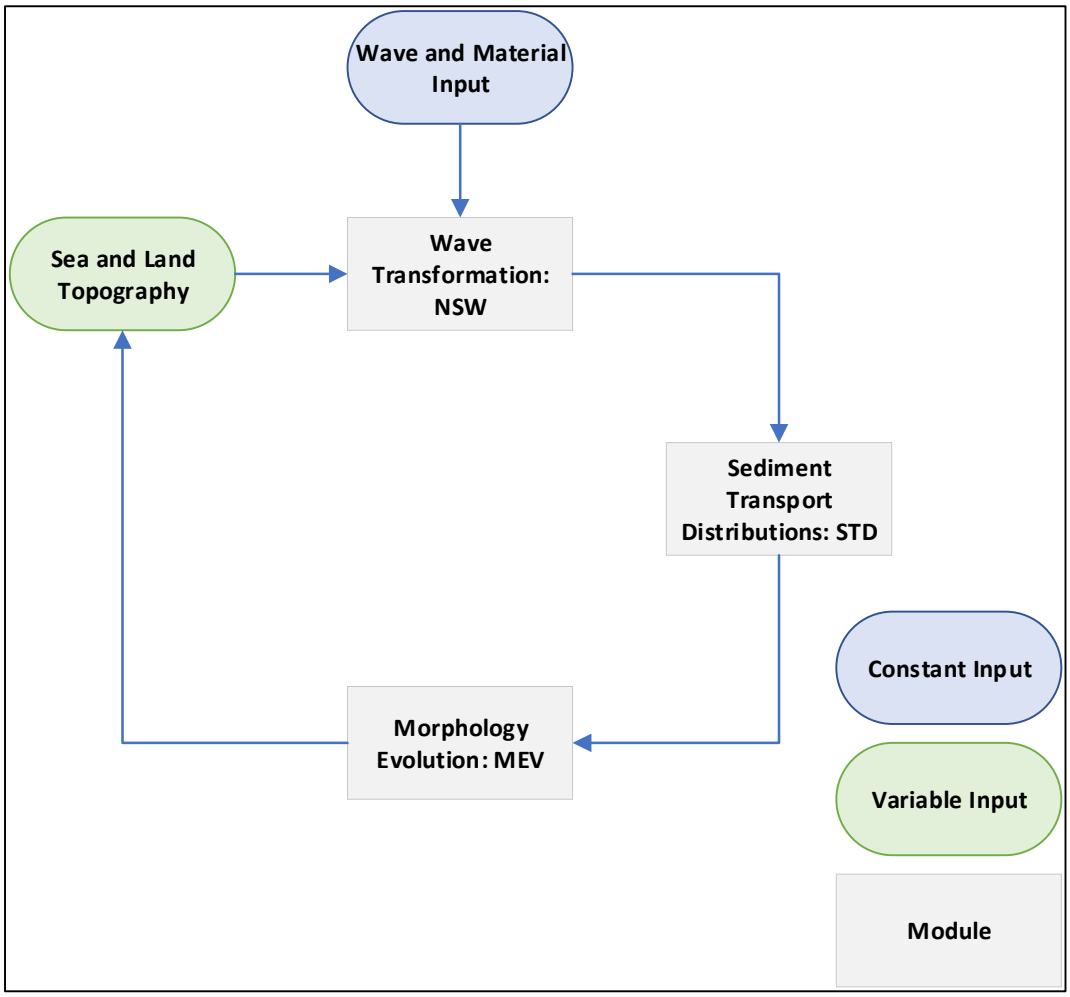


Figure 3.1 Q-2DH model flowchart

Figure 3.1 shows that there are basically two main inputs for the model. The first one is the sea and land topography. This is a variable input, structural information and initial bathymetry conditions should be provided to the model. The model solves module parts and updates bed levels accordingly, and in the next time step, it uses the sea and land topography as the new input. The second one is the wave and material input. This type of input is a constant input, which does not change throughout the model runtime.

The first step (NSW) is the computation of nearshore significant wave height and/or root mean square wave heights and mean wave directions. Computed parameters are taken as constant for a given hydrodynamic time step, since it is a phase-averaged

wave transformation model. Until the bathymetry change affects the wave transformation, parameters are constant. Hydrodynamic time-step is defined constant by the user.

In the second step (STD), bulk longshore sediment transport rate per unit time is computed using extended CERC formula (Komar, 1998), this formula is then distributed over the surf zone. Other than longshore sediment transport, three more different transport mechanisms are introduced in this step. To maintain the equilibrium beach profile, a cross-shore diffusivity term is introduced. An alongshore diffusivity term is introduced to suppress the growth of small-scale noise. A shore relaxation transport term to consider the swash zone profile maintains its equilibrium profile throughout the model.

In the final step (MEV), computed sediment transport quantities are used in a continuity equation to update the bed profile. This updated bed profile is used in the preceding time-step until the model end time.

## 3.2 Model Assumptions and Limitations

Q-2DH Model is a hybrid model incorporating a spectral wave model with a One-Line Model in a two-dimensional environment. Each module has its assumptions and limitations throughout this process to solve numerical processes. In this chapter, these assumptions and limitations are briefly discussed.

### 3.2.1 Wave Transformation (NSW)

Nearshore processes are computed as phase-averaged, which indicates that wave parameters are constant during a wave period or time series of irregular wave trains. This means that the variations during one wave period or time series of irregular wave trains are disregarded. This results in a single wave forcing throughout the model time, whether it is one hour or one year, and even more (Baykal, 2012).

In the offshore wave boundary, wave conditions are assumed to be constant (Smith et al., 2001). The frequency domain's energy distribution is not considered in computations, and multi-directions are represented with a single peak/significant wave period to shorten the computational time. Thus, wave-wave interactions are not considered. Directional waves' domain is defined from $-\pi/2$ to $\pi/2$ with a directional spreading parameter suggested by Mitsuyasu et al. (1975). The wave transformation module considers linear wave shoaling and refraction, depth-induced random wave breaking, and wave diffraction processes. Random waves in the surf zone are assumed to fit a Rayleigh distribution. Waves located greater in the distribution than the limited wave height ratio are assumed to be broken (Baldock et al., 1998; Janssen & Battjes, 2007).

### 3.2.2 Sediment Transport Distributions (STD)

Sediment transport magnitudes are computed using the bulk sediment transport formula. This formula uses phase-averaged wave parameters. Bulk sediment quantities are distributed over the surf zone. In this approach, high angled wave conditions cause relatively high fluctuations in the sediment transport field. Similarly, a great number of bathymetry changes in adjacent computational cells may cause relatively high incoming relative wave angles. This may cause instabilities in the sediment model. Sediment transport computations are applicable for non-cohesive sediments.

### 3.2.3 Morphology Evolution (MEV)

Morphology evolution is governed by a continuity equation that considers alongshore and cross-shore sediment transports. These mechanisms are contributing to bed update in the desired time interval.

In the model, there may be two boundary conditions in the bed; firstly, there is an erodible bed and secondly a non-erodible bed. Both erodible and non-erodible beds

can be introduced to the model. The erodible bed is considered as a non-cohesive sediment bed, and it can accumulate or erode without any limitation. The non-erodible bed is bathymetry, which is a structural element or drypoint (no sediment activity) area. In non-erodible areas, sediment transport is considered as zero.

All these modules successively work until the end of the simulation. The finite difference scheme is applied to morphology evolution both in temporal and spatial space.

## 3.3 Grid System

In the Q-2DH model, the rectangular uniform grid system is used. There are mainly five different discretized spaces in the model. The first four discretized spaces belong to the spatial domain. And the last one is discretized in the directional domain. Initially, there are points that are defined in the model as bathymetry grids. This system is the model's primary (original) grid system, and morphological changes and wave parameters are computed in these points. Other grid systems and points are either supplementary grids defined to compute the sediment flow rates to the original grid points or to compute the bathymetry's topographical orientation. Secondly, there is the staggered grid system. The staggered grid system is used in NSW to solve the two-time step Lax-Wendroff finite difference (1960) method. Also, the staggered grid system is used in the computation of topography orientation. The staggered grid is linearly interpolated from the primary (bathymetry) grid, and two vectors are defined diagonally. The two diagonal vectors result in an equivalent plane which reflects topography's orientation in the original grid point. The components of the normal vector to this plane give the angular orientation of the grid point, and it is used as the orientation of the point in further computations. The methodology is illustrated in Figure 3.2.

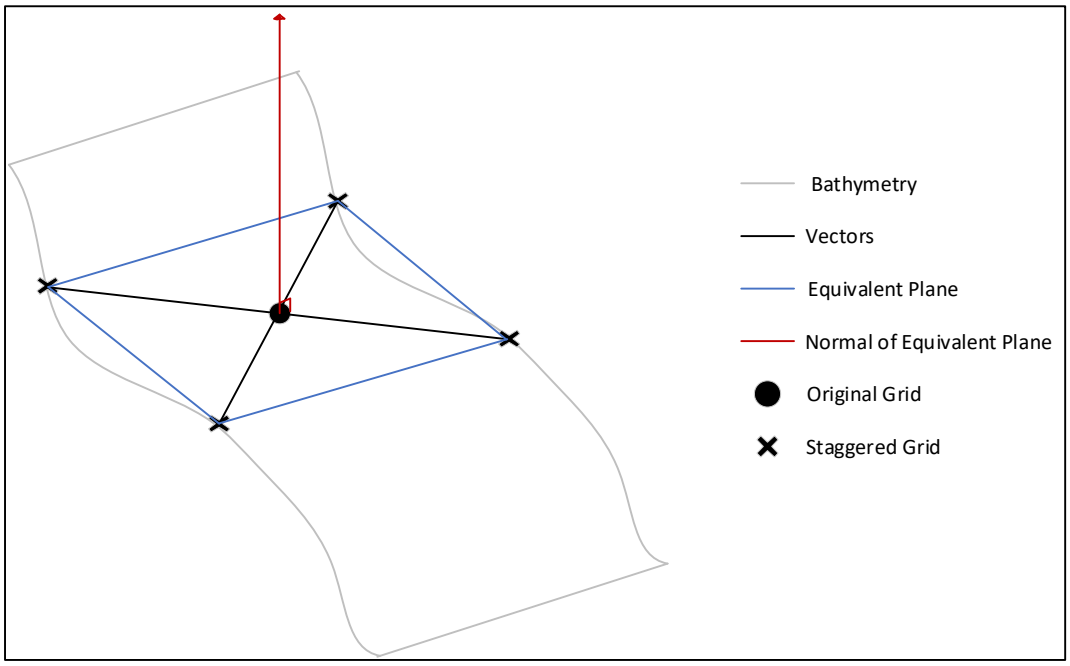


Figure 3.2 Methodology on the orientation of vectors

Thirdly, there is the grid for face centers in the x-direction is available. This grid is used in the computation of sediment transport in the x-direction. Computed sediment transport values at original grid points are interpolated to this coordinate system, and influxes and outfluxes of the original grid points are determined. Similarly, there is the grid for face centers in the y-direction, and it is used in the computation of sediment transport in the y-direction. The computational grids are illustrated in Figure 3.3.

Finally, there is the directional domain. The directional domain of the spectral density is discretized into finite angular grids. Discretization of the directional domain is further explained in Chapter 3.4.

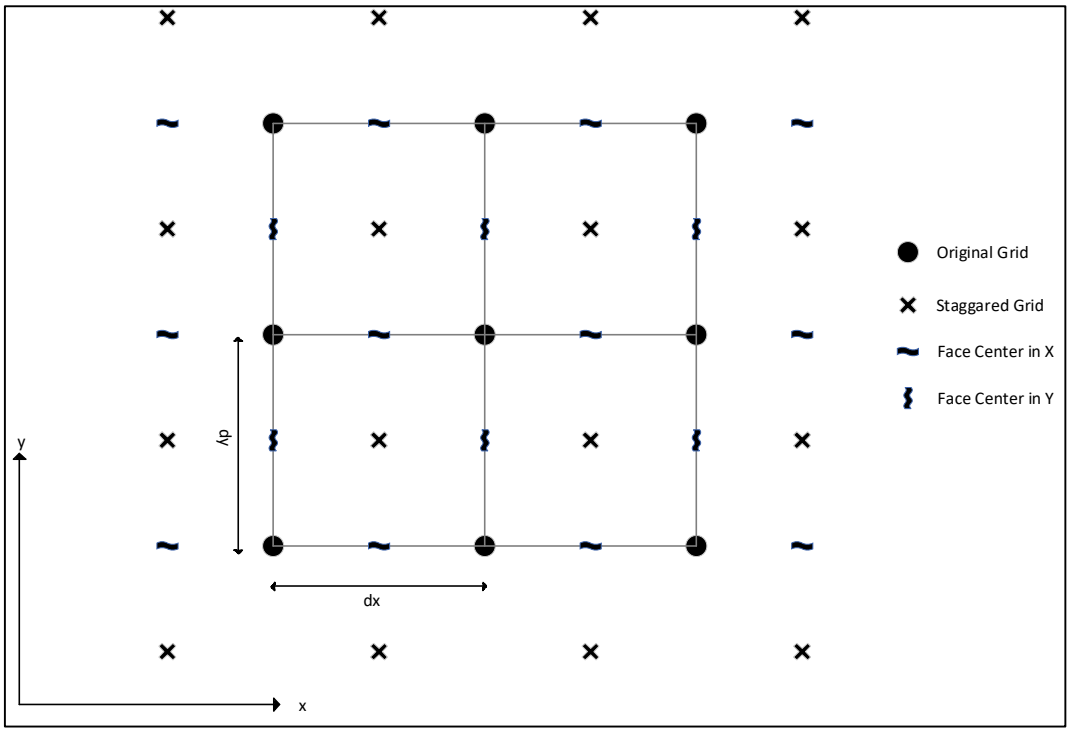


Figure 3.3 Coordinate system in spatial space

## 3.4 Nearshore Spectral Wave Model (NSW)

NSW is a spectral wave model (Baykal, 2012; Baykal, 2014; Baykal et al. 2014). NSW solves the energy balance equation in the computational domain. The energy balance equation with diffraction and breaking term is given in Equation 3.1.

$$\frac{\partial(\vartheta_x S)}{\partial x} + \frac{\partial(\vartheta_y S)}{\partial y} + \frac{\partial(\vartheta_\theta S)}{\partial \theta} = D_b - D_d \tag{3.1}$$

In Equation 3.1, $\vartheta_x$, $\vartheta_y$ and $\vartheta_\theta$ represents propagation velocities in x, y, and directional space, respectively. $S$ is directional wave spectral density ($m^2$/Hz/rad) that changes in the aforementioned three dimensions. $D_b$ is the dissipation rate due to random wave breaking and $D_d$ is the diffraction term introduced by Mase (2001).

For computational ease, it represents directional spectra as peak wave period, and it does not solve waves in the frequency domain. Therefore, wave-wave interactions are neglected in the NSW module.

NSW and the following modules are solved numerically utilized finite difference schemes in order to estimate nearshore wave parameters, sediment transport mechanisms, and morphology evolution. Arbitrary bathymetry is given to the model in a cartesian coordinate system where x-direction is the cross-shore direction, and y-direction is the alongshore direction. Directional space is also discretized and solved in computational cells. Propagation velocities' and directional domain's discretization is represented in Figure 3.4.

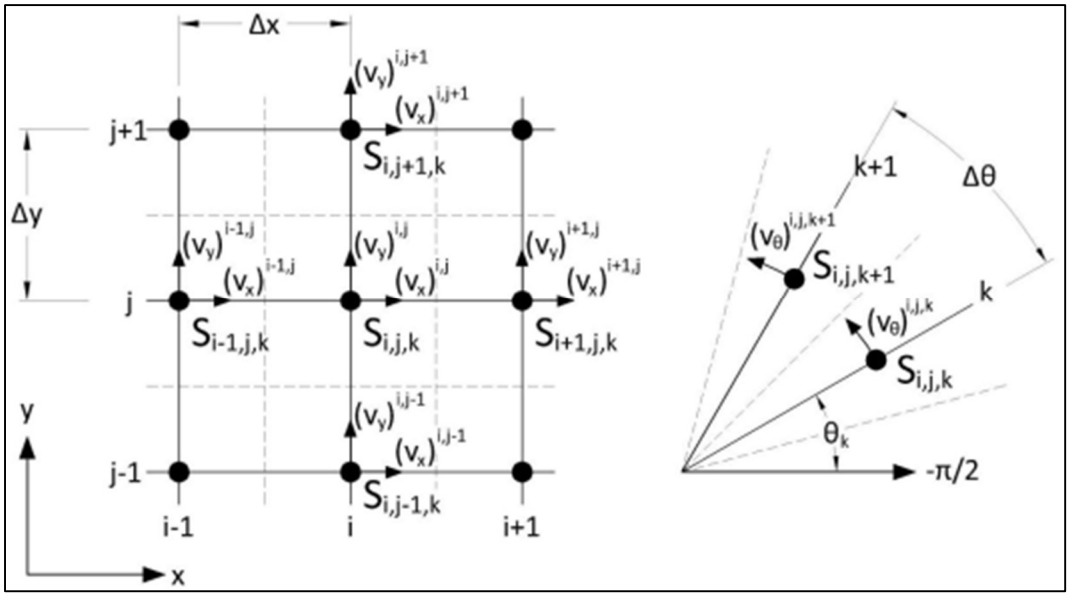


Figure 3.4 The grid system of the model (adopted from Baykal, 2012)

## 3.5 Sediment Transport Distributions (STD)

STD module is the Q-2DH model's sediment transport module. This module represents several physical mechanisms of sediment transport that occurs in the surf zone. It includes bulk longshore sediment transport and the distribution which distributes this bulk sediment transport from shoreline to closure depth and make it sediment transport flux. Cross-shore sediment transport allows beach profile to maintain its equilibrium beach profile on a relatively long-time scale. An alongshore diffusivity transport is introduced to suppress the growth of small-scale noise in the module. Also, a shore relaxation boundary condition is defined to consider the

transport in the swash zone. This term helps the shoreline profile to evolve (i.e., only at the shoreline) to the equilibrium profile.

### 3.5.1 Longshore Sediment Transport

Longshore sediment transport can be defined as the total evolution of shoreline and beach profile due to parallel movement of sediment to the shore by joint activity of tides, wind, and shore parallel currents produced by them (Seymour, 2005). Longshore sediment transport is the main transport mechanism in the Q-2DH model. The model's mechanism depends on interruptions or changes in the longshore gradients through the shoreline. If a parallel straight shoreline without a structure or any sediment interrupting mechanism is introduced to the model and an equilibrium profile is given to the model, there is no expected change in the shoreline. For example, suppose an offshore breakwater is placed in a shoreline. In that case, the seaward side of the breakwater has lower wave heights, thus wave height gradients in the longshore sediment transport formula apply and cause changes in the shoreline and the bathymetry.

Longshore sediment transport is computed based on the extended CERC formula (Komar, 1998). The extended CERC formula includes the second term for the gradients in breaking wave height along the coast. It is introduced by Ozasa and Brampton (1980). Extended CERC formula can be found in Equation 3.2 below,

$$Q = \mu H_{rms,b}^{5/2}\left(\sin(2\beta_b) - \frac{2r}{m}\cos(\beta_b)\frac{\partial H_{rms,b}}{\partial y}\right) \tag{3.2}$$

where $Q$ is the bulk longshore sediment transport, $\mu$ is a constant which is proportional with the empirical parameter $K_1$ of original CERC formula (Equation 2.3). This parameter defines the magnitude of the transport, and the default value is equal to 0.2, which is equivalent to the default value of $K_1$ = 0.7·$H_{rms,b}$ is the root mean square breaking wave height, $\beta_b$ is the angle between breaking wave angle of the wave fronts and the coastline, the constant $r = K_2/K_1$, which is a constant determines the magnitude of the second term and its default value is 1, $m$ is the

average bottom slope of the surf-zone, and $y$ is the alongshore distance of the model area.

Extended CERC formula is chosen in computations due to its second term for wave height gradient. In other common formulas (Kamphuis (1991); Inman and Bagnold (1963)) wave height gradient is not available. Wave height gradient is important in the lee-side of the offshore breakwater. Without the second term, wave height changes in the lee-side of the offshore breakwater are not properly taken into consideration.

Instead of directly using Equation 3.2, it is modified for the Q-2DH model. Firstly, instead of using the angle between breaking wave angle and shoreline ($\beta_b$), the angle between local wave angle ($\theta$) and angle of local bottom orientation ($\alpha$), which is ($\beta$) is implemented. This methodology applies to all computational grids. Illustration of local bottom orientation, local incoming wave angle, and relative incoming angle is illustrated in Figure 3.5.

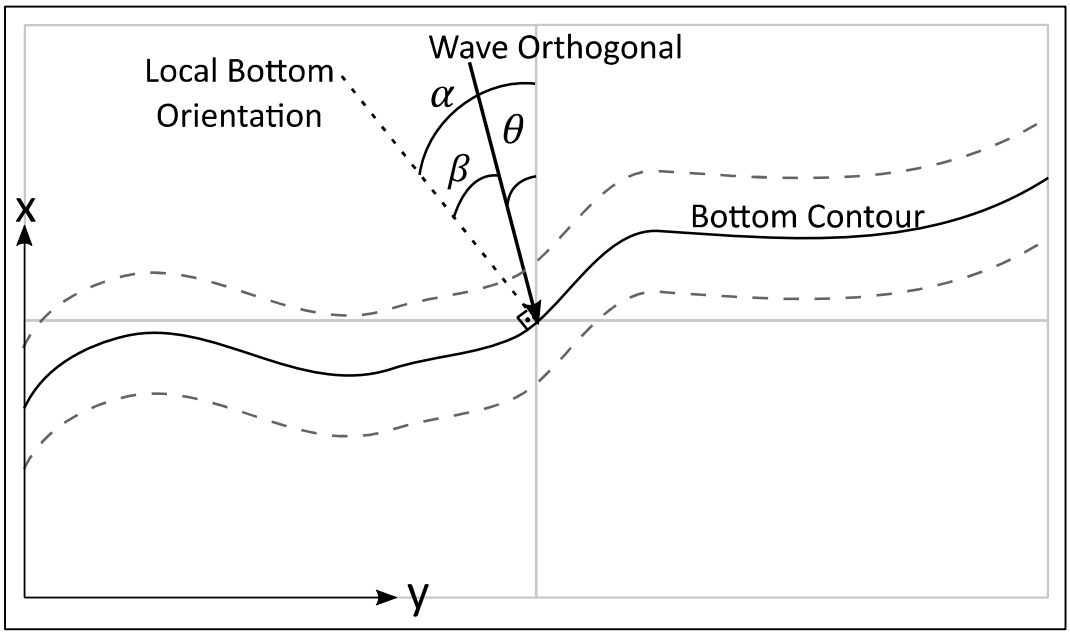


Figure 3.5 Angle between local wave angle and local bottom orientation

Secondly, instead of root mean square breaking wave height, local root mean square wave heights are used. Wave heights and wave angles are varying vastly behind the

structure. The use of local wave properties is more precisely reflect wave behavior around a coastal structure. Bulk longshore sediment transport is computed in the model area with Equation 3.3.

$$Q = \mu H_{rms,b}^{5/2}\left(\sin(2\beta) - \frac{2r}{m}\cos(\beta)\frac{\partial H_{rms}}{\partial y}\right) \quad (3.3)$$

Breaking wave height is found by a depth limiting approach in an equilibrium profile. Breaking wave height is the most offshore wave that meets $H_{rms}(x,y) \geq \gamma_b * d(x,y)$ criterion. When applying the breaking wave height criterion, a linear interpolation is carried out to find breaking wave height if the condition does not coincide with the grid point. $\gamma_b$ is the breaking wave index (the ratio of wave height to the water depth at breaking), and $d\,(x,y)$ is the water depth. $H_{rms}$ is the root mean square wave height, and it is calculated as CIRIA et al. (2007) approach and given in Equation 3.4,

$$H_{rms} = \left(0.6725 + 0.2025\left(\frac{H_s}{d}\right)\right)H_s \quad (3.4)$$

where, $H_s$ is the significant wave height transformed by NSW module, and $d$ is the local depth.

In the Q-2DH model, the breaking wave index can be determined in two ways. The former is entering breaking wave index manually, and the latter is Nairn's (1990) approach. In Nairn's (1990) approach, the breaking index depends on the deep-water root mean square wave height and its corresponding significant wave height. Nairn (1990) approach is given in Equation 3.5,

$$\gamma_b = 0.39 + 0.56 * \tanh\left(\frac{33H_{rms,0}}{1.56T_s^2}\right) \quad (3.5)$$

where, $H_{rms,0}$ is deep water root mean square wave height, and it is equal to deep water significant wave height divided by the square root of two ($H_{s,0}/\sqrt{2}$). $T_s$ is significant wave period. The bulk longshore sediment transport formula is the bulk volume of sediment transported in the surf zone integrated from shoreline to closure depth.

The bulk longshore sediment transport formula is not directly used. The bulk longshore sediment transport formula calculates the sediment transport magnitude in whole profile integrated from the shoreline to the closure depth. This procedure cause problems around the offshore breakwater. Therefore, bulk longshore sediment transport is computed and it is distributed with a distribution depends on wave height and local bathymetry. This allows computations in each grid and better representation due to changing wave height and bathymetries. The bulk longshore sediment transport magnitude is distributed over the surf zone to compute longshore sediment transport flux in each and every computation grid point. Longshore sediment transport flux is computed as in Equation 3.6, Equation 3.7, and Equation 3.8 as follows,

$$q_{lst} = Q\overline{C_3} \tag{3.6}$$

$$q_{lst,x} = -q_{lst} * sin\,(\alpha) \tag{3.7}$$

$$q_{lst,y} = q_{lst} * \cos\,(\alpha) \tag{3.8}$$

with $\overline{C_3}$ is the normalized distribution over the surf-zone, and $\alpha$ is the local bathymetric orientation.

In the Q-2DH model, a distribution is accepted to distribute bulk longshore sediment transport over the surf-zone. The distribution is also normalized to equate the integration of this distribution to one over the surf-zone. Distribution is given in Equation 3.9, Equation 3.10, and Equation 3.11,

$$C_3 = (C_1)^4 * C_2 \tag{3.9}$$

$$C_1 = \frac{d_c - d}{d_c} \tag{3.10}$$

$$C_2 = \left(\frac{H_{rms}}{H_{rms,b}}\right)^{5/2} \tag{3.11}$$

where, $d_c$ is the depth of closure, $d$ is local depth, $H_{rms}$ is the root mean square wave height and $H_{rms,b}$ is the root mean square wave height of breaking wave front.

Depth of closure is defined as the most seaward depth of which there is no significant change in bottom contours and no significant net sediment exchange through onshore and offshore directions. Depth of closure is computed with Hallermeier (1978) approach. Hallermeier (1978) relates closure depth with the significant wave height, which will exceed 12 hours per year, and its corresponding significant wave period and gravitational acceleration. This relationship is given in Equation 3.12,

$$d_c = 2.28 * H_{s,12} - 68.5\left(\frac{H_{s,12}^2}{gT_s^2}\right) \tag{3.12}$$

where, $H_{s,12}$ is the effective significant wave height just seaward of the breaker zone will exceed 12 hours per year. $T_s$ is the significant wave period associated with $H_{s,12}$. And $g$ is the gravitational acceleration.

Komar (1998) developed an expression widely used to distribute bulk longshore sediment transport expressions over the surf-zone. It is qualitatively based on the distribution of longshore current in the cross-shore direction. Komar's normalized shape expression is given in Equation 3.13 and Equation 3.14,

$$f(x) = \frac{4}{\sqrt{\pi}L^3}x^2e^{-(x/L)^2} \tag{3.13}$$

$$L = 0.7X_b \tag{3.14}$$

with, $X_b$ is the width of surf-zone, $x$ is the coordinate in the x-direction. Komar's distribution depends on coordinate in x-direction and the surf-zone width. Hence, only shoreline position controls the distribution. Komar's distribution is not suitable to use in the vicinity of an offshore breakwater. Therefore, the proposed distribution is followed in longshore sediment flux computations.

The proposed distribution is compared with Komar's distribution in a straight parallel beach for bottom slopes of 1/10, 1/20, 1/30, and 1/50 in Figure 3.6-Figure 3.9. In figures, axes are given nondimensional as $x/L_p$, $d/L_p$, $H/H_{s,0}$ and $f(x)$. $x/L_p$ is the distance from shoreline divided by the peak wave length, $d/L_p$ is the depth divided by the peak wave length, $H/H_{s,0}$ is the significant wave height divided by the deep-water significant wave height, and $f(x)$ is the density function.

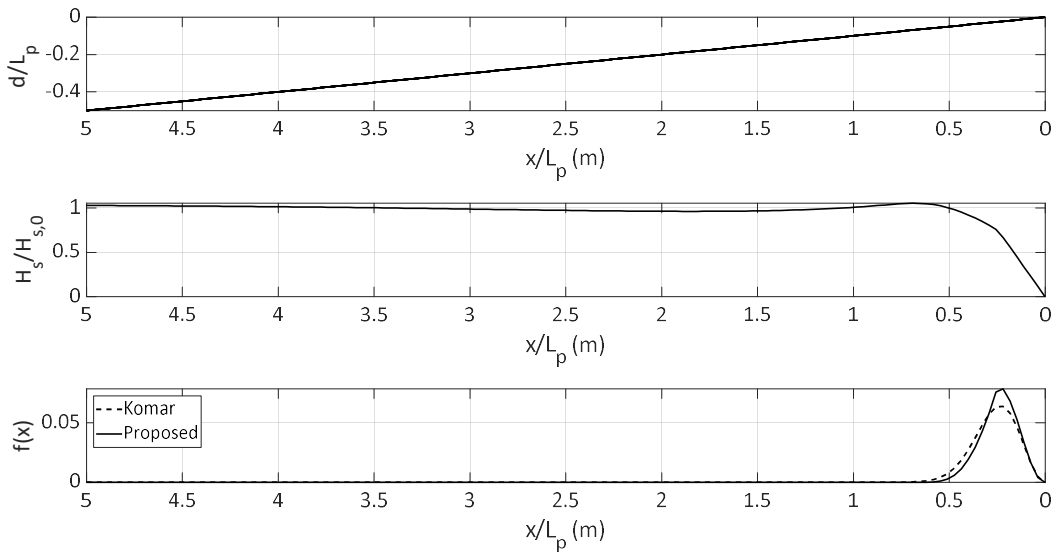


Figure 3.6 Comparison of proposed and Komar (1998) distribution (for 1/10 slope)

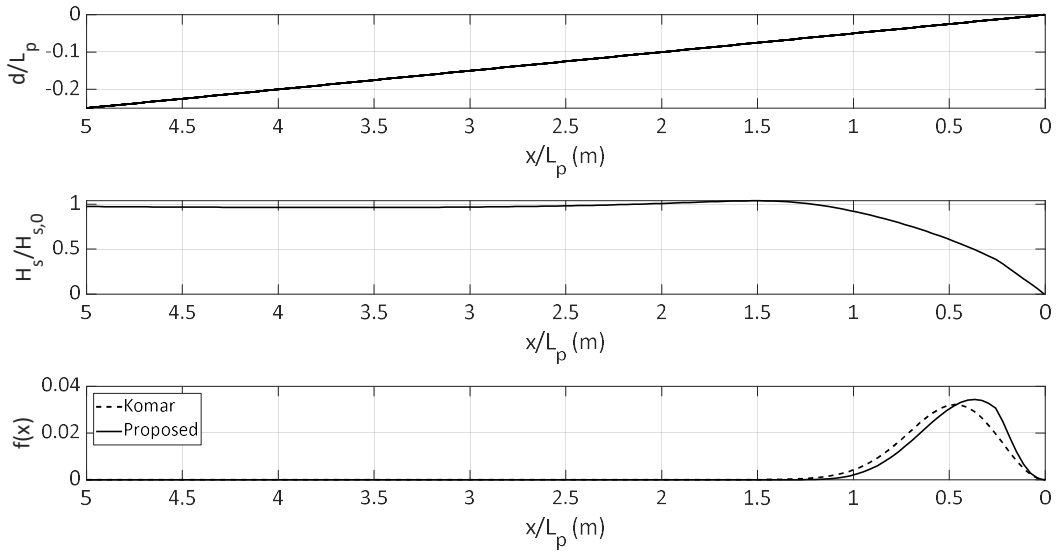


Figure 3.7 Comparison of proposed and Komar (1998) distribution (for 1/20 slope)

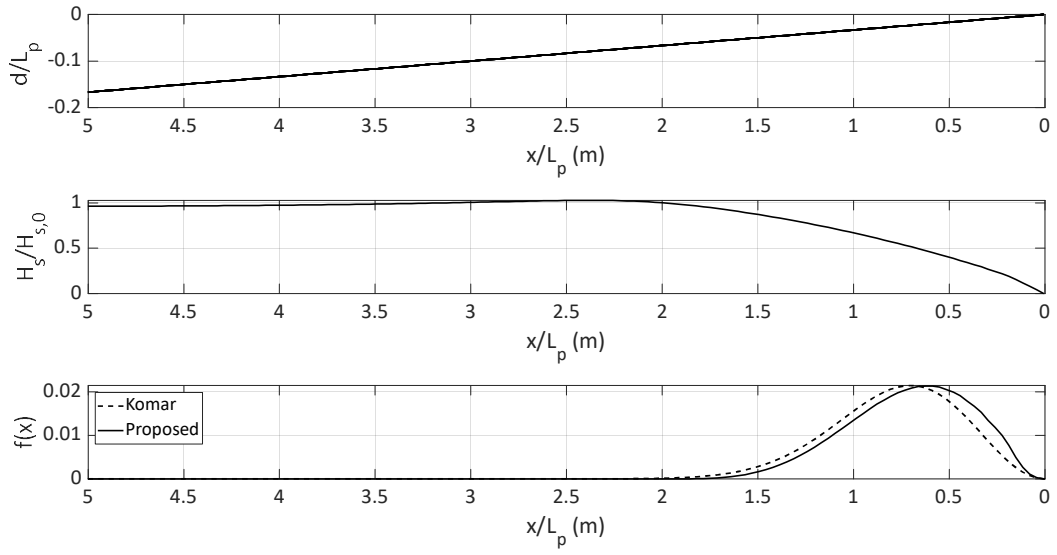


Figure 3.8 Comparison of proposed and Komar (1998) distribution (for 1/30 slope)

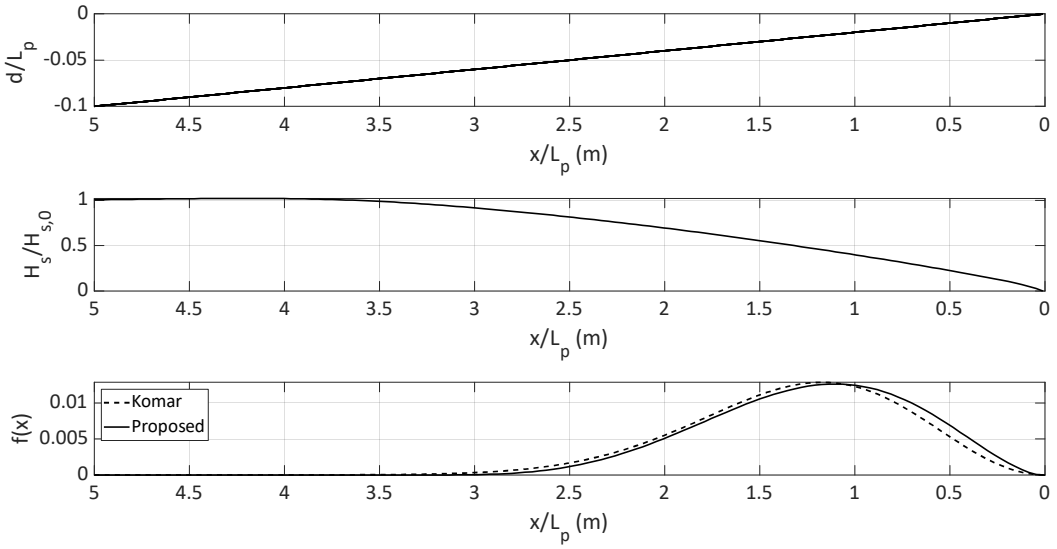


Figure 3.9 Comparison of proposed and Komar (1998) distribution (for 1/50 slope)

In between Figure 3.6-Figure 3.9 proposed distribution and Komar (1998) distribution is compared. For the bottom slope of 1/10 and 1/20, quantitatively, the proposed distribution is slightly higher than Komar's distribution, and qualitatively both distributions are similar. For the bottom slope of 1/30 and 1/50, both distributions are very similar qualitatively and quantitatively.

### 3.5.2 Cross-Shore Sediment Transport

Cross-shore sediment transport can be defined as the total particle movement in the beach and the nearshore region perpendicular to the shore. It occurs as the combined action of tides, waves, winds, and shore perpendicular currents. This process occurs in two ways, the movement of suspended particles and the movement of particles near the bed layer. These can be addressed as suspended sediment transport and bedload sediment transport, respectively (Seymour, 2005). These processes are highly complex and vary in time. Studies suggest that cross-shore transport of beaches is not effective in the long-term. In winter seasons where wave heights are greater than summer seasons, waves transport sediments from nearshore to offshore, causing eroded beaches in winter seasons. In contrast, in summer seasons where waves are lower than winter seasons, waves carry sediment from offshore to onshore to restore the beach back to its summer state. Figure 3.10 illustrates these phenomena and the main components of a beach profile.

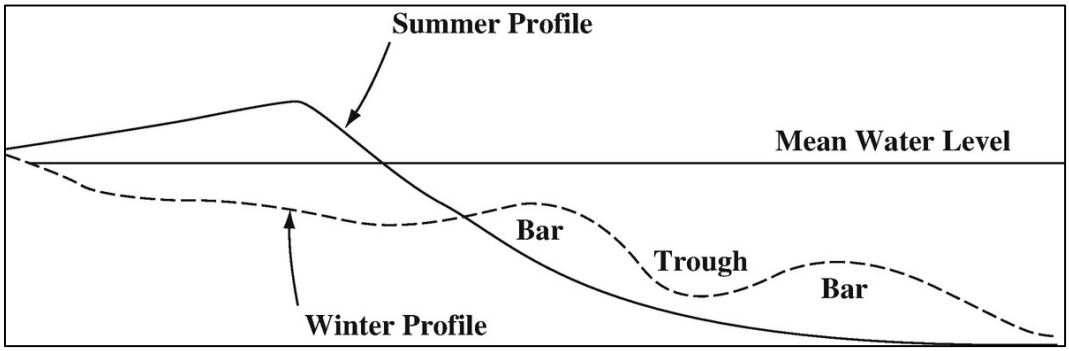


Figure 3.10 Summer and winter beach profiles (adopted from Seymour, 2005)

In the Q-2DH model, cross-shore sediment transport is not introduced as a process-based physical phenomenon. Thus, analysis of winter and summer profiles in the Q-2DH model is not possible. It does not solve time and wave height dependent transport mechanisms. Instead, a parametrization of the cross-shore sediment transport is introduced to change the beach profile to its so-called equilibrium profile on a relatively long timescale as proposed in van den Berg et al. (2011).

Parametrization of cross-shore sediment transport is given in Equation 3.15 below,

$$q_{crs} = -\gamma_x \left( \frac{\partial (d - d_e)}{\partial x} \right) \tag{3.15}$$

where $d$ is the local bathymetry, $d_e$ is the assumed equilibrium profile, $\gamma_x$ is cross-shore diffusivity constant, and it is given in Equation 3.16.

$$\gamma_x = \varepsilon_x \gamma_b^{-1/6} g^{1/2} H_{rms,b}^{11/6} X_b^{-1/3} \varphi(x) \tag{3.16}$$

$\varepsilon_x$ is a non-dimensional constant, $\gamma_b$ is breaking index, $g$ is the gravitational acceleration, $H_{rms,b}$ is the root mean square wave height of the breaking front, $X_b$ is the width of the surf zone and $\varphi(x)$ is the shape function given in Equation 3.17, $X_b$ is computed as the methodology discussed in $H_{rms,b}$ in Equation 3.3,

$$\varphi(x) = \frac{1 + b + \tanh\left(\frac{X_l - x}{L_d}\right)}{1 + b + \tanh\left(X_l / L_d\right)} \tag{3.17}$$

where shape function ($\varphi(x)$) has its maximum value in the surf zone, and it decays to a residual value ($b$) close to zero. $b$ is a constant and controls residual magnitude beyond the closure depth, $X_l = 2X_b$, x is the distance to the shoreline in the x-direction $L_d$ controls the length scale decay until $X_l$.

Equation 3.15 implies that if initial bathymetry is the same as the introduced equilibrium profile, then there would be no transport in the cross-shore direction at the beginning of the simulation. Suppose a different bathymetry rather than the equilibrium profile is introduced initially. In that case, the Q-2DH model computes cross-shore magnitudes different than zero such that the initial bathymetry is to be transformed to the introduced equilibrium profile.

### 3.5.3 Alongshore Diffusivity

The present sediment transport module of the Q-2DH model is a point-based module. Equations and mathematical expressions are explicitly solved in grid points. This means that every grid point has its own attributes and independent of other grids

(except the NSW module). This independence may cause some computational cells to change more than it is expected. Advancement in topographical conditions will result in small scale noise to grow. At the initial stages of the model, these small-scaled noises may not affect the results much, yet with time these small-scale noises will vastly change results or even may lead to instabilities.

Alongshore diffusivity transport is introduced to suppress the small-scale noise in the model. This concept is introduced by van den Berg et al. (2011). This transport mechanism solely depends on the local bottom topography orientation and change of depths in x and y directions. Equation 3.18 gives alongshore diffusivity term,

$$q_d = -\gamma_y \left( \frac{\partial d}{\partial x} sin(\alpha) + \frac{\partial d}{\partial y} cos(\alpha) \right) \tag{3.18}$$

where, $\gamma_y$ is the alongshore diffusivity term. Alongshore diffusivity term is the same as the cross-shore diffusivity term. Alongshore diffusivity constant can be computed as in Equation 3.16; only the difference is $\varepsilon_x$ is used as $\varepsilon_y$. $d$ is local bathymetry in meters, and $\alpha$ is local orientation.

### 3.5.4 Swash Zone Dynamics

The Swash zone is the boundary area where the sea meets the land. In theory, this boundary area can be defined as the area which is starting from the run-down limit in the sea and ending with the run-up limit to the land. However, there are various definitions of swash zone in literature. This area is the most widely used area by beach users. Moreover, due to its visibility, the swash zone is the area in which most of the beach erosion and climate change is associated with (Nielsen, 1999). An illustration of the swash zone can be found in Figure 3.11.

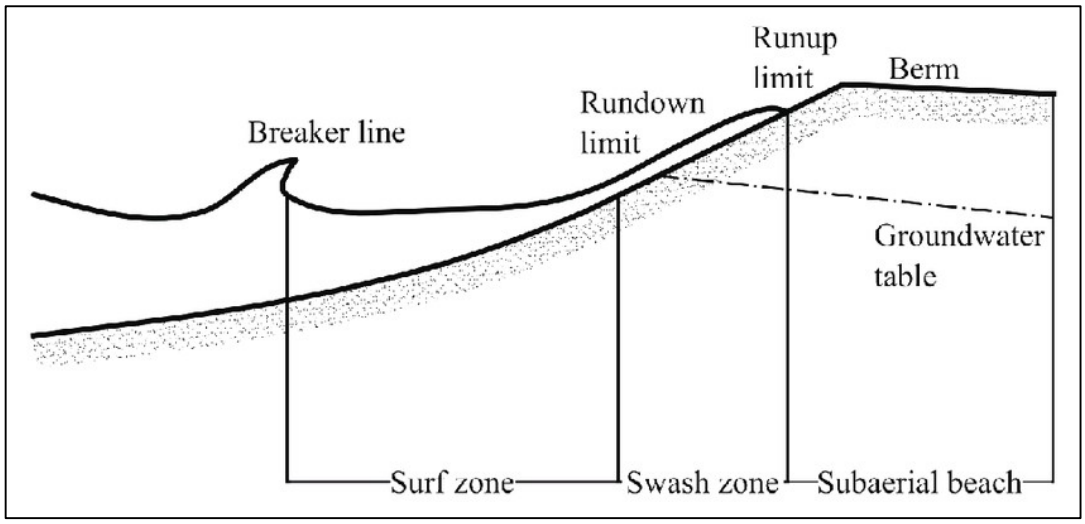


Figure 3.11 Illustration of swash zone (adopted from Lanckriet, 2014)

Swash zone dynamics are highly complex and arduous to model. Modeling swash zone strictly is out of the scope of this model. This model aims to solve coastal sedimentation fast. Therefore, two methodologies are followed to represent swash zone dynamics in the model. Firstly, a wave-induced set-up is computed and introduced to the whole model area. This inundates the swash zone; hence transport mechanisms become available in this region. Secondly, shore relaxation boundary condition is assumed at the shoreline. This assumption allows the model to transport sediment through wet to dry or vice versa regions.

As waves progress through the shoreline, they carry not only energy but also momentum through the shoreline. This momentum transport is called radiation stress. This momentum transport cause stress variations in the shoreline. These stress variations act as forces through the water column. As a result, it raises or tilts the water column. This rise of the mean water level near the shoreline is called wave-induced set-up. Goda (2008) studied bottom slopes from 1/10 to 1/100, wave steepness' from 0.005 to 0.08, and incidence wave angles from 0° to 70° and derived a wave set-up relation which is applicable in most cases. This relation is given for perpendicular incident waves in Equation 3.19 and for oblique waves in Equation 3.20,

$$\zeta_{\theta_0=0}/H_{s,0} = (0.0063 + 0.768m) - (0.0083 + 0.011m)\left(ln\, H_{s,0}/L_0\right) + (0.00372 + 0.0148m)\left[ln\, H_{s,0}/L_0\right]^2 \quad (3.19)$$

$$\zeta = \zeta_{\theta_0=0}(cos\theta_0)^{0.545+0.038lnH_{s,0}/L_0} \quad (3.20)$$

where, $\zeta_{\theta_0=0}$ is wave set-up for perpendicular incident waves, $H_{s,0}$ is deep water significant wave height, $m$ is the average bottom slope of the surf zone, $L_0$ is deep water wavelength, $\zeta$ is wave set-up for oblique incident wave and $\theta_0$ is the offshore incoming wave angle.

At the shoreline, shore relaxation boundary condition is assumed. The shore relaxation can be explained that if swash zone slope is milder than the equilibrium slope at the shoreline, sediment transport is defined from wet grid points to dry grid points. This results in shoreline advance to the offshore direction. In contrast, if the swash zone slope is steeper than the equilibrium slope at the shoreline, sediment transport is defined from dry grid points to wet grid points, resulting in the shoreline retreating landward. This concept is introduced in van den Berg et al. (2011). Equation 3.21 gives shore relaxation transport mechanism. Equation 3.22 and Equation 3.23 gives shore relaxation transport in x and y directions as follows,

$$q_{rel} = -\gamma_s\left(\frac{\partial d}{\partial x}cos(\alpha_s) - \frac{\partial d}{\partial y}sin(\alpha_s) + m_s\right) \quad (3.21)$$

$$q_{rel,x} = -q_{rel} * cos(\alpha_s) \quad (3.22)$$

$$q_{rel,y} = -qrel * sin(\alpha_s) \quad (3.23)$$

where, $\gamma_s$ is the shore relaxation coefficient and it is proportional to $(\Delta x^2)/T_r$. $T_r$ is the relaxation time. $d$ is the local bathymetry, $\alpha_s$ is the orientation at the shoreline and $m_s$ is the local slope at the shoreline.

### 3.5.5 Comparison of Sediment Transport Mechanisms

In summary, longshore, cross-shore, alongshore diffusivity, and swash zone sediment transports are explained in detail. Each transport mechanism has its magnitude, direction, and distribution in cross-shore direction. Longshore sediment

transport is computed, then it is distributed over the surf zone. Its magnitude dependent on the angle between local wave direction and local topographical orientation, mean bottom slope over the surf zone, and local root-mean-square wave height. Its direction is parallel to the local orientation of bottom contours. Cross-shore sediment transport is dependent on two separate mechanisms; one is; the diffusivity parameter in the x-direction, which depends on breaking wave index and root-mean-square wave height; the other one is; the difference between the local slope and the equilibrium slope. Globally, cross-shore sediment transport's magnitude is dependent on diffusivity parameter in cross-shore direction, yet locally it is governed by the difference in slopes. Similarly, alongshore diffusivity transport is dependent on the following two mechanisms; the former is alongshore diffusivity constant where, it is dependent on breaking wave index and root-mean-square wave height, the latter is the local orientation of bottom contours and differences in slope along x and y-direction. It is globally controlled by the alongshore diffusivity constant and locally by bottom contour orientations and the difference in slope along x any direction. Finally, shore relaxation is dependent on local bottom contour and local bottom slope at the shoreline.

All of the above-listed transports are occurring simultaneously. Therefore, total sediment transport is the superposition of all transports. It is important to understand the behavior of sediment transport individually. For a better understanding of the order of magnitude and distribution of sediment transports, all transport mechanisms are plotted and remarked separately in the same plots for different cases. As input, a beach with a curved shoreline and parallel bottom contours with the median sand particle diameter of 0.30 mm and average bottom slope of 1/30 without a structure is selected to evolve to its equilibrium beach profile defined as a Dean profile. For 5, 15, and 45 degrees of deep-water incoming wave angles, initial profile, equilibrium profile, wave transformation, and absolute sediment transport fluxes and its distribution in cross-shore direction at the initiation of the model are presented in Figure 3.12, Figure 3.13, Figure 3.14 and Figure 3.15.

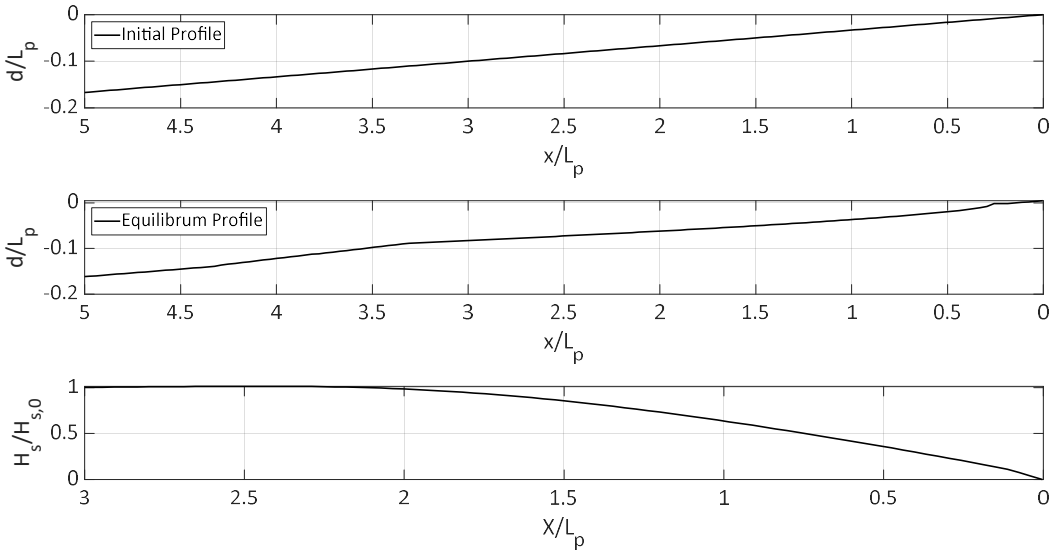


Figure 3.12 Initial, equilibrium beach profile and wave transformation

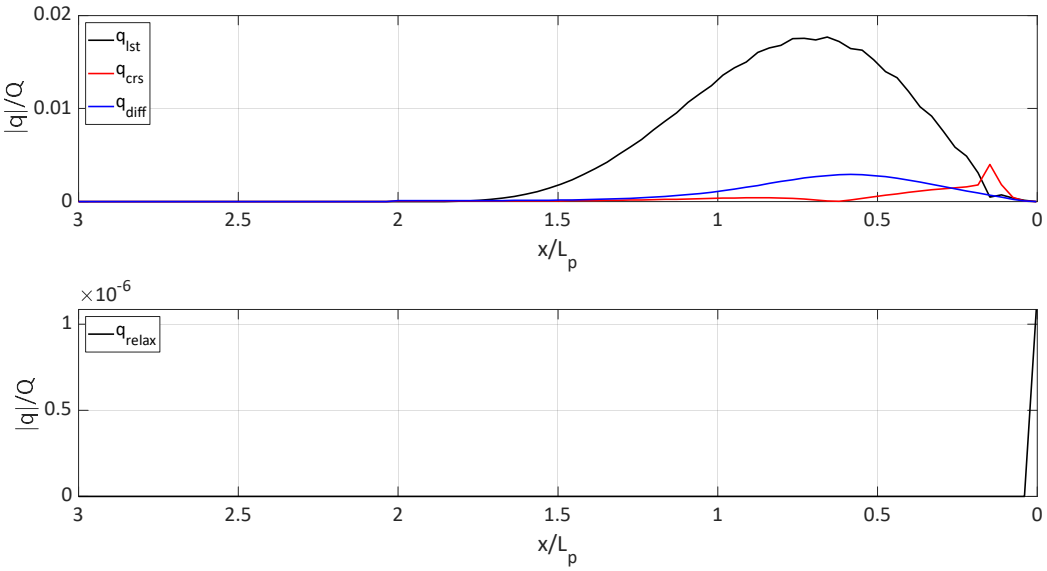


Figure 3.13 Comparison of transport mechanisms (5°)

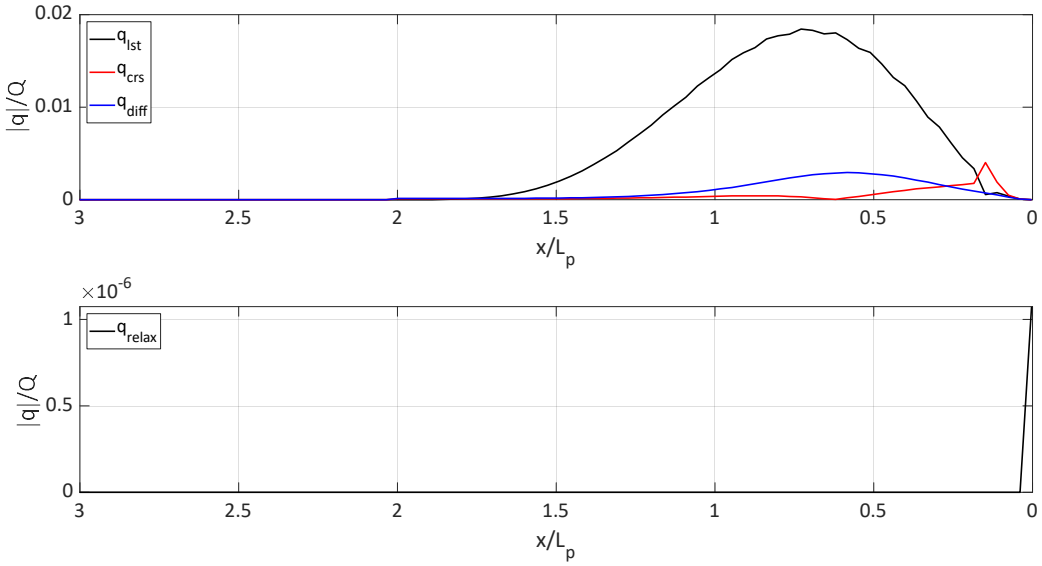


Figure 3.14 Comparison of transport mechanisms (15°)

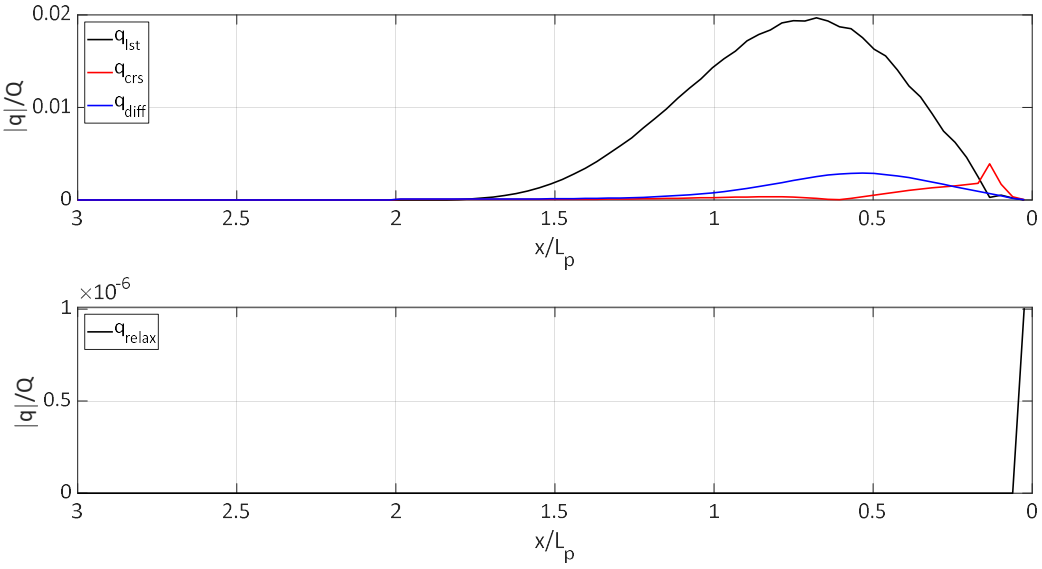


Figure 3.15 Comparison of transport mechanisms (45°)

In figures, axes are given nondimensional as $x/L_p$, $d/L_p$, $H_s/H_{s,0}$, $|q|/Q$, where $x/L_p$ is the distance from the shoreline divided by the peak wavelength, $d/L_p$ is the depth divided by the peak wavelength, $H_s/H_{s,0}$ is the significant wave height normalized by deep water significant wave height and $|q|/Q$ is the absolute sediment transport flux divided by longshore sediment transport magnitude without the angle

term. Figures show sediment transport magnitudes and distributions. With changing deep-water incoming wave angle, only longshore sediment transport magnitude and distribution change at the model's initial phase. Therefore, among transport mechanisms, only longshore sediment transport depends directly on wave angle. Cross-shore, alongshore diffusivity, and shore relaxation transport mechanisms are affected by changing wave angles as a result of changed longshore sediment transport rates; hence they are affected by different bottom topography.

Other than previously mentioned transport methods, sand sources/sinks are not implemented to the model. They are not within this thesis' scope. Although, for future recommendations, phenomena can be implemented via a distribution in the cross-shore direction. Net discharge of source/sink can be distributed in the cross-shore direction with the offshore distance of source/sink will maintain its effectiveness. This distribution's shape can be modified to fit effectiveness of sink/source in cross-shore direction.

## 3.6 Morphology Evolution (MEV)

In the Morphology Evolution module (MEV), sediment transport gradients computed in the STD module at the grid points are interpolated to cell face centers (Figure 3.3). Longshore sediment transport, cross-shore sediment transport, shoreline relaxation boundary, and alongshore diffusivity transports are used to compute depth changes. Bottom changes are computed with the following Equation 3.24.

$$\frac{\partial d}{\partial t} = m_f \left( \frac{\partial q_x}{\partial x} + \frac{\partial q_y}{\partial y} \right) \tag{3.24}$$

In Equation 3.24, $d$ is the local bottom depth, $t$ is time $m_f$ is the morphological acceleration factor, $q_x$ is the total sediment transport in the x-direction, $q_y$ is the total sediment transport in y-direction.

As time progress, even the initial bathymetry is a uniform one; bathymetry will be an arbitrary bathymetry. This arbitrary bathymetry is under the control of an avalanching process. Accretion in some grid points may be higher than its neighboring computational cells. If the bottom slope in neighboring cells exceeds sand grains' limiting slope, sand particles will go through the higher ground to lower ground. This process is called sand avalanching. This limiting (critical) slope is the angle of repose (internal angle of friction). The angle of repose is given 32°-34° for dry sand, and under the wave action, it can reduce to 18° (Reeve et al., 2004; Roelvink et al., 2009). The avalanching algorithm is adopted from Baykal (2012).

Exceedance of limit slope results in sliding of sand particles at the sea depth. The Avalanching is based on Buttolph et al. (2006) and Roelvink et al. (2009). In the morphology module, after every temporal step, in the computation grid's four directions (positive x and y and negative x and y directions), bottom slopes are checked if any of them is exceeding the critical slope. The bottom avalanche check starts from the negative x-direction and continues in the clockwise direction. If one of the slopes exceeds or equal to the critical slope, it is assumed that sand transportation will start from the steepest slope, and water depth will be updated. After the sand transportation, water depths are rechecked if any computational grid exceeds the critical slope. This control mechanism is repeated until all computational grid's slopes are lower than the critical slope until the next time step.

The mathematical expression of the slope checking process is illustrated in Equation 3.25 below,

$$\left|\frac{\Delta d}{\Delta x}\right| = \left|\frac{d_{i,j} - d_{i-1,j}}{\Delta x}\right| > m_{cr} \tag{3.25}$$

where $\Delta d$ is water depth gradient, $\Delta x$ is the spatial resolution in the x-direction, $d$ is water depth and $m_{cr}$ is the critical/limiting slope. It is possible to write the same expression in the y-direction by replacing $\Delta x$ with $\Delta y$ in Equation 3.25.

If Equation 3.25 occurs in the model, an avalanching is assumed to happen, and water depth changes are computed as in Equation 3.26.

$$\Delta d_a = \left( \left| \frac{\Delta d}{\Delta x} \right| - m_{cr} \right) \Delta x \tag{3.26}$$

Water depths in the neighboring cells are recomputed with Equation 3.27 and 3.28,

$$\left.\begin{aligned} d_{i,j}^{a} &= d_{i,j} - \Delta d_a \\ d_{i-1,j}^{a} &= d_{i-1,j} + \Delta d_a \end{aligned}\right\} for\ \frac{\Delta d}{\Delta x} > 0 \tag{3.27}$$

$$\left.\begin{aligned} d_{i,j}^{a} &= d_{i,j} + \Delta d_a \\ d_{i-1,j}^{a} &= d_{i-1,j} - \Delta d_a \end{aligned}\right\} for\ \frac{\Delta d}{\Delta x} < 0 \tag{3.28}$$

where, $d_{i,j}^{a}$ and $d_{i-1,j}^{a}$ is the recomputed water depth after avalanching occurs, $d_{i,j}$ and $d_{i-1,j}$ is the water depth before avalanching occurs, and (i, j)$^{th}$ and (i-1, j)$^{th}$ represent computational cells. Equations 3.26, 3.27, and 3.28 can be rewritten for y-direction as well by replacing $\Delta x$ with $\Delta y$. Computation of morphology is carried out until a user-defined duration. For each time step, if the bottom avalanching module is on, avalanche control occurs until the end of the model.

## 3.7 Numerical Modeling and Boundary Conditions

Q-2DH Model's computational cells are defined as rectangular grid system for numerical modeling. Finite difference schemes are used to model nearshore processes numerically. In the computation of bathymetrical orientation, the procedure explained in Chapter 3.3 is used. Two transverse vectors are defined in the staggered grid system. The normal vector of surface which is created by the two transverse vectors, is used to compute bathymetrical orientation in all grid points individually. Definition of the two transverse vectors are given in Equation 3.29 and 3.30,

$$v_1 = \left| X_{i+1,j}^{stg} - X_{i,j+1}^{stg} \right|_x + \left| Y_{i+1,j}^{stg} - Y_{i,j+1}^{stg} \right|_y + \left| d_{i+1,j}^{stg} - d_{i,j+1}^{stg} \right|_z \tag{3.29}$$

$$v_2 = \left| X_{i+1,j+1}^{stg} - X_{i,j}^{stg} \right|_x + \left| Y_{i+1,j+1}^{stg} - Y_{i,j}^{stg} \right|_y + \left| d_{i+1,j+1}^{stg} - d_{i,j}^{stg} \right|_z \tag{3.30}$$

with, $X^{stg}$ is the x coordinate of the staggered bathymetry system, $Y^{stg}$ is the y coordinate of the staggered bathymetry and $d^{stg}$ is the depth of the staggered

bathymetry system. Nomenclatures after $X^{stg}$, $Y^{stg}$ and $d^{stg}$ represents row and column numbers, respectively. For example, $X_{i,j}^{stg}$ denotes i[th] row and j[th] column of the x coordinate of the staggered bathymetry. Also $|a|_x$ symbolize vectorial representation (magnitude "a" in the x-direction). In this chapter, explained notations are used further.

After computation of the two transverse vectors, the cross product of the two can be found as Equation 3.31 – 3.33.

$$|v_1 x v_2|_x = |v_1|_y * |v_2|_z - |v_1|_x * |v_2|_y \tag{3.31}$$

$$|v_1 x v_2|_y = -(|v_1|_x * |v_2|_z - |v_1|_z * |v_2|_x) \tag{3.32}$$

$$|v_1 x v_2|_z = |v_1|_x * |v_2|_y - |v_1|_y * |v_2|_x \tag{3.33}$$

Projection of cross-product onto free surface gives bathymetry orientation in each computational grid. Projection of cross-product and orientation is given in Equation 3.34 and Equation 3.35,

$$\left|v_{proj}\right| = |v_1 x v_2| - \left(\frac{|v_1 x v_2| * \left|v_{ref}\right|}{\left\|v_{ref}\right\|^2}\right)\left|v_{ref}\right| \tag{3.34}$$

$$\alpha = \arctan\left(\frac{\left|v_{proj}\right|_y}{\left|v_{proj}\right|_x}\right) \tag{3.35}$$

where, $v_{proj}$ is the projected surface vector, $v_{ref}$ is the free surface normal vector, and $\alpha$ is the local bathymetry orientation at the computational cell.

Local bathymetry orientation ($\alpha$) is filtered in the model. There are two reasons to filter $\alpha$; sediment transport direction is not solely affected by a single computational grid, rather it is affected by the overall movement of the current field, also, in some cases where shoreline evolve to a curved one, incoming wave angles and local orientation near the shoreline becomes relatively small, relative wave angle ($\beta$) tends to change its direction, thus causes to change sediment transport direction. A filter is accepted in the Q-2DH model similar to van den Berg et al. (2011) to represent the sediment transport field's overall movement more accurately. A rectangular box is accepted to apply the average filter to local orientation. For the cross-shore

dimension of the filter box, $2*X_b$ and for the alongshore dimension of the filter box, $4*X_b$ is accepted.

Numerical modeling of NSW is done using the first-order backward finite difference scheme in the x-direction, and first-order centered finite difference schemes are practiced in the y-direction. Directional domains contain an explicit up-winding scheme in cross-shore direction and an implicit solution for the unknown density components of alongshore direction and directional space (Baykal, 2012).

NSW module has three different types of boundary conditions: offshore, open-sea, and dissipative beach boundary conditions (Figure 3.16). The offshore boundary condition is a Dirichlet type, and the user defines the offshore boundary condition. Secondly, there is the open-sea boundary condition. This boundary condition is applied where the user defines no existing boundary condition. Water depth in these computational cells is higher than a minimum water depth (i.e., minimum water depth, which can be solved by the NSW module). It is defined as Neumann type boundary condition; the wave spectrum just outside the boundaries is accepted as equal to those placed at the computational area's edge. Finally, there is a dissipative beach boundary condition. This type of boundary condition is accepted at dry points such as lands, islands, and structures. This type of boundary condition is accepted where local water depths are lower than the accepted minimum water depth. Spectral densities are accepted as fully dissipated and are equal to zero in these locations.

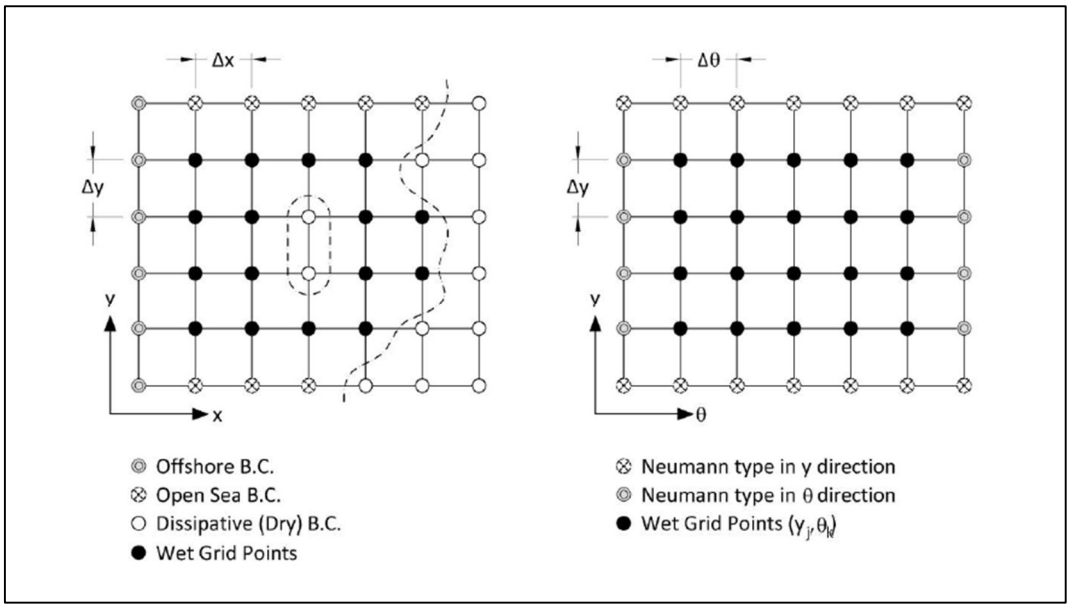


Figure 3.16 Boundary conditions in NSW module (adopted from Baykal, 2012)

In the STD module, transport magnitudes and directions are computed in rectangular grid points. For all transport methods, the most offshore point for a transport mechanism that can exist is the closure depth. Beyond closure depth, sediment transport does not occur. In the landward area, wet computational cells with the minimum depth are the most onshore point for the transport to occur (including wave set-up). Only the Shore Relaxation term is an exception to this statement. It is deliberately defined in the exact shoreline position to reflect the behavior on the shoreline.

In numerical modeling of longshore sediment transport, the wave height gradients in the y-direction are modeled as the first-order centered scheme. Equation 3.3 is rewritten as Equation 3.36.

$$Q_{i,j} = \mu H_{rms,b}^{5/2}\left(\sin(2\beta_{i,j}) - \frac{2r}{m}\cos\left(\beta_{i,j}\right)\frac{H_{i,j+1}^{rms} - H_{i,j-1}^{rms}}{2\Delta y}\right) \qquad (3.36)$$

For the cross-shore sediment transport, there is the gradient of local bathymetry in the x-direction and the gradient of equilibrium profile in the x-direction. These terms are discretized as a first-order centered scheme. Therefore, Equation 3.15 is rewritten as Equation 3.37.

$$q_{i,j}^{crs} = -\gamma_x \left( \frac{d_{i+1,j} - d_{i-1,j}}{2\Delta x} - \frac{d_{i+1,j}^{e} - d_{i-1,j}^{e}}{2\Delta x} \right) \quad (3.37)$$

In numerical modeling of alongshore diffusivity sediment transport, there are gradients of local bathymetry in both x and y directions. Those gradients are discretized from staggered grid system as the methodology explained in this chapter previously. Therefore, all magnitudes and directions are computed directly in computational cells.

Shore relaxation, a sub-header for Swash Zone Dynamics, is numerically modeled as a first-order-centered scheme. Equation 3.21 is rewritten as Equation 3.38.

$$q_{i,j}^{rel} = -\gamma_s \left( \frac{d_{i+1,j} - d_{i-1,j}}{2\Delta x} cos(\alpha_{i,j}^{s}) - \frac{d_{i,j+1} - d_{i,j-1}}{2\Delta y} sin(\alpha_{i,j}^{s}) + m_s \right) \quad (3.38)$$

A forward finite difference scheme solves the MEV module. The scheme is implemented to Equation 3.24, and it is rewritten as Equation 3.39,

$$d_{i,j}^{n+1} = d_{i,j}^{n} + \Delta t m_f \left( \frac{q_{x_{i+1,j}}^{n} - q_{x_{i,j}}^{n}}{\Delta x} + \frac{q_{y_{i,j+1}}^{n} - q_{y_{i,j}}^{n}}{\Delta y} \right) \quad (3.39)$$

where, $d_{i,j}^{n+1}$ is the depth in the next time step, $d_{i,j}^{n}$ is the depth in the current time step, $\Delta t$ is the time increment used in the model, $m_f$ is the morphological acceleration factor, $q_{x_{i+1,j}}^{n}$ is the total sediment transport in the x-direction at the (i+1, j)$^{th}$ computational cell in the current time, $q_{x_{i,j}}^{n}$ is the total sediment transport in x direction at the (i, j)$^{th}$ computational cell in the current time. $\Delta x$ is the spatial resolution in the x-direction. Similarly, $q_{y_{i,j+1}}^{n}$ is the total sediment transport in the y-direction at the (i, j+1)$^{th}$ computational cell in the current time, $q_{y_{i,j}}^{n}$ denotes total sediment transport in y-direction at (i, j)$^{th}$ computational cell in the current time, and $\Delta y$ is the spatial resolution in the y-direction.

In Q-2DH Model, all numerical modeling done is explicitly. This may result in instability problems. Therefore, a numerical stability criterion due to explicit modeling is implemented to the model to limit the time increment ($\Delta t$). The stability

criterion is a Courant-Friedrichs-Lewy type (van den Berg et al., 2011), and it is given in Equation 3.40,

$$\Delta t = cH_{rms}{}^{-3/2} \frac{(min\{\Delta x, \Delta y\})^2}{max\{\varepsilon_x, \varepsilon_y\}} \tag{3.40}$$

where $c$ is a calibration constant and its default value is 0.13, $H_{rms}$ is the root mean square wave height, $\Delta x$, and $\Delta y$ are spatial resolution in x and y directions respectively, $\varepsilon_x$ and $\varepsilon_y$ are non-dimensional constant in Equation 3.16. Their default values are 0.05.

# CHAPTER 4

# MODEL BENCHMARKING

In this chapter Q-2DH model's benchmarking is done. The validity of wave transformation, sediment transport in the surf zone, and morphology evolutions are tested through several cases. To benchmark the model, theoretical and laboratory experiments are considered. For the model's theoretical benchmarking, three different cases are considered; beach cusps, cross-shore sediment transport, and sediment transport in the vicinity of a single groin are considered.

For laboratory experiments, Gravens and Wang's (2007) Test 1 case is considered. In Test 1 case, the formation of tombolo at the lee side of a detached breakwater is studied. It consists of 8 sub-series, which are approximately 190 minutes. To benchmark the model, Test 1 case is studied in two different methods. Firstly, the initial bathymetry of Test 1 is constructed, and the Q-2DH model is executed until the model gives an error. Secondly, each sub-series are executed and analyzed individually.

All cases are selected to illustrate different features of the Q-2DH model. Beach cusps are selected to observe the sediment transport directions in a curved beach. A cross-shore transport case is chosen to indicate the profile behavior under merely cross-shore transport. It restores the equilibrium profile of an arbitrary profile. A single groin case is selected to observe the shoreline accretion in updrift and shoreline erosion in downdrift part of the single groin. In T1C1, the initiation of beach contour development to form salient is illustrated. In between cases, T1C1-T1C7 advancement of salient is inspected. In case T1C8 transition from salient to tombolo is examined. Finally, in the case T1C1-T1C2, the model simulates salient formation before any stability problem occurs and the duration which the model lasts

before stability error occurrence is inspected. All cases are studied, and their properties are summarized in Table 4.1.

Table 4.1 Benchmark studies

| Case Name | $H_{s,0}$ (m) | $T_s$ (s) | $\theta_0$ (°) | Duration (min) | Property |
|---|---|---|---|---|---|
| Beach Cusps | 0.06 | 1.01 | 0 | - | To observe sediment transport direction in curved beach |
| Cross-shore transport | 0.27 | 1.43 | 10 | 334 | To observe morphology change under solely cross-shore transport |
| Single Groin | 2.00 | 6.00 | 30 | 12000 | To observe morphology change in the vicinity of a single groin |
| T1C1 | 0.27 | 1.43 | 10 | 185 | Formation of salient |
| T1C2 | | | | 181 | |
| T1C3 | | | | 185 | |
| T1C4 | | | | 192 | Advancement of salient |
| T1C5 | | | | 176 | |
| T1C6 | | | | 189 | |
| T1C7 | | | | 191 | |
| T1C8 | | | | 184 | Formation of tombolo |
| T1C1-T1C2 | | | | 366 | Formation of salient, duration of the model without stability error |

## 4.1 Beach Cusps

One of the most frequently found shoreline characteristics of sandy and gravel beaches are beach cusps. They appear at the swash zone and are distinguished by elevations of highs and lows with spacing varying between 50-100 meters depending on the beach slope and wave characteristics. High elevation zones of beach cusps are commonly referred to as “beach cusp horn” and have steeper slopes from sea to land area. Low elevation zones appear to be much smoother in slope and typically known as “beach cusp embayment” or simply “bays”. An illustration of beach cusps, beach cusp horns, and beach cusp bays is given in Figure 4.1.

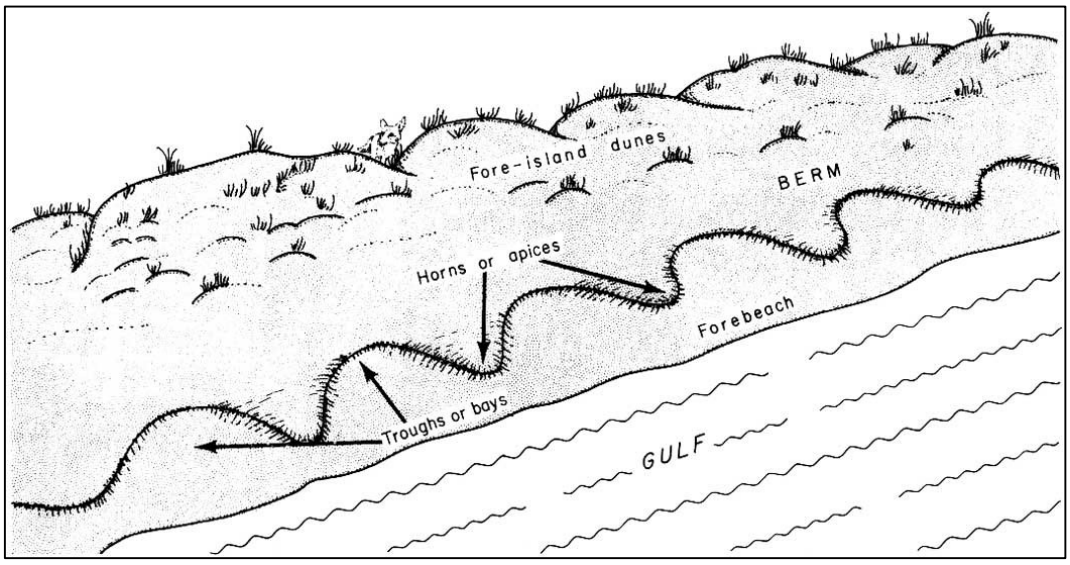


Figure 4.1 Beach cusps (adopted from Weise & White, 1980)

It is important to determine nearshore hydrodynamic conditions accurately in beach cusps. Beach cusps are curved shoreline (concave up in bays and concave down in horns) which cause to change relative incoming wave angles along the shoreline, thus, cause a change in the direction and magnitude of wave-induced currents and the direction and magnitude of alongshore sediment transport along the shoreline. At beach cusps, wave-induced current flows from horns through bays; when two opposite directional currents meet at the center of the bay, it causes a backwash as mini-rip flows from the beach to offshore. In Figure 4.2, flow directions are

illustrated for beach cusps. To examine the alongshore sediment transport around beach cusps, a theoretical analysis has been carried out based on Park and Borthwick's (2001) study on nearshore currents at a sinusoidal beach which is close to the beach cups in nature. Sinusoidal water depths of the model area, $d(x,y)$ for the benchmark case is defined as Equation 4.1,

$$d(x,y) = \begin{cases} for\ x < 11\ m\ and\ x > 16\ m; \\ 0.8 - x/20 \\ for\ 11m \le x \le 16m; \\ 0.05(15-x) - 0.75sin\left(\frac{\pi(15-x)}{5}\right)\left(1 + sin\left(\frac{3\pi}{2} - \frac{2\pi y}{4}\right)\right) \end{cases} \quad (4.1)$$

where $x$ is the coordinate in the cross-shore direction, $y$ is the coordinate in the alongshore direction.

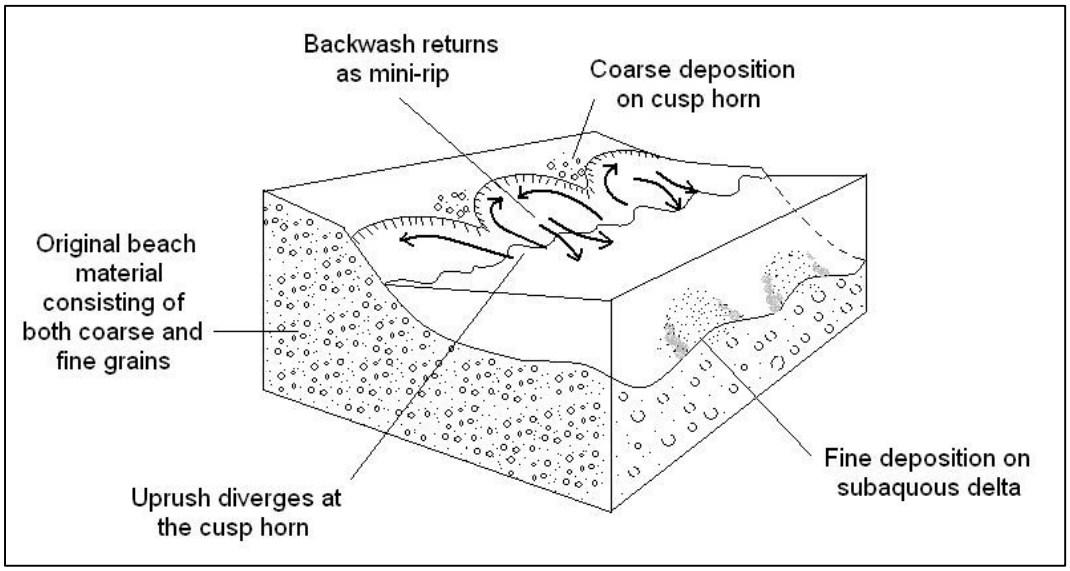


Figure 4.2 Beach cusps hydrodynamics (adopted from Masselink & Hughes, 2003)

In this section, waves are defined in the offshore boundary of the model area. Wave propagation through the shoreline and sediment transport directions as a result of given waves in beach cusps at the initial phase of the model is studied. In Figure 4.3, the computed wave field and sediment transport field are plotted.

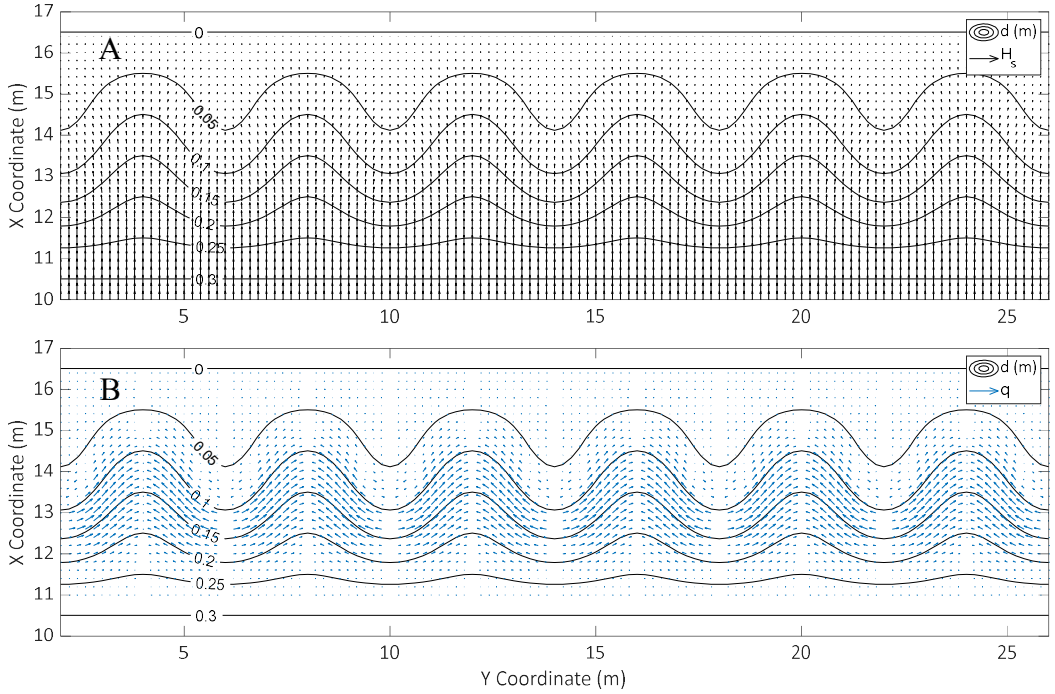


Figure 4.3 Quiver plot of computed wave field (A) and sediment transport (B)

In Figure 4.3, the computed wave field shows that waves are entering the model domain perpendicularly. As waves progress through the beach, bottom topography causes waves to deviate from their perpendicular route to beach cusp horns, which is the expected behavior (refraction) for waves. Sediment transport occurs from beach cups horns to the bay. This is the expected behavior for the sediment transport. However, at the bay center, the return flow cannot be solved with the Q-2DH model. Also, near the head of beach cusp horns, some transport directions cannot be determined correctly. When incoming wave angles and local bottom orientation become relatively small in curved shorelines, the path that refracted waves follows causes the relative incoming wave angle to reverse its direction. This is why the Q-2DH model needs a filter to overcome this obstacle. The need for the filter will be discussed in further chapters. Due to previously mentioned reasons, in further time-steps of the model, the shoreline starts to change; sand accumulation at the center of the bay happens and some discontinuities at beach horns occurs which is not the expected behavior of beach cusps.

## 4.2 Cross-Shore Transport

Cross-shore sediment transport in the Q-2DH model is not introduced as a process-based physical phenomenon as previously explained. A parametrized expression for cross-shore sediment transport is solved. This parameterized expression restores or preserves the so-called user-defined equilibrium profile on a relatively long timescale.

Equation 3.15 implies that if initial bathymetry is the same as the user introduced equilibrium profile, then there is no transport or the transport is limited in the cross-shore direction. If a different bathymetry or different profile than the equilibrium profile is introduced initially, the Q-2DH model changes the initial bathymetry to the introduced equilibrium profile. Instead of constructing a time/wave height dependent new bathymetry, this cross-shore transport mechanism preserves introduced equilibrium bathymetry or reconstructs equilibrium bathymetry in deformed profiles. If a structure is placed in the shoreline's vicinity, the shoreline adapts the structure, and as a result, accretional and erosional zones of the profile diverge from the equilibrium profile. Cross-shore transport restores the equilibrium profile in these profiles.

For an arbitrarily defined initial profile, the Q-2DH model is executed to illustrate the initial profile's advancement in time under solely cross-shore sediment transport with default parameters. Illustrations for different times can be found in Figure 4.4, Figure 4.5, Figure 4.6, and Figure 4.7.

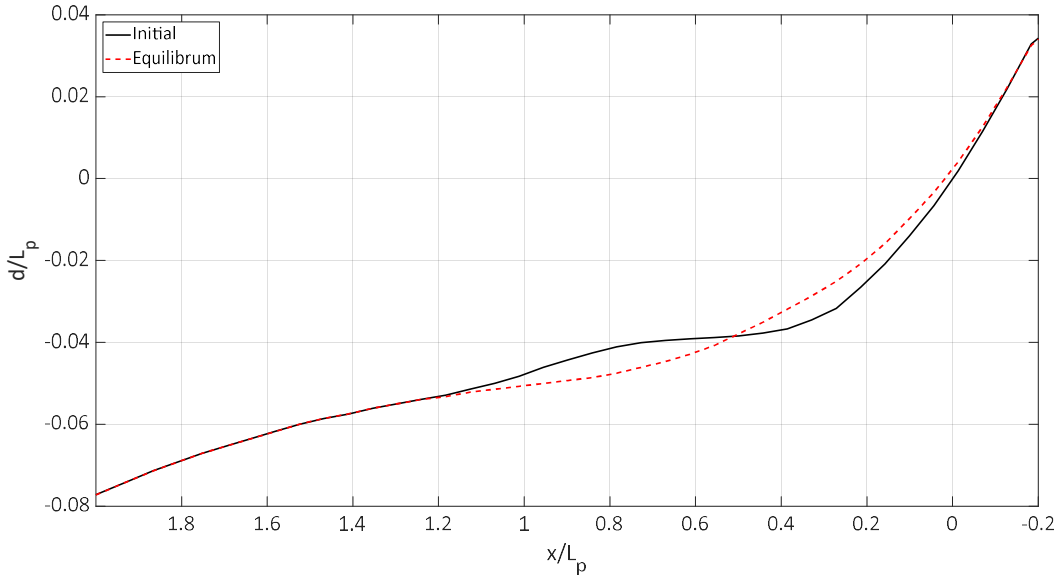


Figure 4.4 Change of beach profile under cross-shore sediment transport (t = 0 seconds)

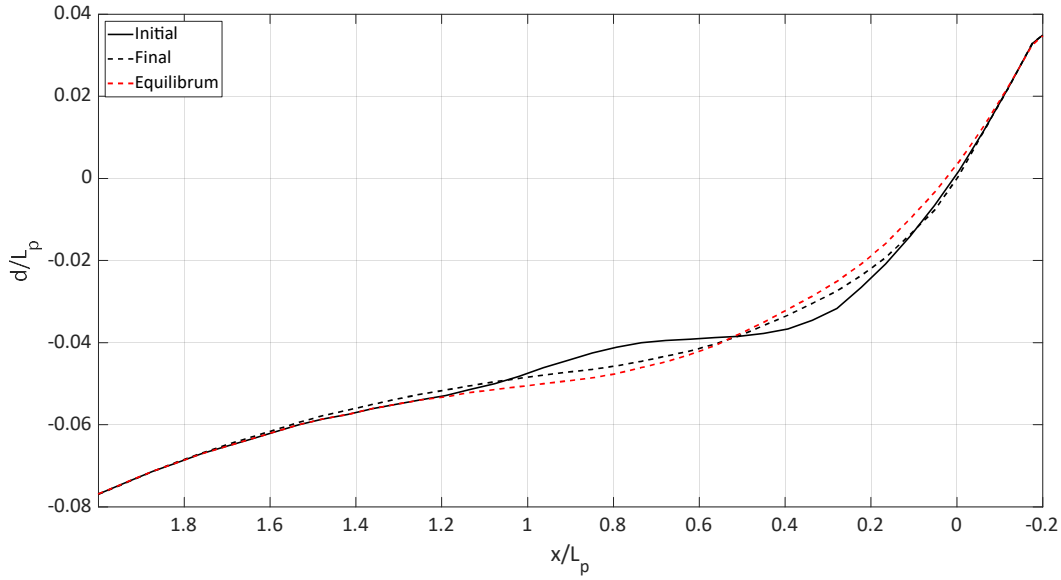


Figure 4.5 Change of beach profile under cross-shore sediment transport (t = 1000 seconds)

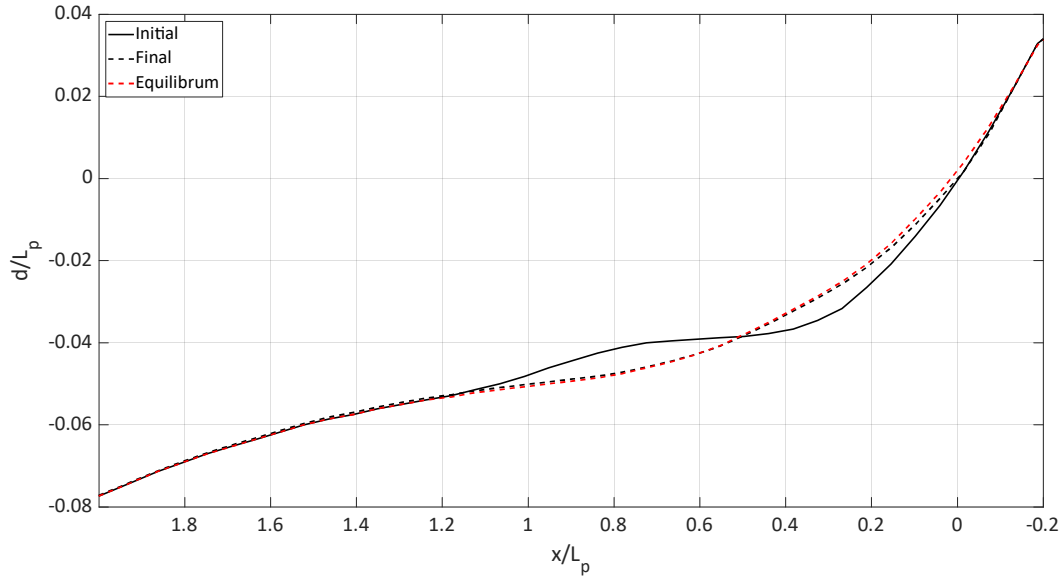


Figure 4.6 Change of beach profile under cross-shore sediment transport (t = 10000 seconds)

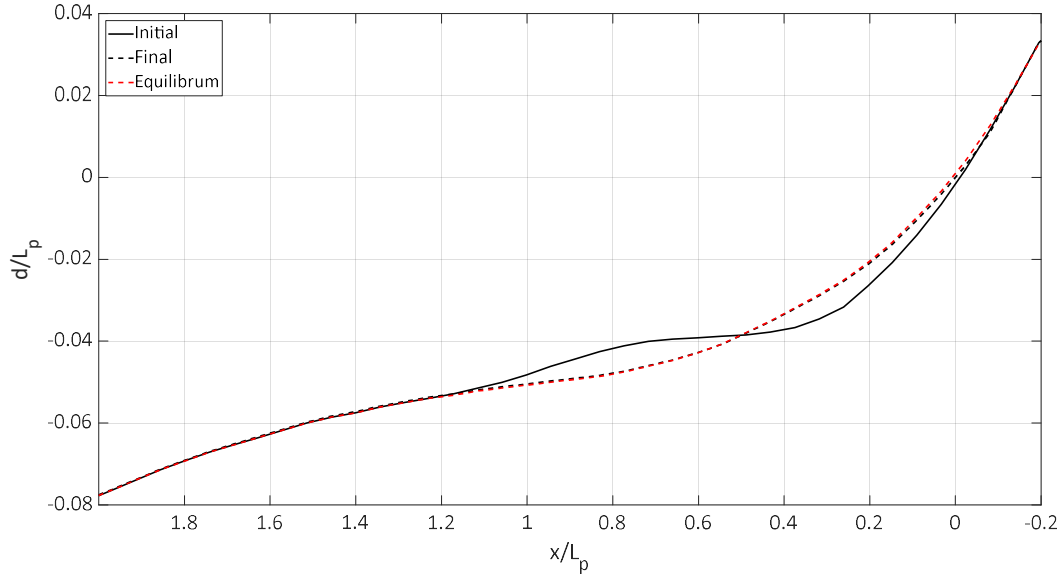


Figure 4.7 Change of beach profile under cross-shore sediment transport (t = 20000 seconds)

In figures, four different times are presented; time at the start, time at 1000 second, time at 10000 seconds, and time at 20000 seconds. In the figures, three different profiles are given; the initial profile, the final profile, and the equilibrium profile. At the start, the initial profile and the final profiles are the same, since cross-shore

sediment transport has not been started yet, at t = 1000 seconds, the profile roughly takes the equilibrium's profile shape, at t = 10000 seconds, the final profile is almost same with the equilibrium profile. At t = 20000 seconds, the final and the equilibrium profile becomes approximately identical. It can be concluded that transport magnitudes are much higher in the initial simulation steps and gradually decreases to zero. Equation 3.15 causes this phenomenon to happen. Thus, at time 10000 seconds, the final profile took the overall shape of the equilibrium profile.

For a better understanding of the cross-shore sediment transport process, the equilibrum profile is defined as the initial profile of the previously study case and the initial profile is defined as the equilibrium profile of the previous case. Profile is subjected to waves and only the cross-shore sediment transport is active among the sediment transport mechanisms in the model domain. Model is simulated for 20000 seconds as the previous case. Model results for cross-shore sediment transport is given in Figure 4.8, Figure 4.9, Figure 4.10 and Figure 4.11.

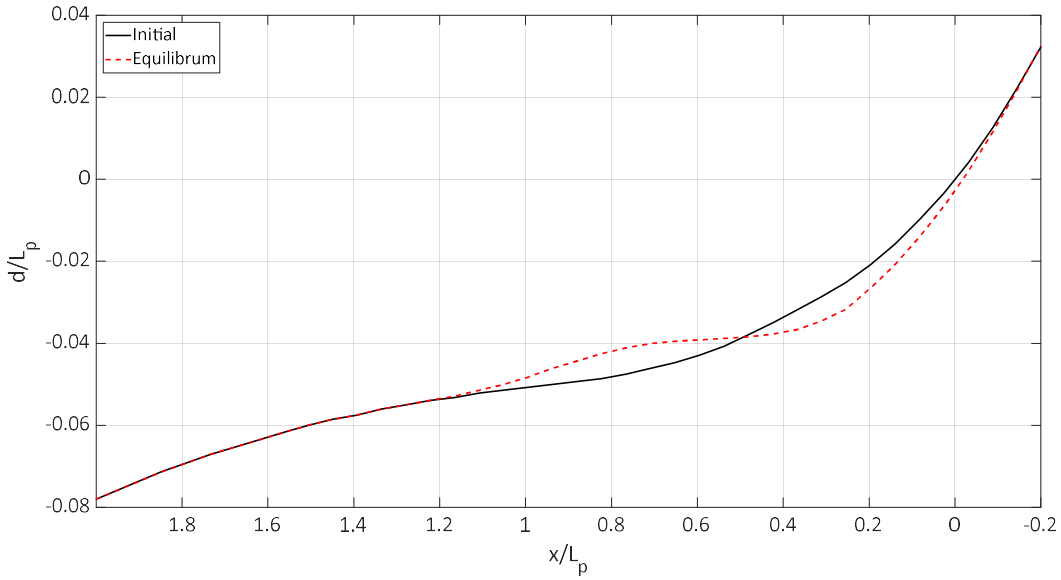


Figure 4.8 Change of beach profile under cross-shore sediment transport (t = 0 seconds)

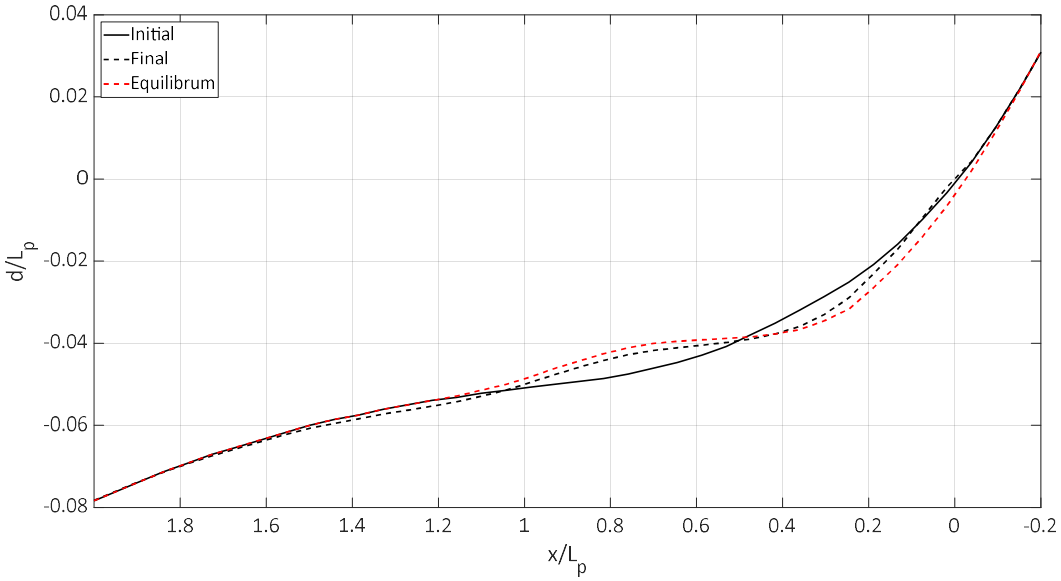


Figure 4.9 Change of beach profile under cross-shore sediment transport (t = 1000 seconds)

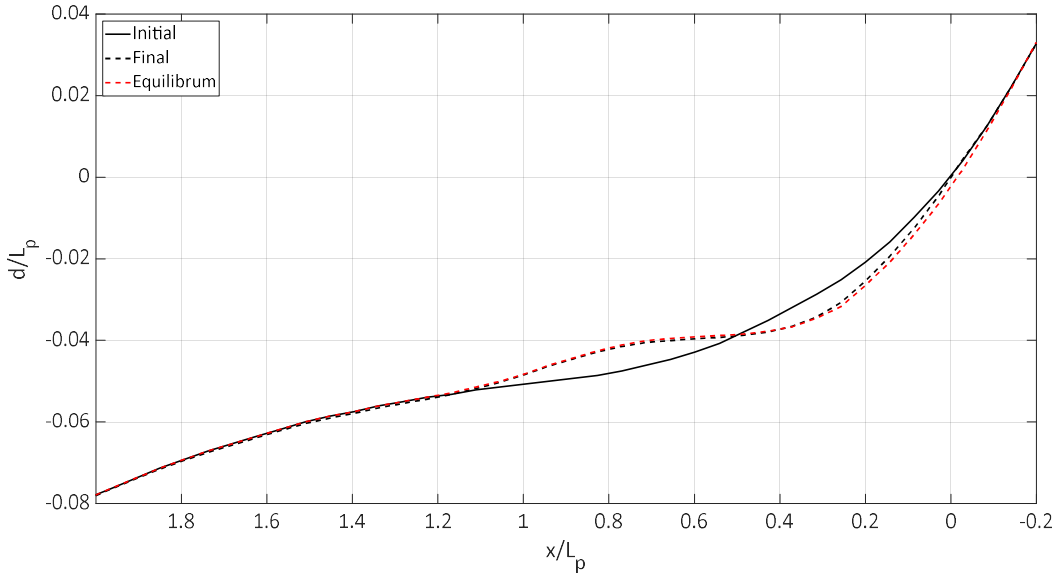


Figure 4.10 Change of beach profile under cross-shore sediment transport (t = 10000 seconds)

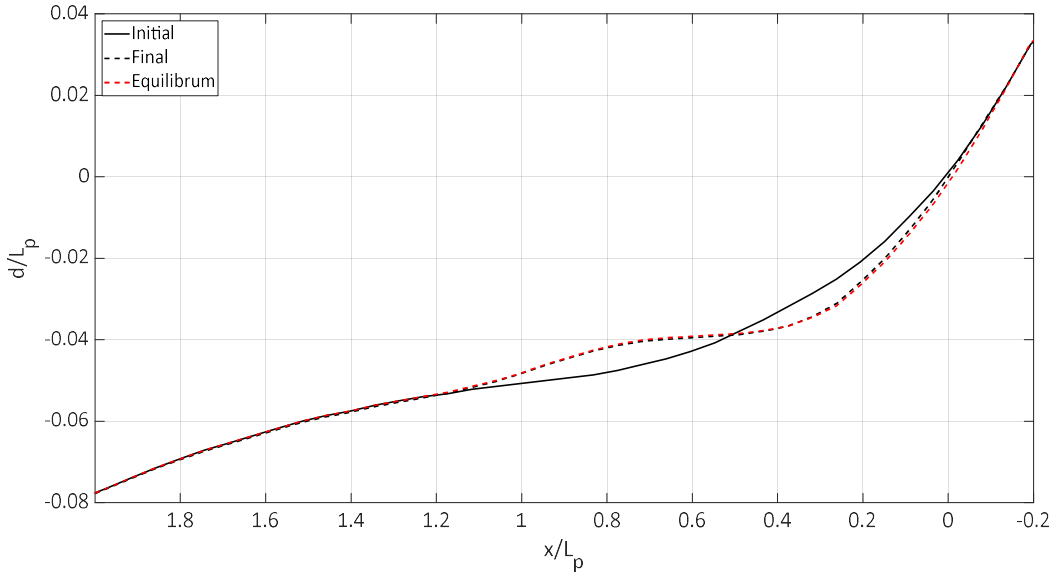


Figure 4.11 Change of beach profile under cross-shore sediment transport (t = 20000 seconds)

In figures, profile in four different times are presented; time at the start, time at 1000 second, time at 10000 seconds, and time at 20000 seconds. Three different profiles are given; the initial profile, the final profile, and the equilibrium profile. Similarly, in initial phases of the model, overall equilibrium profile shape is achieved by the profile. In 20000 seconds, initial profile takes the equilibrium profile's shape.

## 4.3 Single Groin

Groins are the oldest and most widespread structure of beach stabilization. They are connected to the shoreline. Groins are generally perpendicular or almost perpendicular to the shoreline, and their length is usually short compared to jetties and tidal inlets. Groins are built to achieve a minimum dry beach width to minimize storm damage or limit sand flowing alongshore. Groins can be constructed either singular or in series. Whichever is designed for the shoreline, shoreline adapts to the presence of groin(s). In the updrift part of the groin, sand accumulates and causes to

beach width to expand. Due to the conservation of mass, there should be erosion in the groin's downdrift part (USACE, 2007).

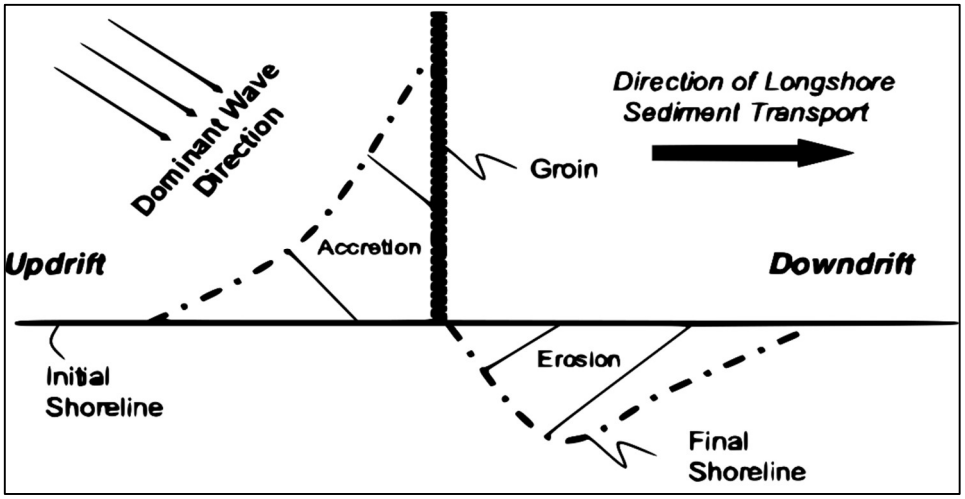


Figure 4.12 Morphology after groin placement in the shoreline (adapted from Artagan, 2006)

A simulation with the Q-2DH model is conducted to analyze the numerical model's action in the case of a single groin under oblique incoming waves on an initially straight parallel shoreline with a uniform bottom slope. Computed wave field and morphology evolution can be found in Figure 4.13.

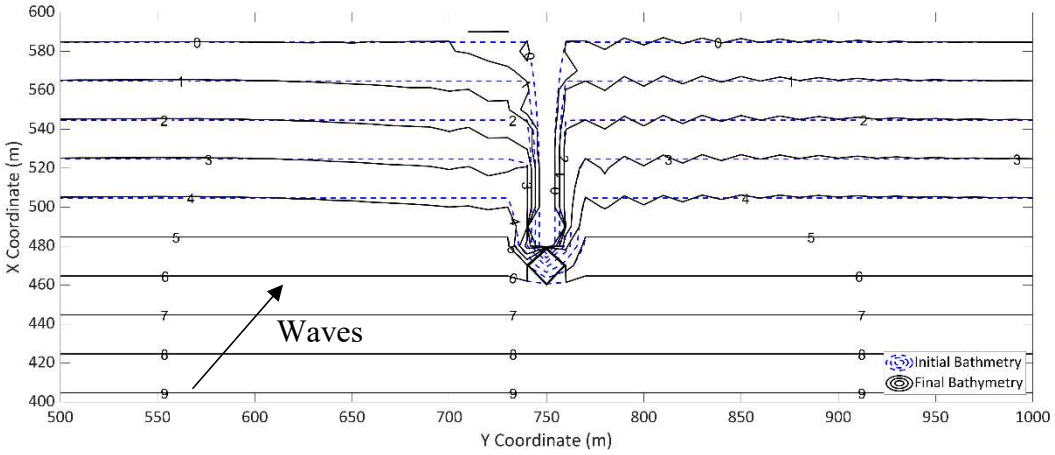


Figure 4.13 Q-2DH model results for single groin

Figure 4.13 illustrates that sediment accumulates in the updrift part of the groin, causing the shoreline to advance. While in the downdrift part, erosion should occur,

yet the Q-2DH model could not accurately solve the downdrift part. There are few reasons behind it; in the down-drift part where waves are diffracted, wave directions computed through a single groin causes accumulation next to the groin. In the further downdrift part of the groin, the wave model computes diffracted waves higher than expected and cause sediment transport magnitudes to come to an equilibrium, causes to not eroded shoreline. Also, in the part where erosion should occur, irregularities occur instead of smoothly transitioned erosion. Irregularities in the model cause instability problems as the morphological time step advances.

## 4.4 Laboratory Experiments

Q-2DH model is tested with the laboratory experiments of Gravens and Wang (2007). They have studied five series of physical model movable bed experiments. The experiments aimed to collect data sets for the testing and validation of sediment transport relationships and provide these data sets for the development of computational model algorithms for the estimation of tombolo processes in the vicinity of headland structures (offshore breakwater and T-groin). Every series of laboratory experiments consisted of several sub-series; in each sub-series, waves and currents were produced in the basin, and hydrodynamic data were obtained. Wave heights, alongshore current velocities, mean water elevations, and gross sediment transport fluxes were measured during experiments. Between cases, the beach profiles were surveyed, and, in some cases, the sand traps were cleaned, and the beach profile was reconstructed to the equilibrium profile. Series designed to acquire data sets for the development of tombolo in the shadow zone of a detached breakwater are addressed as “Test 1” and “Test 2”. To benchmark the Q-2DH model, “Test 1” is used within the scope of this study.

Test 1 cases were executed in a sub-series of 8 runs (T1C1 through T1C8) and each sub-series are approximately 190 minutes. Each one is on a natural beach with a 4-meter-long rubble mound breakwater centered in the alongshore direction (between

Y=26 m to Y=22 m) and located 4 meters distanced from the initial shoreline. The initial layout of the Test 1 case can be found in Figure 4.14.

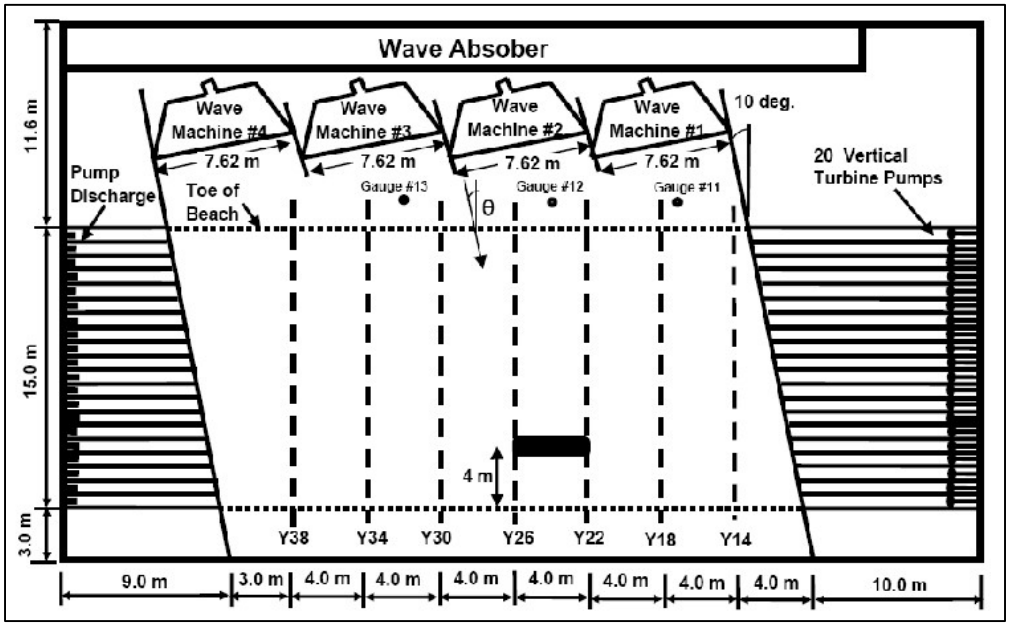


Figure 4.14 Initial layout of Test 1 (adopted from Gravens & Wang (2007))

Alongshore current which is produced by waves were recirculated from the downstream end of the basin to the upstream end. After sub-series T1C2 (time = 6 hours) and T1C5 (time = 15 hours), sediment traps are emptied, and the equilibrium beach profile is reconstructed. Movable bed material is chosen as very well sorted quartz sand with a median grain size of 0.15 mm.

As previously discussed, laboratory experiments are studied in two different ways; each sub-series of Test 1 (from T1C1 to T1C8) is studied individually, and Test 1 is studied from the beginning until the Q-2DH model gives stability error (end of T1C2). Performance of wave height computations are studied with areal computation of mean absolute percent error (MAPE). Results of morphology evolution are studied through three different methods; Brier Skill Score (BSS) (Brier, 1950) is computed for each case and for three different depth intervals (0-0.08, 0.08-0.16, and 0-0.16), which will be addressed in further as BSS1, BSS2, and BSS3 respectively. BSS3 is the equivalent of whole depth interval in the lee-side of the breakwater. Mean

absolute percent error (MAPE) is computed in two different ways; based solely on shoreline change and based on initial and final bathymetry. MAPE is given in Equation 4.2,

$$MAPE = \frac{1}{n}\sum_{i=1}^{n}\left|\frac{y_i - x_i}{x_i}\right| \tag{4.2}$$

where $MAPE$ is the mean absolute percent error, $y_i$ is the prediction value, $x_i$ is the true value, and $n$ is the total number of data points.

BSS is a function of score that test the accuracy of the probabilistic forecast. It is widely used in sediment transport and morphology evolution. BSS compares the mean square difference between the observed and predicted value. Excellent correlation takes one from BSS. Predicting initial values as prediction gives zero BSS score. If the prediction is even distant from initial values, the BSS score would be negative. BSS for two dependent variables (for bathymetry in two dimensions) is given in Equation 4.3,

$$BSS = 1 - \frac{\sum_{i=1}^{n}\sum_{j=1}^{k}\left(d_{i,j}^{p} - d_{i,j}^{m}\right)^2}{\sum_{i=1}^{n}\sum_{j=1}^{k}\left(d_{i,j}^{b} - d_{i,j}^{m}\right)^2} \tag{4.3}$$

with $d_{i,j}^{p}$ is the predicted sea depth at the (i, j)$^{th}$ cell, $d_{i,j}^{m}$ is the measured sea depth at the (i, j)$^{th}$ cell and $d_{i,j}^{b}$ is the initial sea depth at the (i, j)$^{th}$ cell.

Van Rijn et al. (2003) offered some ranges to measure bottom evolution performance, and they are presented in Table 4.2.

Table 4.2 Error ranges for BSS

| Qualification | Morphology, BSS |
|---|---|
| Excellent | 1.0 - 0.8 |
| Good | 0.8 - 0.6 |
| Reasonable / Fair | 0.6 - 0.3 |
| Poor | 0.3 - 0 |
| Bad | < 0 |

### 4.4.1 T1C1

T1C1 consists of 185 minutes experiment duration with waves and wave generated currents. Q-2DH model is calibrated to T1C1 case, and the same calibration parameters are used in further cases as well. For the bathymetry, the domain is divided into regularly spaced computational cells with 0.2 meters. To eliminate the lateral boundary effects (to ensure longshore currents to occur in the model area), the model is elongated 20 meters through the left and right side, approximately one model width in the alongshore direction. In the offshore direction, T1C1's offshore depth is 0.70 meters; model depth is extrapolated to an offshore depth, which is 1.69 meters for able to give offshore wave condition of Test 1. So, there exists a total of 113 rows (X-Range = 1.6 to 24) and 301 columns (Y-Range = -6 to 54) of computational cells in the one-time interval. Other model parameters for T1C1 is listed as follows; $H_{s,0}$ = 0.27 m, $T_{s,0}$ = 1.42, $\theta_0$ = 10°, $\gamma_b$ = 0.78, $s_{max}$ = 10, $\varepsilon_x$ = 0.5, $\varepsilon_y$ = 0.5, $\gamma_s$ = 6.24*10$^{-6}$, $m_f$ = 0.37, $\mu$ = 0.20, $d_c$ = 0.37 m and $\Delta_t$ = 0.2 s. $H_{s,0}$, $T_{s,0}$, $\theta_0$, $\gamma_b$ and $s_{max}$ is calibrated to satisfy wave conditions of the T1C1, $\varepsilon_x$, $\varepsilon_y$, $\gamma_s$ and $m_f$ is determined by trial and error to obtain the quantitative and qualitative advancement of shoreline in T1C1 and $\Delta_t$ is selected as the maximum value to satisfy the stability criterion as mentioned earlier. Wave height variation in the cross-shore direction in profiles Y30 and Y24, alongshore wave height variation in profile X5.2, and sediment transport flux in profile Y24 are given in Figure 4.15.

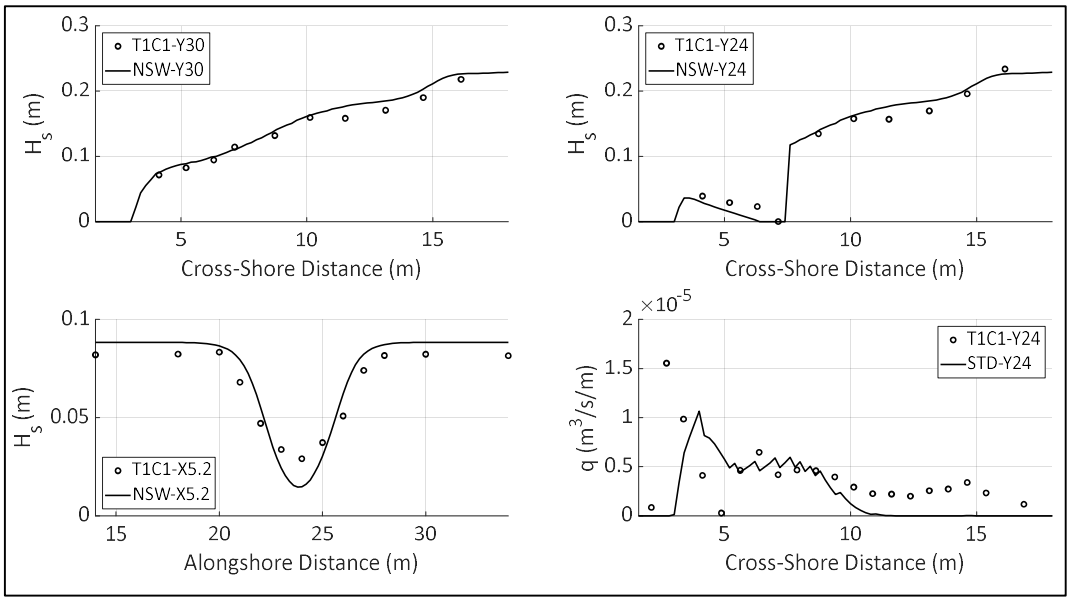


Figure 4.15 Wave height variation along Y30 (upper-left), Y24 (upper-right), X5.2 (lower-left) and sediment transport flux in Y24 (lower-right)

van den Berg et al. (2011) suggest that in the computation of orientation of the coast, instead of directly using the shoreline orientation, use of mean bathymetric orientation in the surf-zone is advised. Since wave characteristics in the surf-zone are not solely affected by the shoreline, it is affected by mean surf-zone orientation. Therefore, in their article, the mean of the surf-zone is computed in a defined box. This defined box's dimensions are introduced as four times of surf-zone width in alongshore direction and two times of surf-zone width in cross-shore dimension. In the Q-2DH model, a similar approach is followed. As previously explained, the Q-2DH model is not using shoreline orientation; rather, it uses local wave angles in computational cells, so a filter is applied to each computational cell to take effect of neighboring cells in the computation of the orientation. An illustration of the applied filter-box at the Y=26$^{th}$ and X=5$^{th}$ grid is given in Figure 4.16.

Significant wave heights of Gravens and Wang's Test 1 case are measured in alongshore direction between Y=14 m to Y=34 m and in cross-shore direction between X=4.125 m to X = 16.125 m with total of 125 points. MAPE for significant wave heights are computed in these points. Measurement points are illustrated in Figure 4.17.

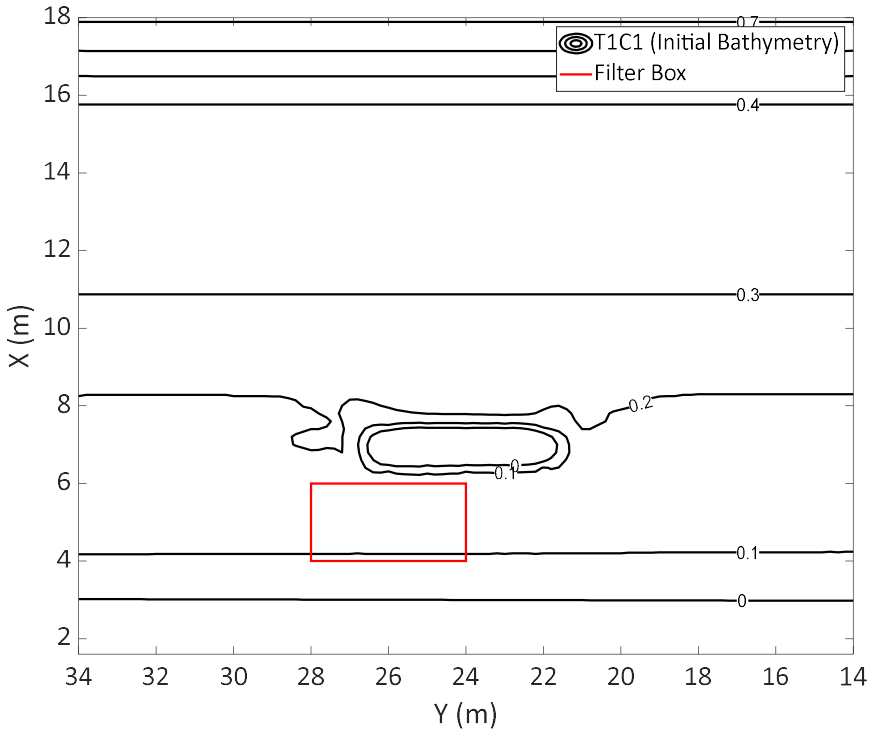


Figure 4.16 Filter box for local orientation at Y=26, X=5 grid

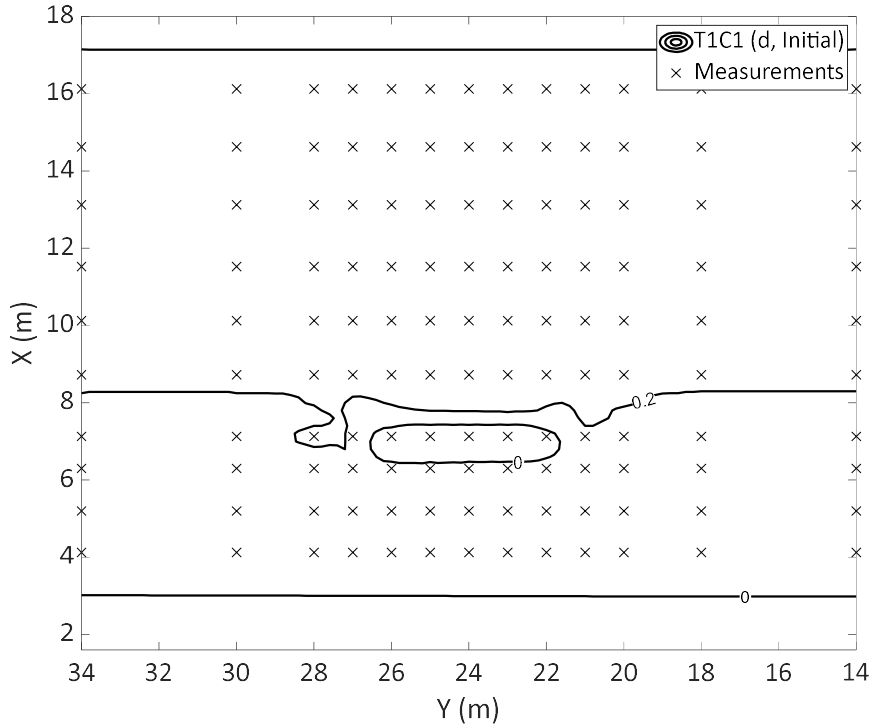


Figure 4.17 Measurement points of significant wave heights

Significant wave heights are computed and they are compared with experiment's results for T1C1 case in Figure 4.18.

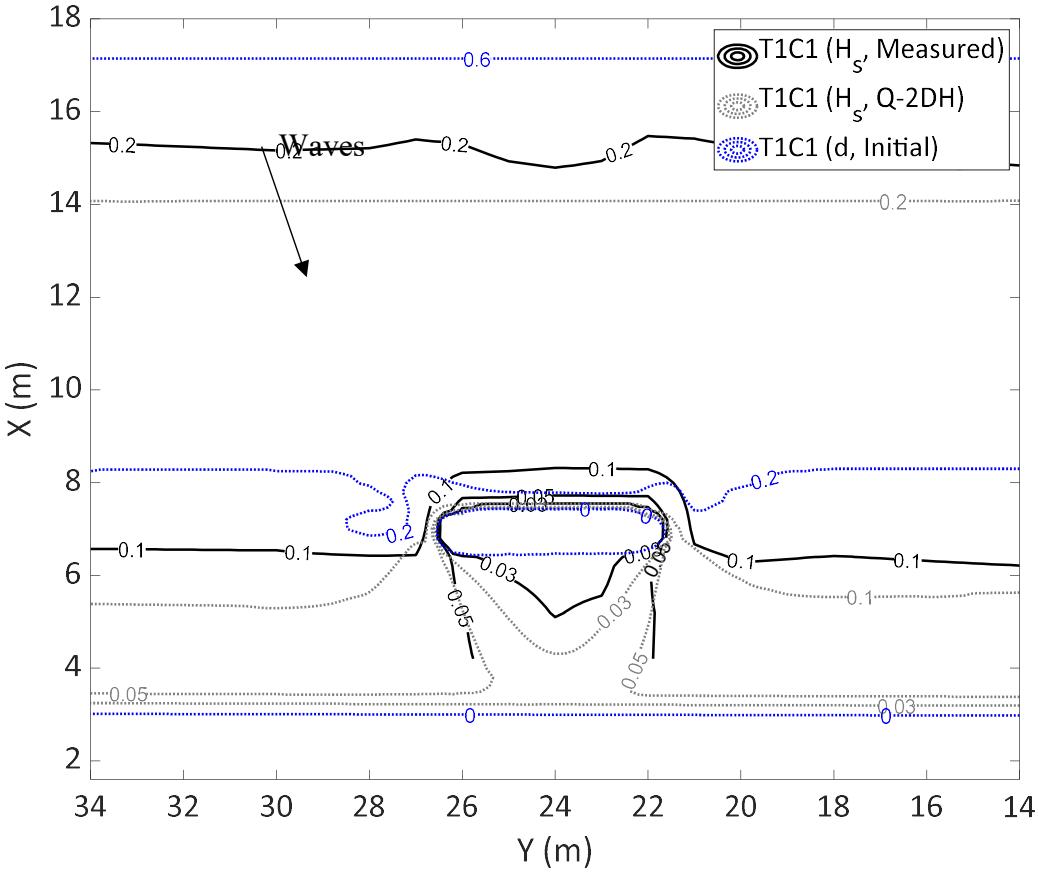


Figure 4.18 Comparison of significant wave heights of T1C1 (Measured) and T1C1 (Q-2DH)

MAPE is computed as 0.12 for significant wave heights with respect to the measured significant wave heights for the whole area. Measured and computed wave heights show some discrepancy in the whole model area.

No-filter condition and an average filter condition are studied, and results are compared in the Q-2DH model. Firstly, the T1C1 case is studied with mentioned parameter without any filter is applied to orientation. The comparison between Gravens and Wang's T1C1 and Q-2DH model's T1C1 is presented in Figure 4.19.

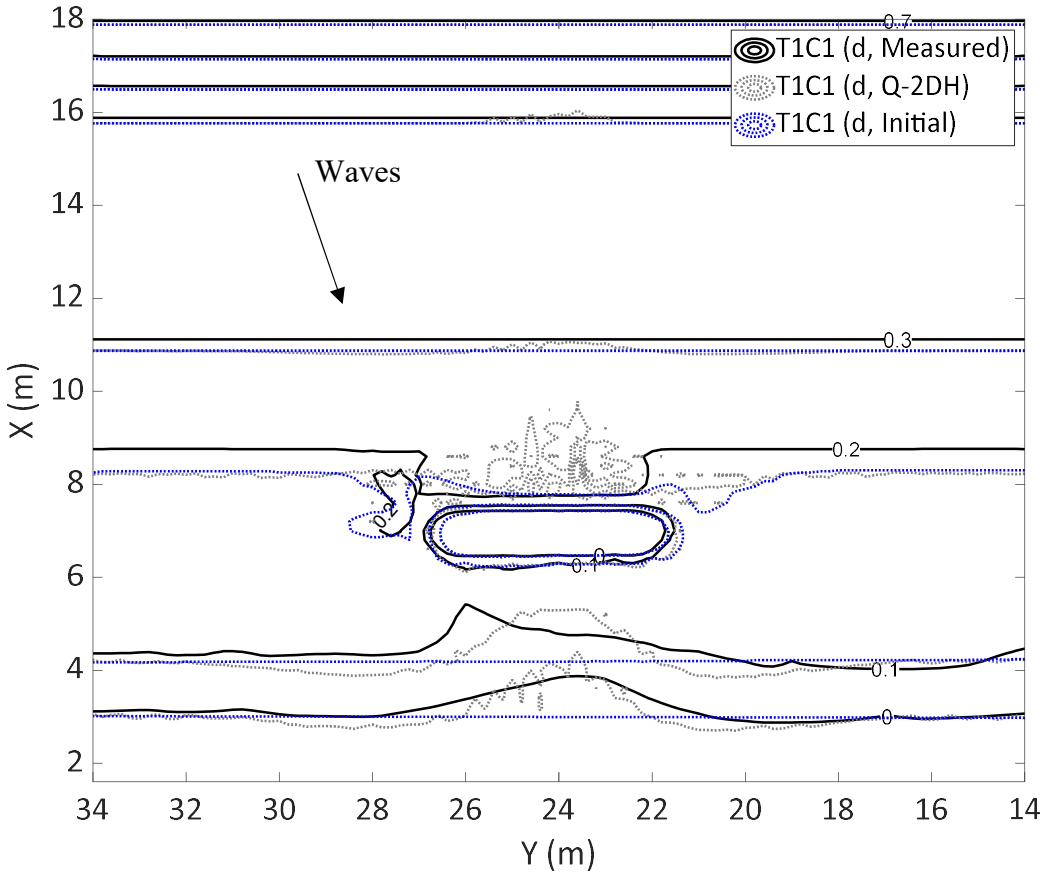


Figure 4.19 Comparison of depths for T1C1-Measured and T1C1-Q-2DH (Unfiltered)

In Figure 4.19, solid black lines are Gravens and Wang's measured result of T1C1, gray dotted lines are Q-2DH model's unfiltered T1C1 result, and blue dotted lines are the initial beach state of T1C1. According to the unfiltered result, in the breakwater's lee side, the measured case's 0.1-m depth contour is sloping through the left side. 0-meter contours are close with the model result. There are irregularities in the Q-2DH model's 0-meter contour. Maximum shoreline advancement is 0.88-meter, the retreat is 0.11 meters in measurement, and the advancement is 1.40 meters, and the retreat is 0.29 meters in the Q-2DH model. In both MAPE computation, extended lateral boundaries are not considered. Q-2DH model's shoreline MAPE with respect to measurements are found to be 0.0020 and areal MAPE is computed as 0.26. BSS for unfiltered condition is found as 0.72, 0.54 and 0.61 for BSS1, BSS2

and BSS3 respectively. Similarly, in the computation of BSS, only the lee-side of the offshore breakwater is considered. Van Rijn et al. (2003) states that “BSS is extremely sensitive to small changes when the denominator is low.” This means that if the whole area is selected for the BSS computation, depths that are not changed both in the model and in measurements through the modeling cause to BSS score to lower. However, in this problem, it is preferred to test the change of shoreline in the vicinity of the offshore breakwater. Moreover, to be able to understand morphology change with respect to changing depth intervals, three cases are considered; BSS1, which is calculated with lower depths, BSS2 computed with higher depths, and BSS3 computed with all depth in the lee-side of the offshore breakwater. BSS1 includes a depth interval of 0-0.08 m, BSS2 includes a depth interval of 0.08-0.16, and BSS3 includes 0-0.16.

Secondly, T1C1 is studied with the average filter; for filter size, two times of surf-zone width is accepted in alongshore direction, and one surf-zone width is accepted in cross-shore direction. Measured results and Q-2DH model results are compared in Figure 4.20. In Figure 4.20, there are irregularities in bottom contours in sides and offshore side of the offshore breakwater. Moreover, the shoreline path is very close to the measured shoreline; the 0.1-meter contour is not aligned to the breakwater's left side. For the average filter case, maximum shoreline advancement is 0.80 meters, and maximum shoreline retreat is 0.39 meters. Areal MAPE is computed as 0.26 with respect to measurements. MAPE for shoreline change is computed as 0.0024 for averaged filter case with respect to measurements. BSS1, BSS2, and BBS3 are computed as 0.83, 0.62, and 0.71 respectively for this case, which is classified as good.

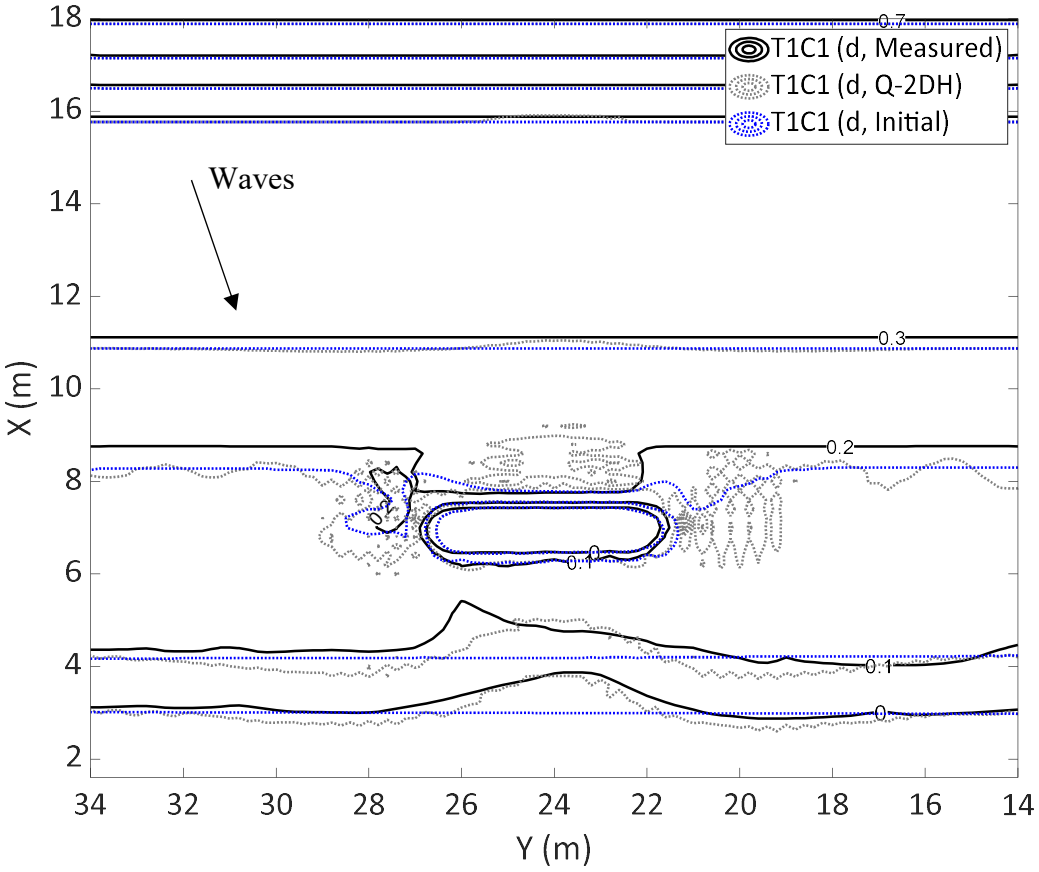


Figure 4.20 Comparison of depths for T1C1-Measured and T1C1-Q-2DH (Average filtered)

To sum up, for the T1C1 case, unfiltered and average filter cases are studied. For each case, MAPE for shoreline change, areal MAPE and BSS values for the offshore breakwater's lee-side are computed. BSS and MAPE criteria are assessed for unfiltered and average filter cases. Considering BSS and MAPE, in further simulations average filter is used to model experiments.

### 4.4.2 T1C2

T1C2 consists of 181 minutes of the experiment under wave and wave generated current. All parameters which are determined in the T1C1 case are used to model the T1C2 case. The same number of computational cells are defined both in the x and y-

direction. Computed significant wave heights and measured significant wave heights are compared in Figure 4.21.

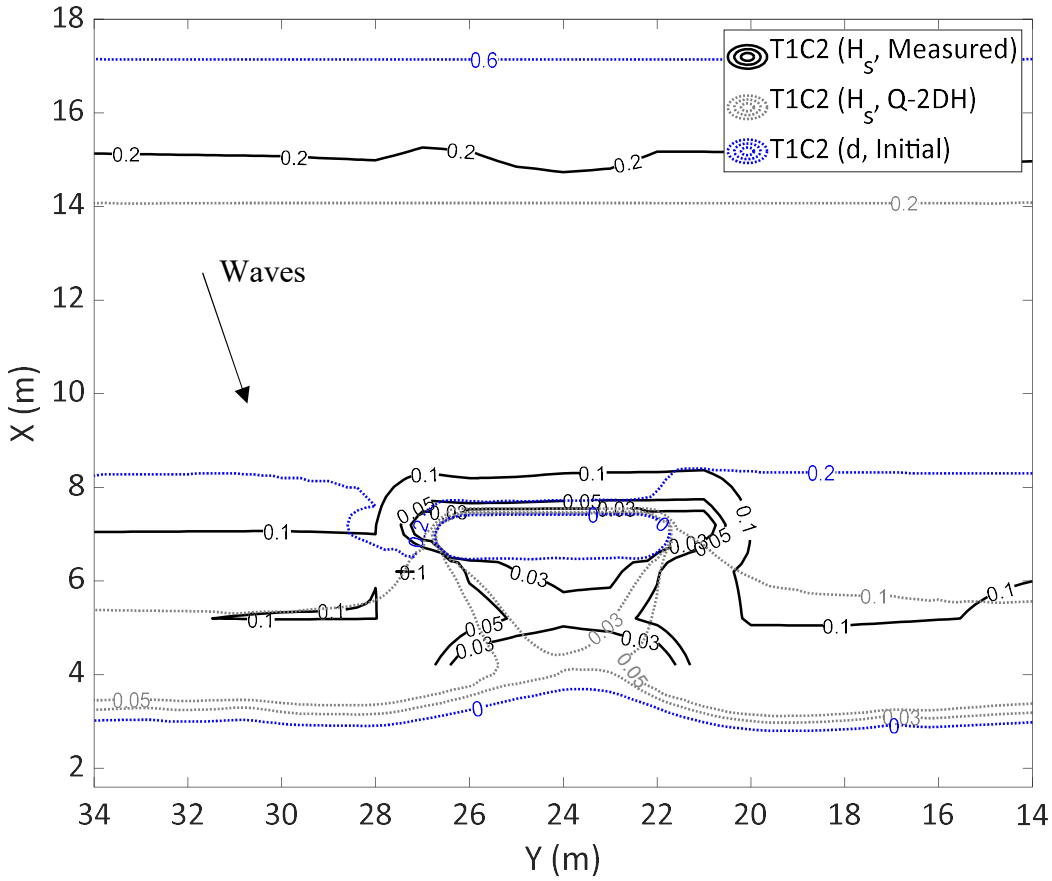


Figure 4.21 Comparison of significant wave heights for T1C2 (Measured) and T1C2 (Q-2DH)

MAPE for Q-2DH's significant wave height is computed as 0.12 with respect to T1C2 experiment results. Measured depth results are co-plotted with Q-2DH results in Figure 4.22.

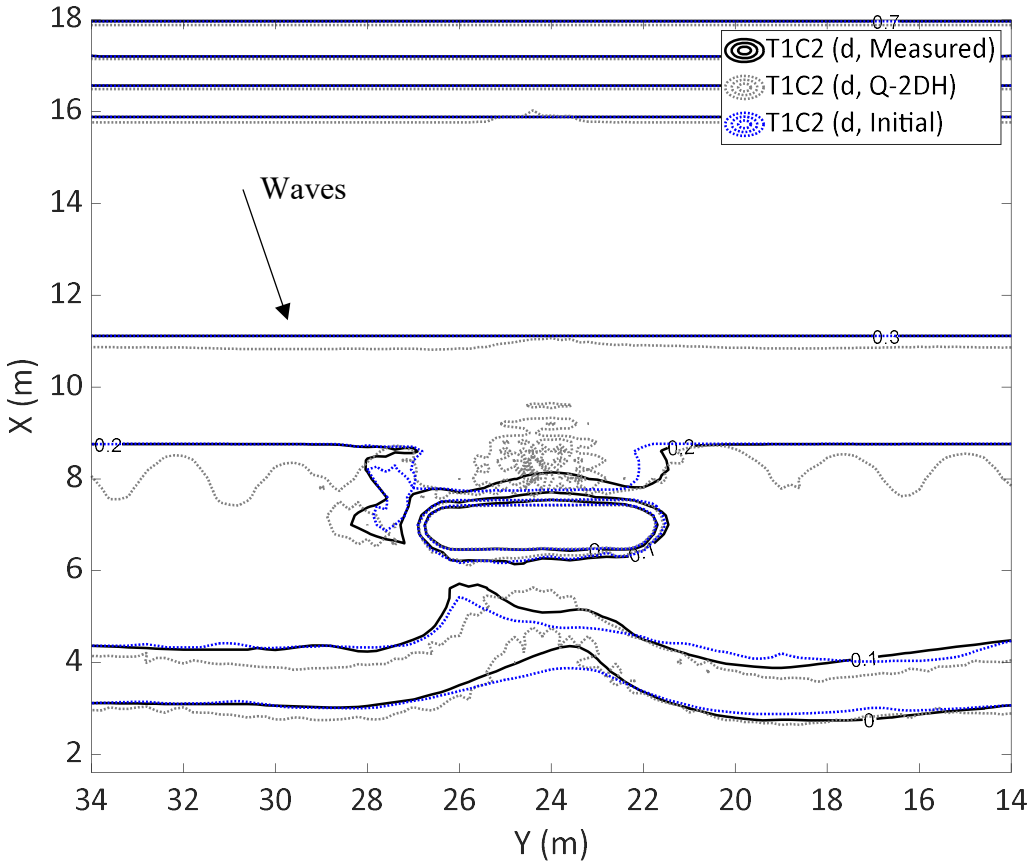


Figure 4.22 Comparison of depths for T1C2 (Measured) and T1C2 (Q-2DH)

Figure 4.22 shows that the Q-2DH model overestimates the shoreline advancement in the T1C2 case; the 0.1-meter contour is similar to the measurement's case. Maximum shoreline advancement for measurement with respect to the T1C1 result is computed as 0.48 meters, and for the Q-2DH model, it is computed as 1 meter. The maximum shoreline retreat is 0.34 meters for the model and 0.25 meters for the experiment. Areal MAPE is computed as 0.37 and MAPE for shoreline is 0.0011. BSS1, BSS2 and BSS3 are computed as 0.71, -0.45 and 0.50 respectively.

### 4.4.3 T1C3

T1C3 lasts 185 minutes. It consists of wave and wave generated current in the model basin. The equilibrium profile is reconstructed from Y38 to Y30 before the

experiment. All parameters defined in the T1C1 case are used in the T1C3 case as well. The same number of computational cells are defined in both the x and y-direction.

Significant wave heights are compared for measured and Q-2DH cases and illustrated in Figure 4.23.

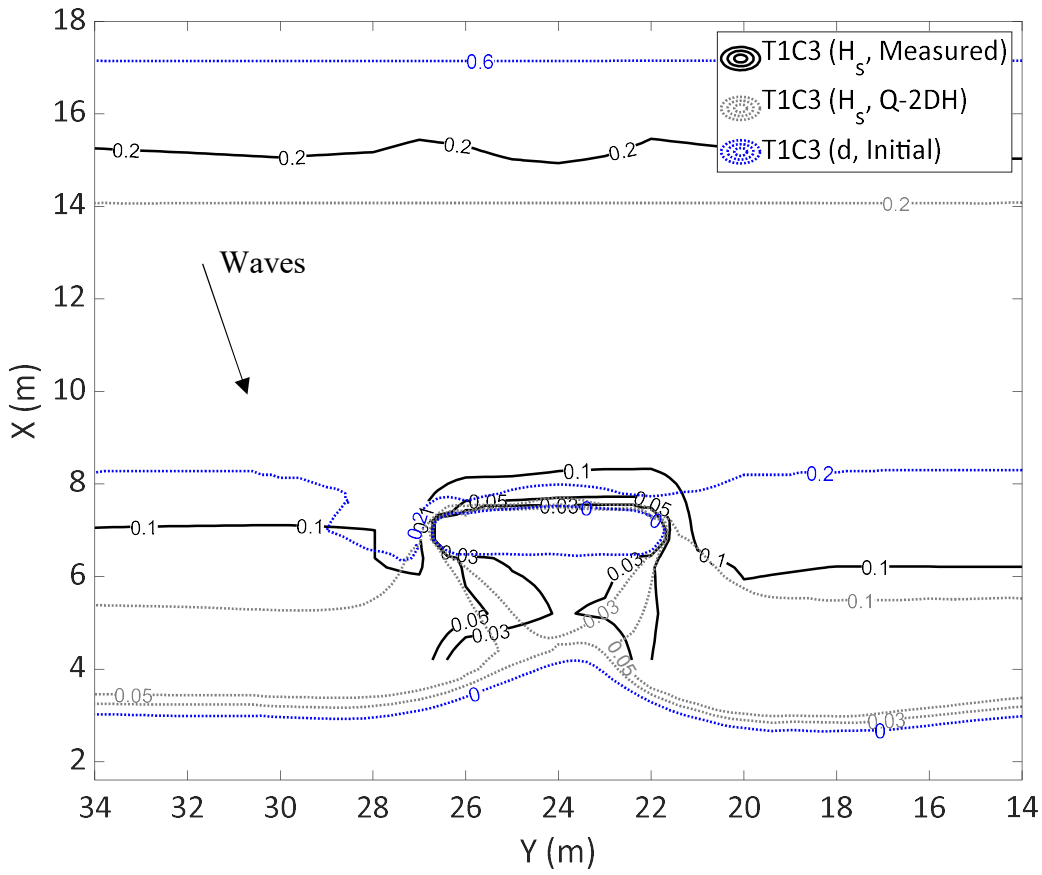


Figure 4.23 Comparison of significant wave heights for T1C3 (Measured) and T1C3 (Q-2DH)

MAPE of the significant wave heights is computed for the Q-2DH model with respect to measurements as 0.11. Depths of measured and computed results are plotted in Figure 4.24.

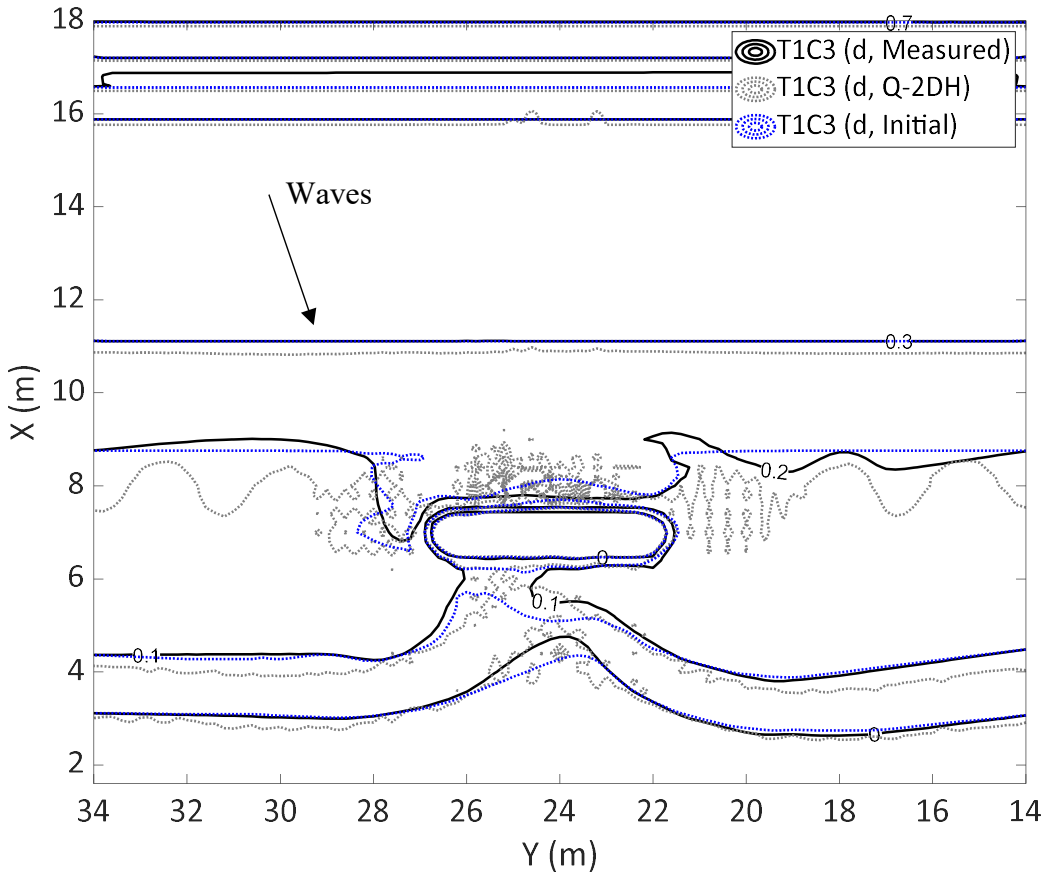


Figure 4.24 Comparison of depths for T1C3 (Measured) and T1C3 (Q-2DH)

In Figure 4.24, the shoreline is very similar to experimental results. 0.1-meter contour is quantitively similar in the lee-side of the breakwater. In the Q-2DH model, the 0.1-meter contour is started to incline the left side, which is similar to the experiment's behavior. In model 0.1-meter, contour's left and right sides of the offshore breakwater stay behind those of experiments. Maximum advance and retreat in shoreline with respect to T1C2 case computed as 0.54 and 0.20 meter for Q-2DH model, 0.49 and 0.11 meter for the experiment. MAPE of shoreline is computed as 0.0258 for the T1C3 case and MAPE for areal is computed as 0.29. BSS1, BSS2 and BSS3 are computed as T1C4 -1.26, 0.07 and -0.42 respectively.

### 4.4.4 T1C4

T1C4 consists of 192 minutes run with waves and wave generated currents. All parameters which are defined in T1C1 is reused in this case. Computed significant wave height and measured significant wave heights are co-plotted in Figure 4.25.

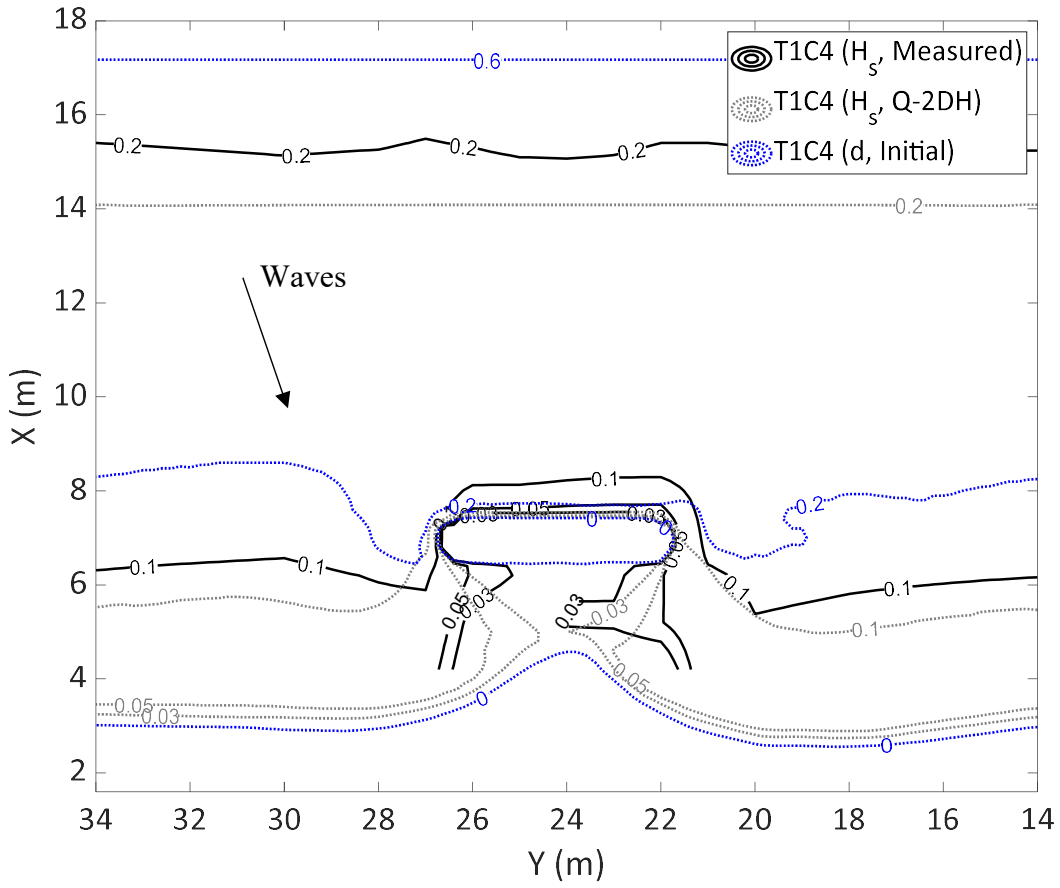


Figure 4.25 Comparison of significant wave height for T1C4 (Measured) and T1C4 (Q-2DH)

In Figure 4.25, significant wave heights of Q-2DH and measurements are plotted. MAPE for the significant wave field is computed as 0.14 with respect to measurements. Depths of experiment results and model results are illustrated in Figure 4.26.

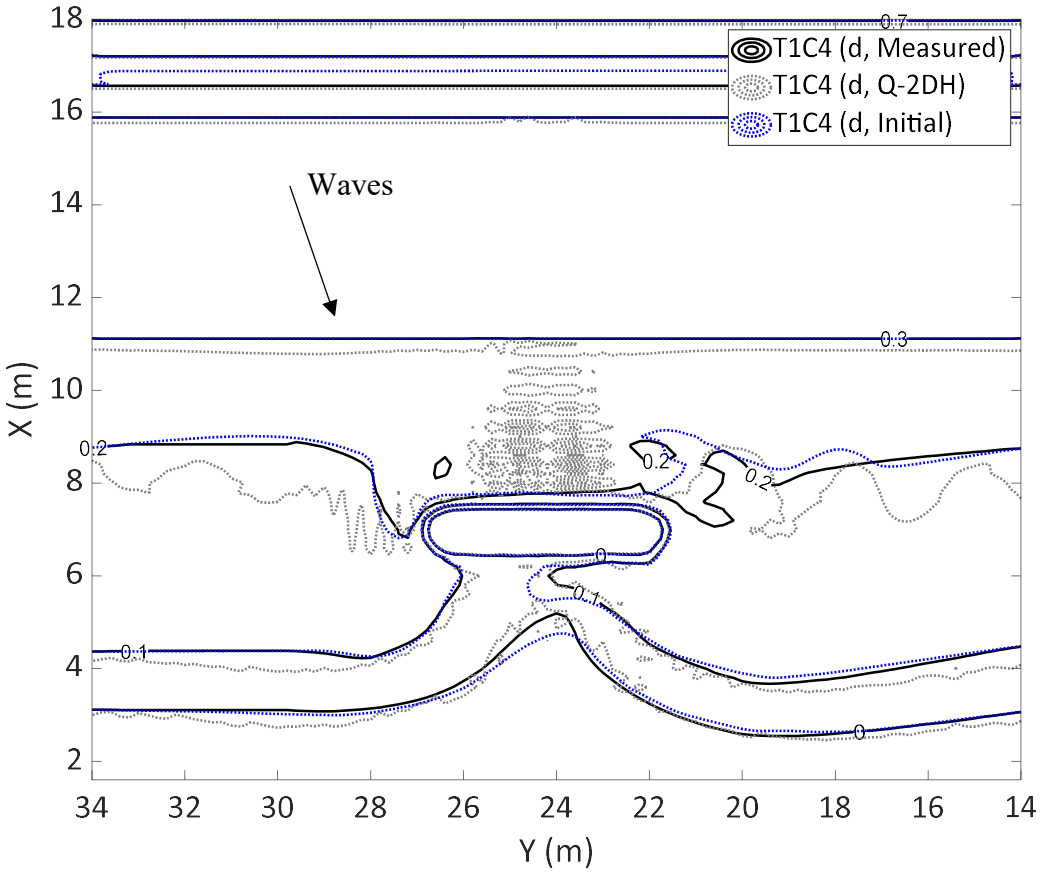


Figure 4.26 Comparison of depths for T1C4 (Measured) and T1C4 (Q-2DH)

In Figure 4.26, T1C4's experiment measurements and numerical model results are compared. Gray dotted lines are Q-2DH's results, solid black lines are experiment results, and blue dotted lines are the initial position of contours. In the lee-side of the breakwater, contour lines are quantitatively and qualitatively similar to each other. In left and right side of breakwater erosion occurs relatively more than experiment results. Maximum advance and retreat along the shoreline with respect to T1C3 case computed as 0.72 and 0.30 meter for model and 0.44 and 0.18 meter for the experiment. Areal MAPE is computed as 0.22 and MAPE for shoreline computed as 0.0068. BSS1, BSS2 and BSS3 are computed as -1.45, -0.03 and -0.65 respectively.

### 4.4.5 T1C5

T1C5 lasts 176 minutes. Waves and wave generated currents occur in the basin. Q-2DH model is used to study T1C5 with previously defined parameters in the T1C1 case. Significant wave heights of measured and the model is given in Figure 4.27.

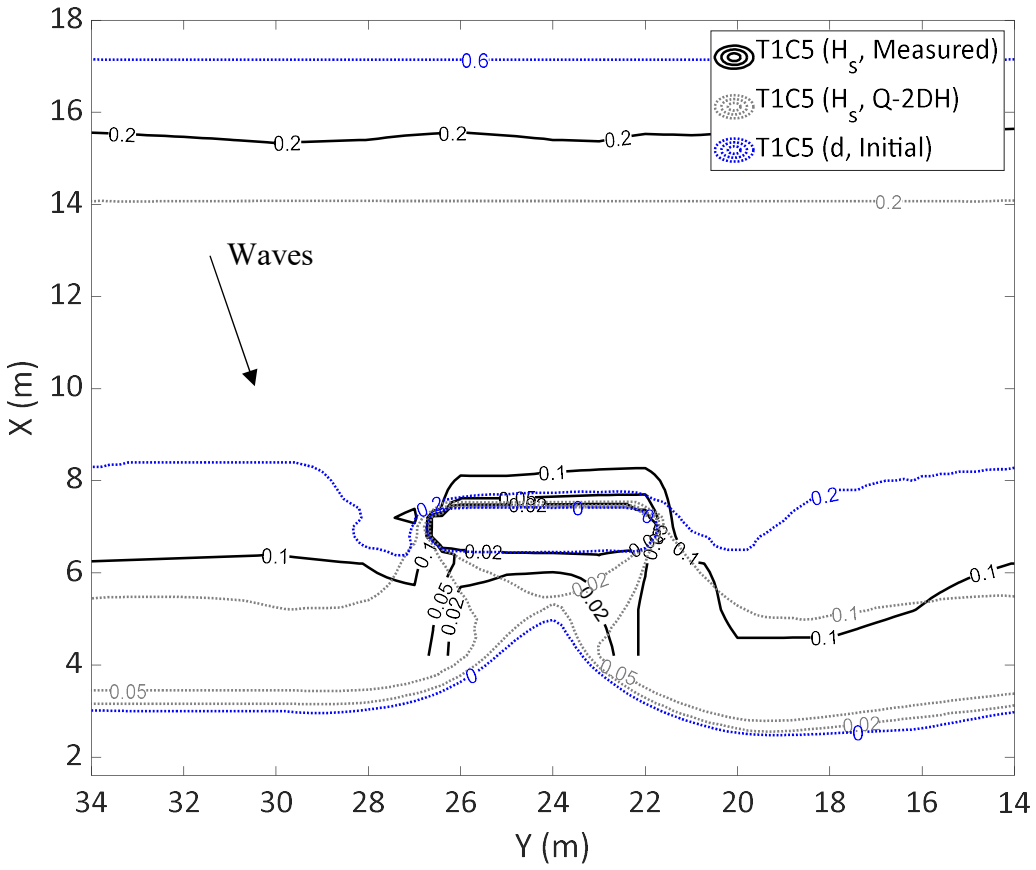


Figure 4.27 Comparison of significant wave heights for T1C5 (Measured) and T1C5 (Q-2DH)

MAPE is computed for T1C5 case as 0.16. Depth comparison of measured and predicted results are given in Figure 4.28.

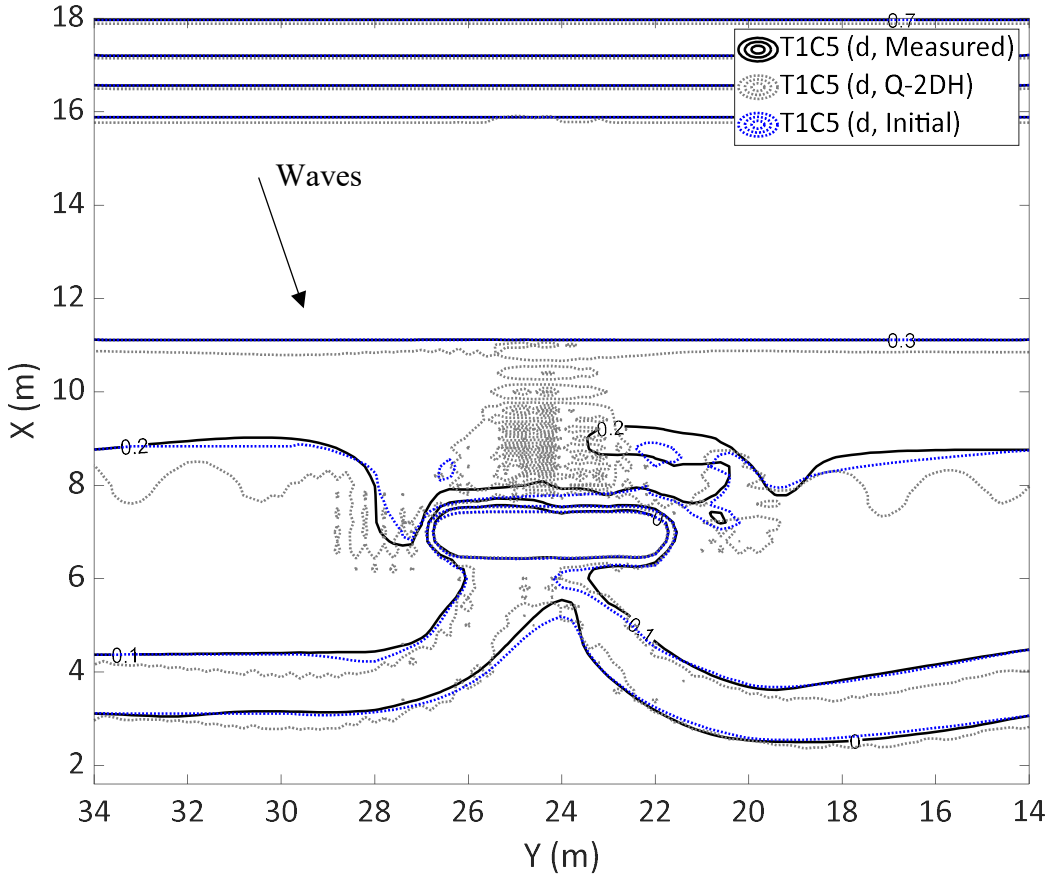


Figure 4.28 Comparison of depths T1C5 (Measured) and T1C5 (Q-2DH)

In Figure 4.28, T1C5's experiment measurements and numerical model results are compared. In the lee-side of the breakwater, the 0.1-meter contour and shoreline are closely similar to experimental results. On the breakwater's left and right side, the shoreline recedes more in model results than experiments. Maximum advance and retreat in shoreline with respect to T1C4 case computed as 0.82 and 0.33 meter for model and 0.37 and 0.11 meter for the experiment. MAPE for shoreline computed as 0.0019 and areal MAPE is computed as 0.29. BSS1, BSS2 and BSS3 are computed as -2.93, -0.91 and -2.00 respectively.

### 4.4.6 T1C6

T1C6 is a 189 minutes experiment run consist of waves and wave generated currents. Before executing T1C6, the beach profile was reconstructed to the equilibrium profile in profiles Y38 to Y30 in the updrift part. Parameters for Q-2DH are defined previously in the T1C1 case is used in T1C6. Comparison of significant wave height for measurements and computations are given in Figure 4.29.

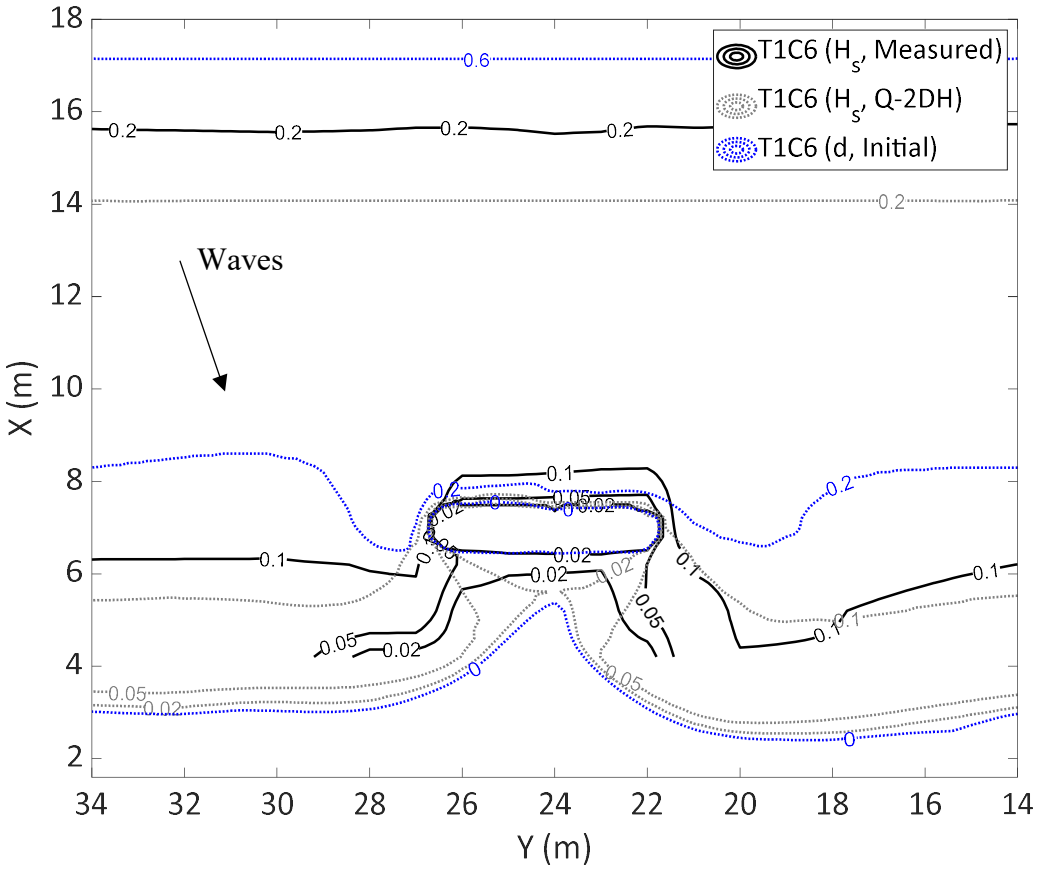


Figure 4.29 Comparison of significant wave heights for T1C6 (Measured) and T1C6 (Q-2DH)

MAPE for T1C6 is computed as 0.15 with respect to measurements. Comparison of depth measurements and the model depth results are compared in Figure 4.30.

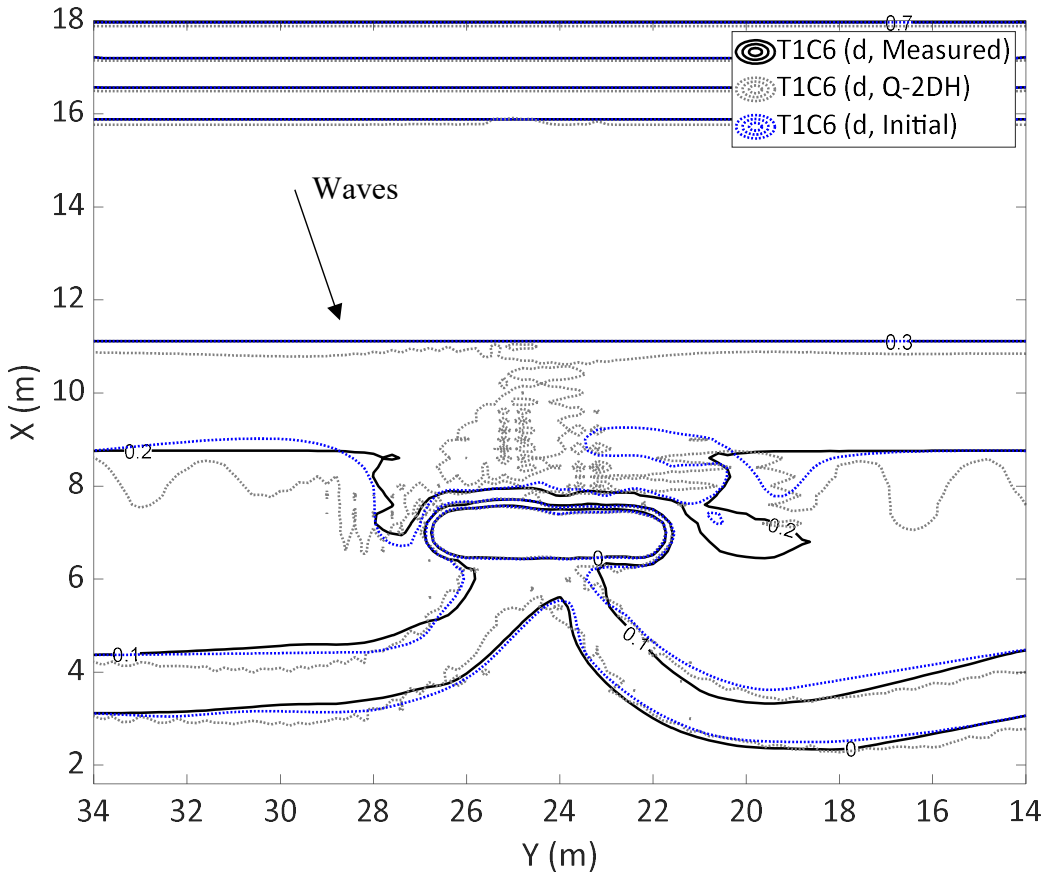


Figure 4.30 Comparison of depths for T1C6 (Measured) and T1C6 (Q-2DH)

Figure 4.30 shows that both shoreline and 0.1-meter contour is close to experimental results. In the updrift (left) part, the shoreline and 0.1-meter contour are much more advanced than the model. And in the downdrift part (right side), erosions are similar, yet around Y18, experiment contours are advanced than model results. Regarding the T1C5 case, maximum shoreline advance and recede are found to be 0.78 and 0.56 meters for the Q-2DH model and 0.23 and 0.31 meters for the experiment case. MAPE for shoreline change is 0.0067 and MAPE for areal is computed as 0.22. BSS1, BSS2 and BSS3 are found as -2.78, -1.21 and -2.22 respectively.

### 4.4.7 T1C7

T1C7 involves a 191-minute laboratory experiment with waves and wave generated currents. Model parameters of T1C1 are used here as well. Comparison of Q-2DH's and measurement's significant wave heights are illustrated in Figure 4.31.

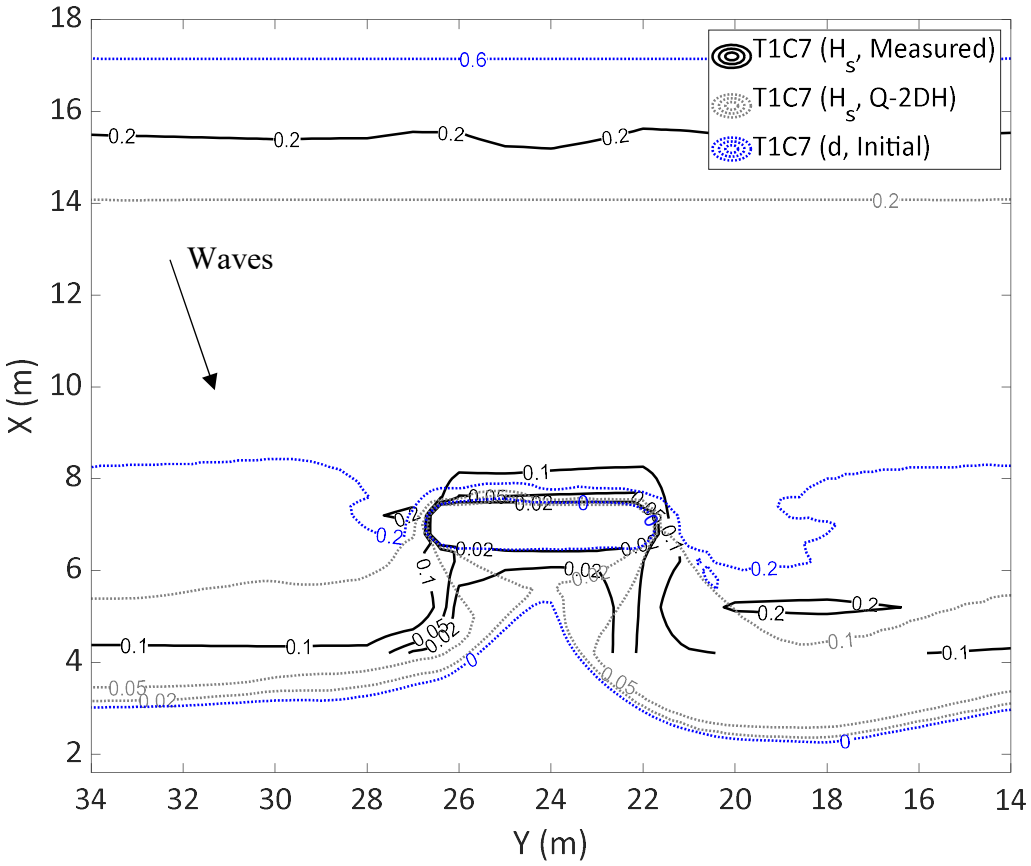


Figure 4.31 Comparison of significant wave height for T1C7 (Measured) and T1C7 (Q-2DH)

MAPE for significant wave height is computed as 0.18 for T1C7 case. Comparison of measurement and model results are illustrated in Figure 4.32.

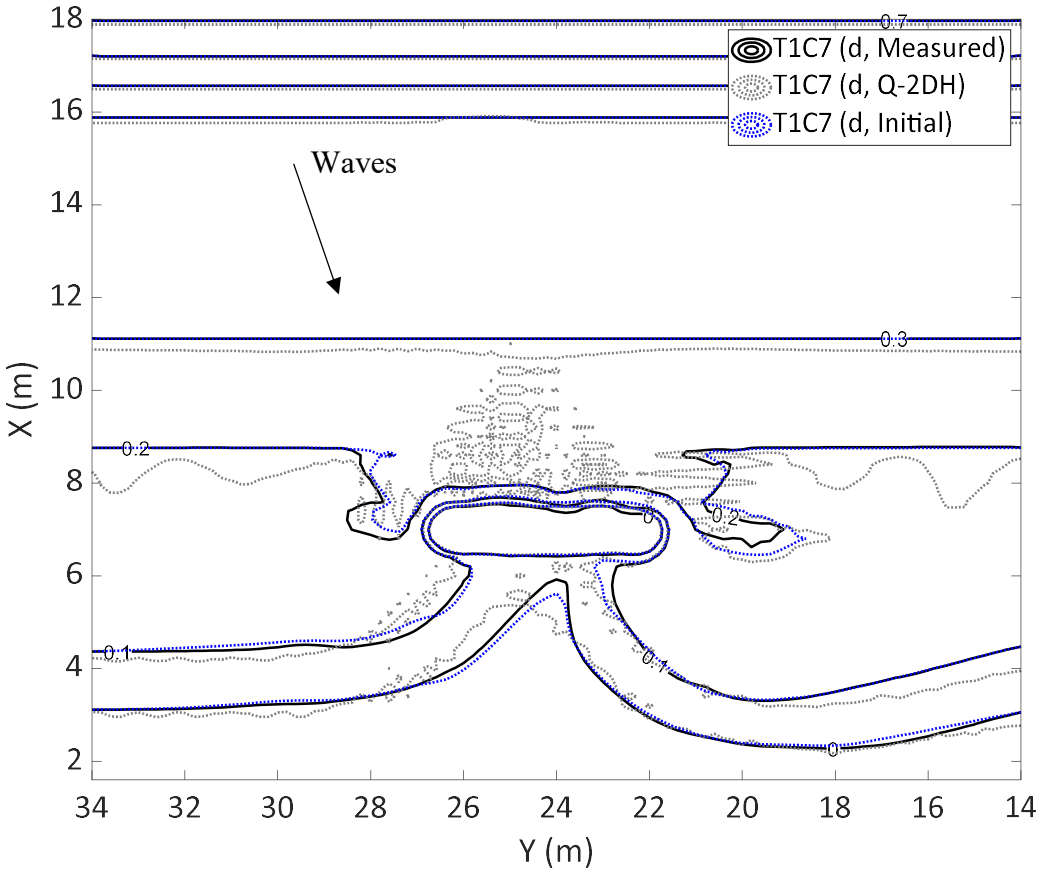


Figure 4.32 Comparison of depths for T1C7 (Measured) and T1C7 (Q-2DH)

In Figure 4.32, the model results' shoreline could not advance through the breakwater, and instead it thicknesses along the alongshore direction are increased. 0.1-meter contour is similar to experimental results. Areal MAPE is computed as 0.28 and MAPE for shoreline change is computed as 0.0036. BSS1, BSS2 and BSS3 are found to be -8.47, -2.99 and -6.43.

### 4.4.8 T1C8

T1C8 is 184 minutes of run with waves and wave generated currents. In experiment results, after the completion of T1C8, tombolo formation occurs in the offshore breakwater lee-side. To model T1C8, Q-2DH model parameters, which are defined

in T1C1, is used. Firstly, computed significant wave heights with Q-2DH and measured results are compared for T1C8 case in

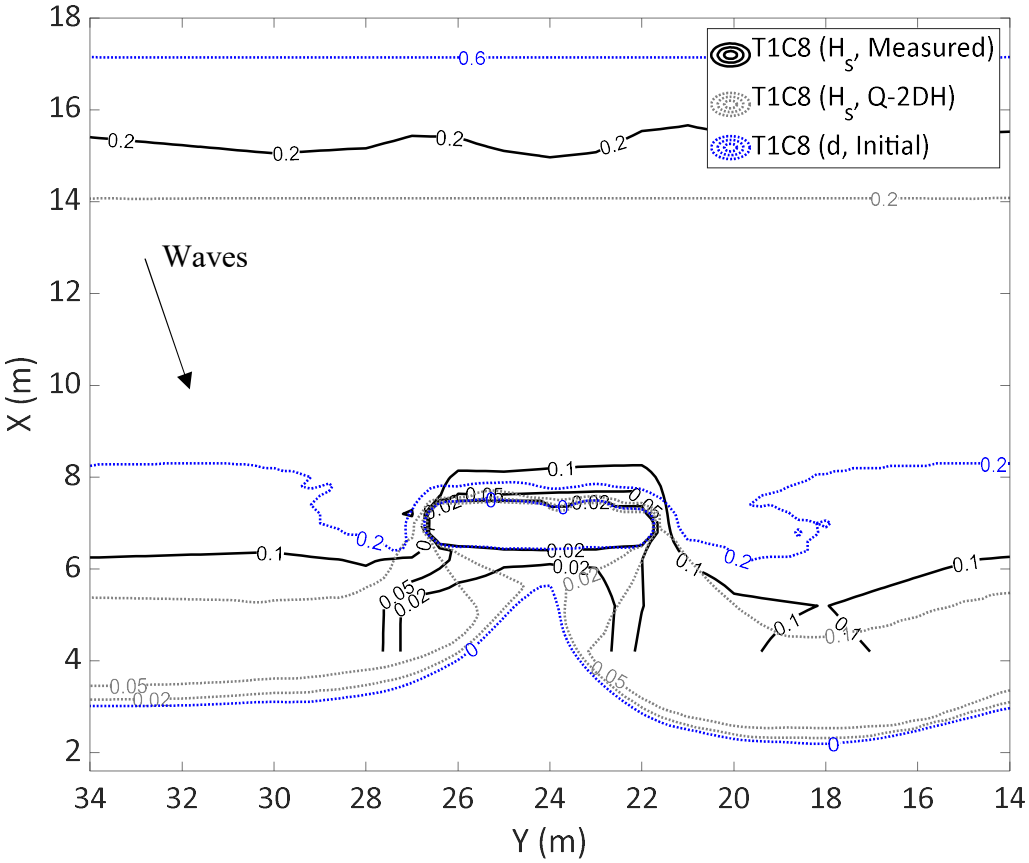


Figure 4.33 Comparison of significant wave heights for T1C8 (Measured) and T1C8 (Q-2DH)

MAPE for significant wave height is computed as 0.16. Comparative depth results of measurements and the model is given in Figure 4.34.

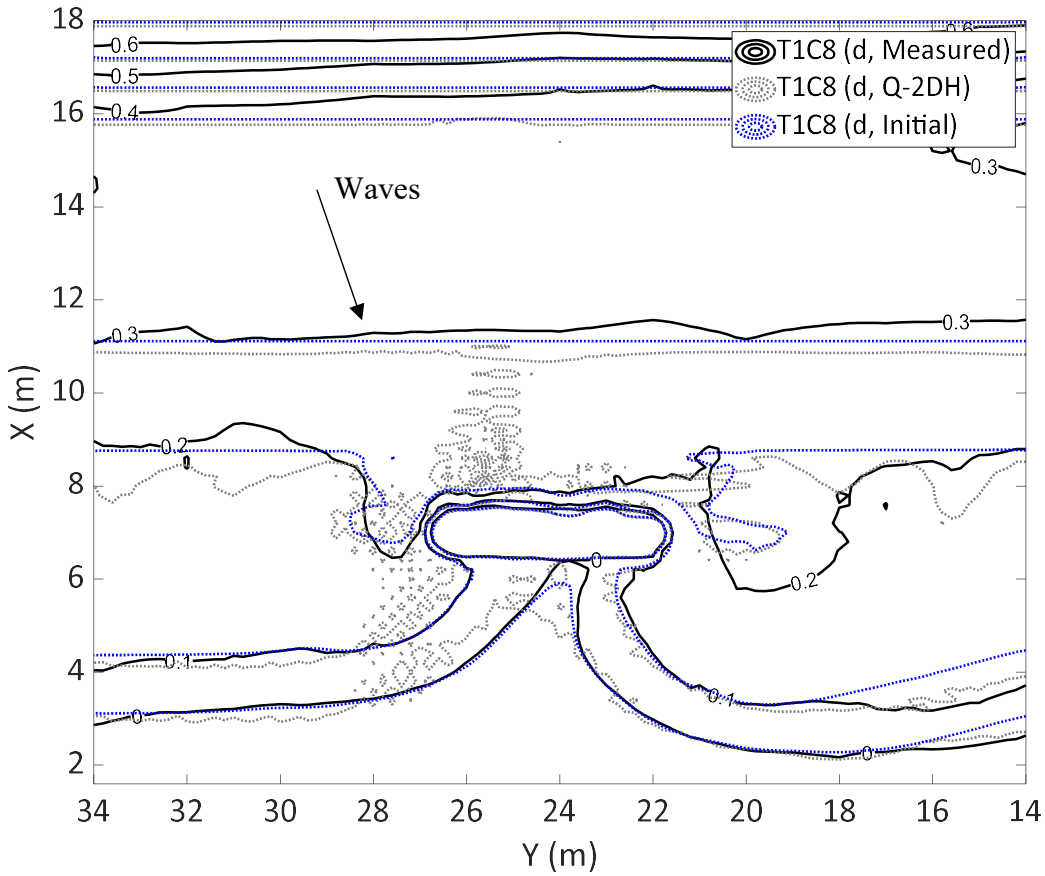


Figure 4.34 Comparison of depths for T1C8 (Measured) ant T1C8 (Q-2DH)

Figure 4.34 illustrates that the model's shoreline could not form a tombolo in the offshore breakwater lee-side. Although, the 0.1-meter contour is similar to the experiment's 0.1-meter contour. Areal MAPE is computed as 0.31 and MAPE for shoreline change is computed as 0.01. BSS1, BSS2 and BSS3 are found as -7.93, -2.95 and -6.07 respectively for T1C8 case.

### 4.4.9 T1C1-T1C2

Q-2DH model is studied to work from the beginning of the experiment until the model's interruption due to an error which is equivalent to the end of T1C2. The total model run time is 366 minutes. For the Q-2DH model, previously defined parameters are used. Comparison of significant wave heights for this case is the same as the

T1C1 case which is shown in Figure 4.18. Comparison of depths for measured and modeled results are given in Figure 4.35.

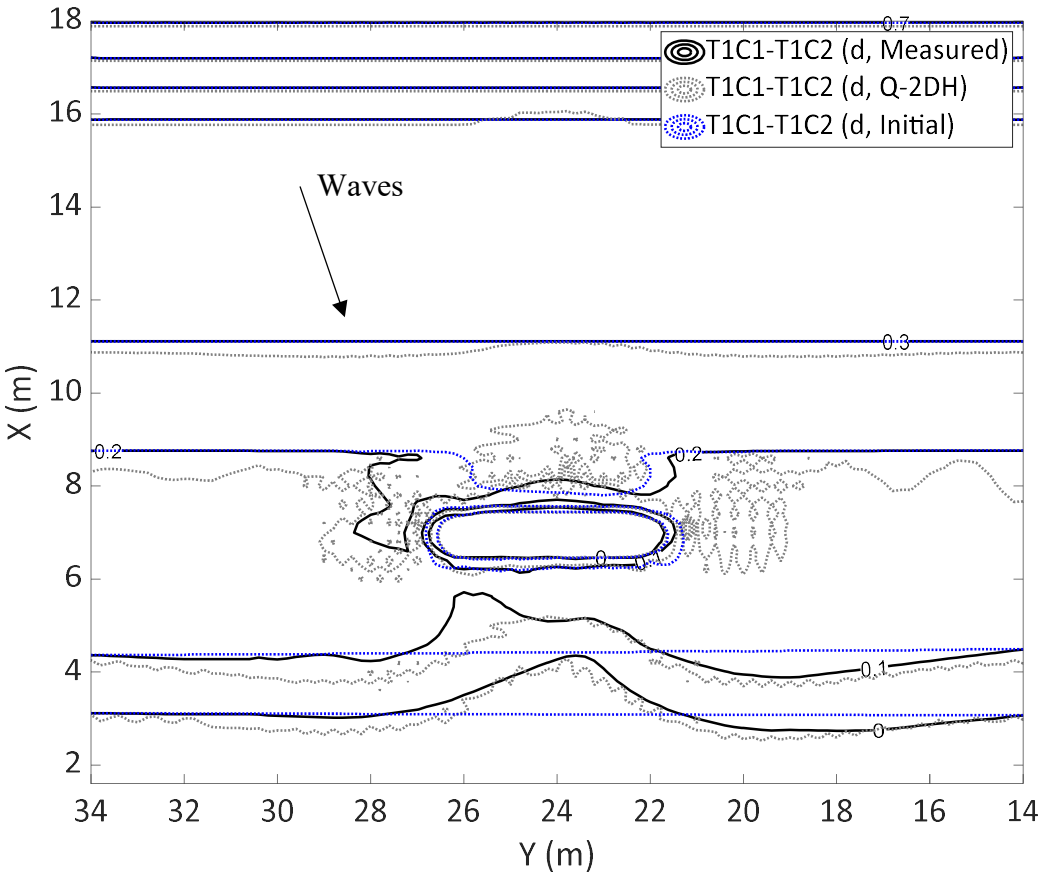


Figure 4.35 Comparison of depths for T1C1-T1C2 (Measured) and T1C1-T1C2 (Q-2DH)

Figure 4.35 shows that both shoreline and 0.1-meter contour is close to experimental results. In the updrift (left) part, the shoreline and the 0.1-meter contour are much more advanced than the model. And in the downdrift part (right side), erosions are similar, yet around Y18, experiment contours are positioned more offshore side than model results. With respect to initial bathymetry, maximum shoreline accumulation and recede is found to be 1.19 and 0.56 meter respectively for the Q-2DH model and 1.27 and 0.34 meter for experiment case. MAPE for shoreline change is 0.0015, areal MAPE is 0.37 and BSS1, BSS2, and BSS3 are computed as 0.85, 0.58, and 0.74 for this case.

The summary of significant wave height results is tabulated in Table 4.3.

Table 4.3 Summary of significant wave height results

| *Case Name* | *T1C1* | *T1C2* | *T1C3* | *T1C4* | *T1C5* | *T1C6* | *T1C7* | *T1C8* | *T1C1-T1C2* |
|---|---|---|---|---|---|---|---|---|---|
| MAPE | 0.12 | 0.12 | 0.11 | 0.14 | 0.16 | 0.15 | 0.18 | 0.16 | 0.12 |

The summary of topography results is tabulated in Table 4.4.

Table 4.4 Summary of topography results

| *Case Name* | *Duration (min)* | *MAPE (Areal)* | *MAPE (Shoreline)* | *BSS1** | *BSS2*** | *BSS3**** |
|---|---|---|---|---|---|---|
| T1C1 | 185 | 0.26 | 0.0024 | 0.83 | 0.62 | 0.71 |
| T1C2 | 181 | 0.37 | 0.0011 | 0.71 | -0.45 | 0.5 |
| T1C3 | 185 | 0.29 | 0.0258 | -1.26 | 0.07 | -0.42 |
| T1C4 | 192 | 0.22 | 0.0068 | -1.45 | -0.03 | -0.65 |
| T1C5 | 176 | 0.29 | 0.0019 | -2.93 | -0.91 | -2 |
| T1C6 | 189 | 0.22 | 0.0067 | -2.78 | -1.21 | -2.22 |
| T1C7 | 191 | 0.28 | 0.0036 | -8.47 | -2.99 | -6.43 |
| T1C8 | 184 | 0.31 | 0.01 | -7.93 | -2.95 | -6.07 |
| T1C1-T1C2 | 366 | 0.37 | 0.0015 | 0.85 | 0.58 | 0.74 |

* (0-0.08 m), ** (0.08-0.16 m), *** (0-0.16 m)

In summary, in this chapter Q-2DH model's performance is studied comparatively with laboratory experiments. First of all, each individual case is studied separately to observe the performance and possible causes of errors in the model. Then, initial bathymetry is studied until the model poses a problem and stops executing which is

approximately at the end of the T1C2 case. For significant wave heights, it is computed that all MAPE values are in the range of 0.12-0.18. Interval of MAPE does not vary much. Therefore, significant wave height computations' accuracy are approximately equal and it does not contain high error. It is observed that, in almost all cases, MAPE for shoreline change is in the range of 0.0011 to 0.01, which are not highly scattered, and it can be defined as correlative with measurements. If shoreline position change is purely the criteria for the model's success, then it can be concluded that estimations are close to measurements. Areal MAPE is computed in the range of 0.22-0.37 for every cases. Considering the interval, model results are not highly scattered from experiment measurements. On the other hand, BSS1 values that indicate the model's performance in lower depths (0-0.08 m) vary vastly in each case. BSS1 interval is between 0.85 to -8.47. Where 0.85 can be classified as excellent and -8.47 as bad (Table 4.2). Overall, in initial cases (T1C1, T1C2, and T1C1-T1C2) BSS1 scores are very high. As salient progresses through the offshore breakwater (T1C3 to T1C8), BSS1 significantly reduces. BSS2 values, which indicate the higher depths' performance (0.08-0.16 m) are ranging in the interval of 0.62 to -2.99. Estimation of morphology evolution in higher depths are lower than estimation in lower depths. A similar pattern exists in BSS2 as well; as cases progress from T1C1 to T1C2 BSS2 scores start to reduce. BSS3, which represents the whole area in the breakwater's lee-side, varies from 0.74 to -6.43. 0.74 can be classified as good, and -6.43 is bad. The same behavior exists in BSS3 as well; as salient progresses through the offshore breakwater, BSS3 values are reducing. In initial cases, T1C1, T1C2, and T1C1-T1C2 cases, all BSS scores are in the interval of good/excellent. That means, regarding both MAPE for shoreline change and all BSS, the Q-2DH model successfully models those three cases. However, in further cases (T1C3 to T1C8), the Q-2DH model could not successfully model cases. As the shoreline advances through the offshore breakwater, incoming wave angles and orientation of bottom contours behind the offshore breakwater are increasing. An increase in angles causes the model not to represent the sediment transport behind the offshore breakwater accurately and lead to instabilities in the model. Also, from the figures, it can be

concluded that there exist many irregularities in the computational cells in the model's contour maps. Transitions in neighboring cells are not smooth. Those irregularities accumulate over time, and it causes the model to give probable stability errors due to highly chaotic bathymetry.

# CHAPTER 5

## CONCLUSIONS AND FURTHER RECOMMENDATIONS

This thesis's major focus is to develop a quasi-2-dimensional numerical model to numerically model shoreline changes under wave action in the vicinity of coastal structures, which is applicable in both the medium and long term. Goals are; computation of wave field in the vicinity of structures with the use of a spectral wave model (NSW), rather than geometric/parametric computations as in one-line models and to incorporate aforementioned wave solver (NSW) to compute longshore sediment transport directly and to distribute the transport rates based on nearshore wave characteristics, thus increasing the accuracy of estimation of shoreline behavior. Also, computation of cross-shore and swash zone sediment transport mechanisms without complex expressions are among goals. Hence, eliminating complex nearshore circulation computations as in complex 2D and 3D models. In summary, to develop a Q-2DH model applicable in medium to long-term applications with precise modeling compared to one-line models and a faster computation tool than complex 2D and 3D models. To benchmark the model, investigation of computed sediment field with theoretical cases (beach cusps, cross-shore sediment transport, single groin) and validation of the model results with laboratory measurements are studied.

Q-2DH model consists of 3 modules. The first module is the wave transformation module (NSW; Baykal, 2012). It is a phase-averaged spectral wave module that solves the energy balance equation. The second module is the sediment transport module (STD). STD consists of longshore sediment transport, cross-shore sediment transport, alongshore sediment diffusivity, and swash zone transport. For the longshore sediment transport, a bulk sediment transport formula is used, and it is distributed over the surf zone. For cross-shore sediment transport, an expression based on van den Berg et al. (2011) is defined to preserve the equilibrium profile in

a relatively long-time scale. An alongshore diffusivity term is based on van den Berg et al. (2011) is defined to eliminate the growth of small-scale error is introduced. In swash zone dynamics, wave set-up term adopted from Goda (2008) is introduced to include sediment transport around the shoreline, and a shore relaxation term (van den Berg et al., 2011), which operates a branch of cross-shore sediment transport, is included to the model. Explained transport mechanisms are computed over the two-dimensional grid system. The third module is the morphology module (MEV). MEV computes bottom topography change under the aforementioned sediment transport mechanisms in a defined time interval.

Developed sub-modules and Q-2DH model is tested and validated under theoretical cases and laboratory experiments of Wang and Gravens (2007). As theoretical cases, three different situations are considered; beach cusps, cross-shore sediment transport, and single groin. Beach cusps are curved shoreline, and they are studied to validate sediment transport directions. Overall, the model successfully reflects transport directions in beach cusps. However, in situations where the incoming wave angle and local orientation is low, transport directions can be reversed. Moreover, in beach cusps, a return flow occurs in the middle of bays through the offshore direction. This flow transports sediments to offshore direction cause to preserve beach cusp layout. In the Q-2DH model, return flow is not represented. As previously discussed, cross-shore sediment transport is not process-based, and it preserves an equilibrium profile. An arbitrary profile is subjected to waves to transform its equilibrium profile to illustrate the cross-shore sediment transport. In the initial phases of the model, most of the overall equilibrium shape is acquired, and in approximately 20000 seconds, the profile reached its equilibrium profile. Finally, a single groin case is considered to observe the model's results in the vicinity of a groin. In the updrift part, the model accumulates sediment. However, in the downdrift part, the model fails to erode the beach. In the scope of laboratory experiments, Gravens and Wang's (2007) experiments from T1C1 to T1C8 are studied to validate the Q-2DH model in the presence of an offshore breakwater. When the cases are individually studied, the Q-2DH model is quantitively successful

in estimating shoreline changes for all cases. According to BSS scores, areal analysis suggests the model is successful in T1C1, T1C2, and T1C1-T1C2 cases. The model is successful in the initial phases of experiments. As the shoreline advances through the offshore, high local orientation angles and high incoming wave angles occur, and they cause instabilities and lead to model failure.

For further recommendations on the model, when high incoming wave angles and high local orientations are combined, the model cannot accurately predict the areal change in topography. Moreover, there is an instability accumulation exists in the model. After the model initiates and as time progresses, irregularities become distinguishable in sediment transport magnitudes and bottom topography. These irregularities cause the shoreline to be crinkled. Thus, causing instabilities in sediment transport magnitudes, accumulation of further instabilities. To deal with this problem; development of further filters or algorithms, their effects on irregularities and the shoreline change can be investigated and implemented to the model. Also, curved shorelines with the presence of a structure, sand sources/sinks, tides and currents can be studied with Q-2DH model. Q-2DH model can be enhanced to represent the behavior around the single groin. Sediment transport expressions can be altered to consider the wave model's behavior in the downdrift part, or the wave model can be enhanced for the downdrift part. Solving the above-given drawbacks, the Q-2DH model might be a base for a widely applicable, fast, and precise computing tool for sediment transport problems.

## REFERENCES


Artagan, S.S. 2006. A One Line Numerical Model for Shoreline Evolution under the Interaction of Wind Waves and Offshore Breakwaters, M.Sc. Thesis, METU, Ankara

Bailard, J. A. 1981. An Energetics Total Load Sediment Transport Model for a Plane Sloping Beach, Journal of Geophysical Research 86, C11, 938-954

Bakker, W. T. 1968. The Dynamics of a Coast with a Groin System. Proc. 11th Int. Conf. on Coastal Eng., ASCE, London, 492-517

Baldock, T.E., Holmes, P., Bunker, S. & Van Weert, P. 1998. "Cross-shore Hydrodynamics within an Unsaturated Surf Zone," Coastal Eng., 34, pp.173-196.

Baykal, C. 2006. Numerical Modeling of Wave Diffraction in One-Dimensional Shoreline Change Model., M.Sc. Thesis, METU, Ankara, Turkey

Baykal, C. 2012. Two-Dimensional Depth-Averaged Beach Evolution Modelling, Ph.D. Thesis, METU, Ankara, Turkey

Baykal, C., 2014. Development of a numerical 2-dimensional beach evolution model. Turkish Journal of Earth Sciences, vol.23, 215-231.

Baykal, C., Ergin, A. & Güler, I., 2014. Two-Dimensional Depth-Averaged Beach Evolution Modeling: Case Study of the Kizilirmak River Mouth, Turkey. Journal of Waterway Port Coastal and Ocean Engineering, vol.140.

Booij, N., Ris, R.C. & Holthuijsen, L.H., 1999. A third-generation wave model for coastal regions, 1, model description and validation. J. Geophys. Res., 104 (C4): 7649-7666.

Briand, M.H.G. & Kamphuis, J.W. 1993. Sediment transport in the surf zone: A quasi 3-D numerical model. Coastal Eng., Vol.20, pg.135-156

Brier, G. W. (1950). Verification of Forecasts Expressed in Terms of Probability. Monthly Weather Review, 78 (1), 1.

Brøker-Hedegaard, I., Deigaard, R. & Fredsoe, J. 1991. Onshore/offshore Sediment Transport and Morphological Modelling of Coastal Profiles. Proc. ASCE Specialty Conf. Coastal Sediment' 91. 643-657

Bruneau, N., Bonneton, P., Pedreros, R., Dumas, F. & Idier, D. 2007. A New Morphodynamic Modelling Platform: Application to Characteristic Sandy systems of the Aquitanian Coast, France. Journal of Coastal Research, Special Issue 50, 932-936

Buttolph, A.M., Reed, C.W., Kraus, N.C., Ono, N., Larson, M., Camenen, B., Hanson, H., Wamsley, T. & Zundel, A.K. 2006. Two-dimensional depth-averaged circulation Model CMS-M2D: Version 3.0, Report 2, Sediment

Transport and Morphology Change. Technical Report ERDC/CHL TR-06-9, Coastal and Hydraulics Laboratory, US Army Engineer Research and Development Center, Vicksburg, MS.

Capobianco, M., Hanson, H., Larson, M., Steetzel, H., Stieve, M.J.F., Chatelus, Y., Aarninkhof, S. & Karambas, T. 2002. Nourishment design and evaluation: applicability of model concepts, Coastal Engineering, Vol. 47, 113-135

CIRIA, CUR & CETMEF 2007. The Rock Manual. The use of rock in hydraulic engineering (2nd edition). C683, CIRIA, London.

Cowell, P., Roy, P. S. & Jones, R.A. 1994. Simulation of LSCB using a morphological behavior model, Marine Geology, 126, 45-61

Dabees, M.A., 2000. Efficient Modeling of Beach Evolution, Ph.D. Thesis, Queen's University, Kingston, Ontario, Canada

Dabees, M.A. & Kamphuis, J.W. 1998. ONELINE, a Numerical Model for Shoreline Change. Proc. 27th Int. Conf. On Coastal Eng., ASCE, Copenhagen, 2668-2681

Dabees, M.A. & Kamphuis, J.W. 2000. NLINE: efficient modelling of 3-D beach change. Proc. 27th Coastal Eng. Conf., ASCE, 2700–2713.

Dally, W.R. & Dean, R.G. 1984. Suspended Sediment Transport and Beach Profile Evolution, Journal of Waterway, Port, Coastal and Ocean Engineering, Vol 110, No. 1, 15-33

Dally, W.R., Dean, R.G. & Dalrymple, R.A., 1985. Wave height variation across beaches of arbitrary profile. J. Geophys. Res., 90(C6): 11,917-11,927.

Dang, V. T. 2006. Development of a Mathematical N-line Model for Simulation of Beach Changes Ph.D Thesis. University of New South Wales.

Davies, A. G., van Rijn, L. C., Damgaard, J. S., van de Graad, J. & Ribberink, J. S. 2002. Intercomparison of research and practical sand transport models, Coastal Engineering, 46, 1-23

DHI, Danish Hydraulic Institute. 2001. LITPACK Coastline evolution, User's Guide and Reference Manual. Ed. DHI, Lingby, Denmark

DHI, Danish Hydraulic Institute. 2005. MIKE21/3, Coupled Model FM Technical Documentation, Shoreline Morphology Module, Lingby, Denmark

Ebersole, B.A., Cialone, M.A. & Prater, M.D., 1986. Regional coastal processes numerical modeling system: Report 1: RCPWAVE - a linear wave propagation model for engineering use. Tech. Rep. CERC 86-4. US Army Corps of Engineers, CERC. Vicksburg, Miss.

Esen, M. 2007. An implicit one-line numerical model on longshore sediment transport, M.Sc. Thesis, METU, Ankara, Turkey

Fleming, C. A. & Hunt, J. N. 1976. Application of a sediment transport model, Proc. 15th Int. Conf. on Coastal Eng., ASCE, 1184-1202

Fredsoe, J. & Deigaard, R. 1992, Mechanics of Coastal Sediment Transport, Advanced Series on Ocean Engineering, World Scientific.

Goda, Y. 2008. Wave Setup and Longshore Currents Induced by Directional Spectral Waves: Prediction Formulas Based on Numerical Computation Results. Coastal Engineering Journal, 50(4), 397-440.

Gravens, M.B. & Wang, P. 2007. Data report: Laboratory testing of longshore sand transport by waves and currents; morphology change behind headland structures. Technical Report, ERDC/CHL TR-07-8, Coastal and Hydraulics Laboratory, US Army Engineer Research and Development Center, Vicksburg, MS.

Hallermeier, R.J. 1978. Uses for a Calculated Limit Depth to Beach Erosion,Proc. 16th Int. Conf. on Coastal Engrg., ASCE, New York, pg.1493-1512

Hanson, H., Aarninkhof, S., Capobianco, M., Jimenez, J.A., Larson, M., Nicholls,R.J., Plant, N.G., Southgate, H.N., Steetzel, H.J., Stive, M.J.F. & de Vriend, H.J., 2003. Modelling of Coastal Evolution on Yearly to Decadal Time Scales, Journal of Coastal Research, Vol.19, No.4, 790-811

Hanson, H. & Kraus, N.C. 1989. Genesis: Generalized Model for Simulating Shoreline Change, Technical Report CERC-89-19, Report 2 of a Series, Workbook and User's Manual. US Army Corps of Engineers, Waterways Experiment Station, Vicksburg, MS, USA.

Hanson, H. & Larson, M. 1998. Seasonal shoreline variations by cross-shore transport in a one-line model under random waves. Proc. of 26th International Coastal Eng. Conf., ASCE, 2682-2695.

Hanson, H., Larson, M. & Kraus, N.C. 2001. A new approach to represent tidal cunents and bathymétrie features in the oneline model concept. Proc., Coastal Dynamics '01, ASCE, 172-181.

Hanson, H., Larson, M., Kraus, N.C., & Capobianco, M. 1997. Modeling of seasonal variations by cross-shore transport using one-line compatible methods. Proc., Coastal Dynamics '97, ASCE, 893-902.

Hanson, H. & Larson, M. 2000. Simulating Coastal Evolution Using a New Type of N-line Model. Proc. 27th Coastal Eng. Conf. ASCE, 2808–2821.

Hoan, L.X. 2010. Long-Term Simulation of Coastal Evolution. Ph.D. Thesis, Lund, Sweden

Inman, D. L. & Bagnold, R. A. 1963. Littoral Processes, in The Sea, M. N. Hill, (ed.), Vol. 3, pp. 529-533, New York, Wiley.

Janssen, T.T. & Battjes, J.A. 2007. "A note on wave energy dissipation over steep beaches." Coastal Eng., 54, 711-716

Kamphuis, J. W. 1991a, Alongshore Sediment Transport Rate, Journal of Waterway, Port, Coastal and Ocean Engineering, 117(6):624–640.

Kamphuis, J. W. 1991b, Alongshore Sediment Transport Rate Distribution, in Coastal Sediments, 170–183.

Kamphuis, J.W. 2000. Introduction to Coastal Engineering and Management. World Scientific Publishing, Singapore

Kriebel, D.L. & Dean, R.G. 1984. Beach and Dune Response to Severe Storms. Proc. 19th Int. Coastal Eng. Conf. ASCE, 1584-1599

Komar, P.D. 1998. Beach Processes and Sedimentation, 2nd Edition. Prentice Hall, Englewood Cliffs, N.J.

Kristensen, S. E., Drønen, N., Deigaard, R., & Fredsoe, J. 2013. Hybrid morphological modelling of shoreline response to a detached breakwater. Coastal Engineering, 71, 13-27. doi: 10.1016/j.coastaleng.2012.06.005

Kristensen, S. E. 2012. Marine and Coastal Morphology: medium term and long-term area modelling, Ph. D. Thesis, Technical University of Denmark, Lyngby, Denmark

Lanckriet, T. 2014. Near-Bed Hydrodynamics and Sediment Transport in The Swash Zone. 10.13140/2.1.4163.4883.

Larson, M., Kraus, N.C & Connell, K.J. 2006. Cascade Version 1: Theory and model formulation. ERDC TNSWWRP-06-7. Vicksburg, Mississippi: U.S. Army Engineer Research and Development Center.

Larson, M., Kraus, N.C & Hanson, H. 2002. Simulation of regional longshore sediment transport and coastal evolution - the 'Cascade' model. Proc. of 28th Coastal Eng. Conf., World Scientific Press, Singapore, 2612-2624.

Larson, M. & Kraus, N.C. 1989. SBEACH: Numerical Model for Simulating Storm-Induced Beach Change. Technical Report CEREC-89-9, Coast. Eng. Res. Ctr., U.S. Army Eng. Waterway Experiment Station, Vicksburg, Miss.

Larson, M., Kraus, N.C. & Hanson, H. 1990. "Decoupled numerical model of three-dimensional beach range." Proc. 22nd Coastal Eng. Conf., ASCE, 2173–2185.

Lax, P. D., Wendroff B., 1960. Systems of conservation laws. Commun. Pure Appl. Math. 13 (2): 217–237. doi:10.1002/cpa.3160130205.

LeMéhauté, B. & Soldate, M., 1978. Mathematical modeling of shoreline evolution. Proc. 16th Int. Conf. on Coastal Eng., ASCE, 1163-1179

Mase, H., 2001. Multidirectional random wave transformation model based on energy balance equation. Coastal Eng. Journal 43 (4), 317–337.

Masselink, G. & Hughes M.G., 2003, Introduction to coastal processes and geomorphology, Hodder Arnold, London

Militello, A., Reed, C. W., Zundel, A. K. & Kraus, N. C. 2004. Two-dimensional depth-averaged circulation model M2D: Version 2.0, Report 1: Documentation and user's guide, ERDC/CHL TR-04-02, U.S. Army Engineer Research and Development Center, Vicksburg, MS.

Miller, J.K. & Dean R.G. 2004. A simple new shoreline change model, Coastal Engineering, Vol. 51, 531-556

Mitsuyasu, H., Suhaya, T., Mizuno, S., Ohkuso, M., Honda, T., & Rikiishi, K. 1975. Observations of the directional spectrum of ocean waves using a cloverleaf buoy. J. Phys. Oceanogr., 5, 750–760

Nairn, R.B. 1990. Prediction of cross-shore sediment transport and beach profile evolution. Ph.D thesis, Imperial College, London, 391 pp.

Nielsen P., 1999. Groundwater dynamics and salinity in coastal barriers. J. Coastal Res., 15: 732-740.

Ozasa, H. & Brampton, A.H. 1980. Mathematical modelling of beaches backed by seawalls. Coastal Eng. 4, 47–63.

Park, K.-Y., & Borthwick, A.G.L. 2001. Quadtree grid numerical model of nearshore wave-current interaction. Coastal Engineering Vol.42, pp.219-239

Pelnard-Considere, R. 1956. Essai de Theorie de L'Evolution des Form de Rivage en Plage de Sable et de Galets, 4th Journess de l'Hydraulique, Les Energies de la Mer, Question III, Rapoort No. 1, 289-298

Perenne, N. 2005. MARS: a Model for Applications at Regional Scale,"Documentation Scientifique Ver.1.0. User Manual, 45.

Price, W.A., Tomlinson, D.W. & Willis, D.H., 1973. Predicting Changes in the Plan Shape of Beaches, Proc. 13th Int. Conf. on Coastal Eng., ASCE

Reeve, D., Chadwick, A. & Fleming, C. 2004. Coastal Engineering: Processes, theory and design practice, Spon Press, Taylor & Francis Group, 461p.

Roelvink, J. A. & Broker, I. 1993. Cross-shore profile models, Coastal Engineering, Vol. 21, 163-191

Roelvink, J. A., Meijer, T. J., Houwman K., Bakker, R. & Spanhoff, R. 1995. Field validation and application of a coastal profile model. Proceedings, Coastal Dynamics' 95, ASCE, 818-828

Roelvink, D., Reniers, A., van Dongeren, A., van Thiel de Vries, J., McCall, R. & Lescinski, J. 2009. Modelling storm impacts on beaches, dunes and barrier islands. Coastal Eng. 56, 1133-1152.

Roelvink, D., A. J. H. M. Reniers, A. Van Dongeren, J. Van Thiel de Vries, J. Lescinski & R. McCall 2010. XBeach model description and manual. Unesco-IHE Institute for Water Education, Deltares and Delft University of Technology. Report June, 21, 2010.

Roelvink, J. A. & G. K. F. M. Van Banning 1995. Design and development of DELFT3D and application to coastal morphodynamics, Oceanogr. Lit. Rev., 11(42), 925.

Saint-Cast, F. 2002. Modélisation de la morphodynamique des corps sableux en milieu littoral. Bordeaux, France: University of Bordeaux I, Ph.D. thesis, 247.

Seymour R.J. 2005. Cross-Shore Sediment Transport. In: Schwartz M.L. (eds) Encyclopedia of Coastal Science. Encyclopedia of Earth Science Series. Springer, Dordrecht. https://doi.org/10.1007/1-4020-3880-1_104

Seymour R.J. 2005. Longshore Sediment Transport. In: Schwartz M.L. (eds) Encyclopedia of Coastal Science. Encyclopedia of Earth Science Series. Springer, Dordrecht. https://doi.org/10.1007/1-4020-3880-1_199

Schoonees, J. S. & Theron, A. K. 1993. Review of the field data base for longshore sediment transport. Coastal Eng., 19(1), 1–25.

Schoones J. S. & Theron, A. K. 1996. Improvement of the Most Accurate Longshore Sediment Transport Formula. Proc. 25th Int. Conf. on Coastal Engineering, ASCE: 3652-3665

Shimizu, T., Kumagai, T. & Watanabe, A. 1996. Improved 3-D beach evolution model coupled with the shoreline model (3D-shore). Proc. 25th Coastal Eng. Conf., ASCE, 2843–2856.

Shore Protection Manual (SPM), 1984. U.S. Government Printing Office, Washington D.C.

Smith, G. A. 2012. Wave Induced Sediment Mobility Modelling: Bedforms, Sediment Suspension and Sediment Transport. Ph.D. Thesis, Swinburne University.

Smith, J.M., Sherlock, A.R. & Resio, D.T. 2001. "STWAVE: Steady-state spectral wave Model User's Manual for STWAVE Version 3.0." CE-ERDC/CHL 1R-01-1, U.S. Army Engineer Research and Development Center, Coastal and Hydraulics Laboratory, Vicksburg, MS

Stieve, M. J. F. & Battjes, J. A. 1984. A Model for Offshore Sediment Transport. Proc. 19th Int. Coastal Conference, ASCE, 1420-1436

Şafak, I. 2006. Numerical Modeling of Wind Wave Induced Longshore Sediment Transport, M.Sc. Thesis, METU, Ankara

U.S. Army Corps of Engineers (USACE), 2007. Coastal Engineering Manual (CEM), Engineer Manual 1110-2-1100, U.S. Army Corps of Engineers, Washington, D.C. (6 volumes).

van den Berg, N., Falqués, A., & Ribas, F. 2011. Long-term evolution of nourished beaches under high angle wave conditions. Journal of Marine Systems, 88(1), 102-112. doi: 10.1016/j.jmarsys.2011.02.018

van Rijn, L. C., Walstra, D.J.R., Grasmeijer, B., Sutherland, J., Pan, S. & Sierra, J. P. 2003. The predictability of cross-shore bed evolution of sandy beaches at the time scale of storms and seasons using process-based profile models, Coastal Engineering, Vol. 47, 295-327

Vitousek, S., P. L. Barnard, P. Limber,L. Erikson & B. Cole 2017. A model integrating longshore and cross-shore processes for predicting long-term shoreline response to climate change, J. Geophys. Res. Earth Surf., 122, 782–806, doi:10.1002/2016JF004065.

Warner, J. C., B. Armstrong, R. He & J. B. Zambon 2010. Development of a coupled ocean–atmosphere–wave–sediment transport (COAWST) modeling system, Ocean Model., 35(3), 230–244.

Warner, J.C., Sherwood, C.R., Signell, R.P., Harris C.K. & Arangoc, H.G. 2008. Development of a three-dimensional, regional, coupled wave, current, and sediment-transport model. Computers & Geosciences 34, 1284–1306

Weise B.R., White, W.A. 1980. Padre island national seashore: a guide to the geology, natural environments, and history of a Texas barrier island, Guidebook 17, Texas Burau of Economic Ecology

Wright, L. D. & Short, A. D. 1984. Morphodynamic variability of surf zones and beaches: a synthesis, Marine Geology, Vol. 26, 93-118

Zheng, J. & Dean, R.G. 1997. Numerical models and inter-comparisons of beach profile evolution, Coastal Engineering, Vol. 30, 169-201